Imperial College London
Department of Physics

Ultra-Relativistic Thermal Production of Electrons and Positrons

Jonathan Jacob Beesley

Submitted in part fulfilment of the requirements for the degree of
Doctor of Philosophy in Physics of Imperial College London
September 2022.

Abstract

This thesis investigates ultra-relativistic processes of thermal production of electrons and positrons, and the theories involved in their description. It first focuses on collisional ionisation and excitation rates in a partially-ionised plasma, presenting correction factors to them that account for special relativity in the free electron motion as a function of temperature and the threshold energy. These results are extended to de-excitation and three body recombination using detailed balance.

It then turns to the production of electron-positron pairs from Breit-Wheeler two-photon collision in the black-body field, and presents an analytic expression for the high-temperature limit of the total rate. It then examines the same physical process using the formalism of "external fields", in which the black-body is treated as as a thermal ensemble of classical field profiles. It presents a novel formal scheme for this calculation, and then presents the results of a numerical scheme that approximates this field ensemble by 1D spatial "Sauter pulses". It is found that pair-production calculated by this means exceeds that calculated by Breit-Wheeler by a large factor, and the energy spectrum of produced particles is presented.

Then, work comparing different theoretical formalisms of vacuum-destabilising background fields in QED is presented. It is first shown how solving the Dirac equation with peculiar boundary conditions can give probability amplitudes for fermion scattering and pair creation/annihilation. It is then demonstrated for a broad class of external fields that four fermion propagators used in the literature are equivalent: Schwinger's "proper-time" propagator; the "causal propagator" used in the "Bogoliubov transformation" method; and two defined using analytic continuation. To do so, we re-derive Schwinger's proper-time expression for the propagator as a statement relating solutions of the inhomogeneous Dirac equation to those of the inhomogeneous "proper-time Dirac equation". We then show that all four propagators return solutions of the inhomogeneous Dirac equation that satisfy the same boundary condition.

Acknowledgements

I would like, first of all, to thank my supervisor, Steven Rose: constant in support, generous with time, patient with the strange places I insisted on taking my PhD. Sometimes by the productive clash of our contrasting approaches, I have learned through our collaboration what I have of how to be a research scientist.

I am profoundly grateful to my parents, who, besides the obvious contingency of my academic life on their efforts, accepted me back into my childhood home to weather the COVID storm, and therefore under whose generous care I have completed my PhD.

I would also like to thank Felix Mackenroth, for our discussions on an early attempt at the Schwinger mechanism project. Thanks also to the students in the plasma group, fellow travellers towards our PhDs, who made my time at Imperial, however sporadic, very enjoyable.

Copyright Declaration

Statement of Originality

The content of this thesis is original unless otherwise cited or acknowledged in the text, and was completed either independently or in collaboration with my supervisor, Steven Rose.

Jonathan Beesley

September 2022

Published Work from Thesis

Some of the novel results from this thesis are published in the following articles.

[1] J. J. Beesley & S. J. Rose. Free electron relativistic correction factors to collisional excitation and ionisation rates in a plasma. *High Energy Density Phys.*, 33:100716, 2019.

[2] J. J. Beesley. On the Equivalence of Causal Propagators of the Dirac Equation in Vacuum-Destabilising External Fields. *Found. Phys.*, 52(1):27, 2022

[3] J. J. Beesley & S. J. Rose. High-temperature limit of Breit–Wheeler pair production in a black-body field. *Results Phys.*, 41:105917, 2022.

The work published in these articles makes up the substances of chapters 3, 7 and 4, respectively.

'We cannot say at what point "technique" begins or where it ends.'

T.S. Eliot

Contents

Abstract **3**

Acknowledgements **5**

Important Symbols and Notation **17**

1 Introduction **23**

2 Theoretical Background **31**

2.1 QED in a Background Classical Field? 32

2.2 The Bogoliubov Transformation Method 40

2.2.1 Formal Summary 41

2.2.2 Points of Interest 44

2.3 Proper Time 45

2.4 The Schwinger Mechanism 46

2.5 Thermal Theory 52

2.5.1 General Thermal Quantum Field Theory 53

2.5.2 Pair Production by the Black-Body Field 55

3 Free Electron Relativistic Correction Factors to Collisional Excitation and Ionisation Rates in a Plasma **57**

3.1 Calculation of Rates 59

3.1.1 Method 59

3.1.2 Excitation Rate 61

3.1.3 Ionization Rate 62

3.2 De-excitation and Recombination Rate Corrections 63

3.3 Conclusion 64

4 Breit-Wheeler Pair Production in a Black-Body Field at High Temperatures 67

4.1 Closed-Form Expression for the High-Temperature Limit 67

4.2 Discussion and Energy Spectrum 72

5 The Schwinger Mechanism in a Black-Body Field 78

5.1 Formalism for Treating the Black-Body Field as an External Field 81

5.1.1 The Classical Probability Distribution over Classical Background Fields . 81

5.1.2 Numerical Generation of a Distribution of Local Black-Body Field Profiles 84

5.2 Pair-Creation Rate from a Statistical Ensemble of Sauter Pulses 89

5.2.1 High-Temperature Limit of Nikishov's Sauter Pulse Result: Total Pair-Creation Rate 91

5.2.2 High-Temperature Limit of Nikishov's Sauter Pulse Result: Energy Spectrum 94

5.2.3 Using Sauter Pulses to Estimate Black-Body Pair-Production 95

6 The Feynman-Cauchy Problem 105

6.1 Precise Statement of the General Result 107

6.2 Proof for a Vacuum-Destabilising External Field 109

6.3 Discussion 113

7 Causal Propagators of the Dirac Equation 115

7.1 The Inhomogeneous Proper-Time Dirac Equation 117

7.1.1 Basic Definitions 117

7.1.2 A Representation of $\mathcal{H}_{\text{S.T.}}$ in which the Dirac Hamiltonian is Diagonal . . 120

7.1.3 A Representation of $\mathcal{H}_{\text{P.T.}}$ in which $\hat{H}_{\text{P.T.}}$ is Diagonal 124

7.1.4 Generalised Eigenvectors of $\hat{H}_{\text{P.T.}}$ 126

7.1.5 Projecting a Vector in $\mathcal{H}_{\text{P.T.}}$ onto a Vector in $\mathcal{H}_{\text{S.T.}}$ 128

7.1.6 The Differential Equations 134

7.2 The "Causal Propagator" of Fradkin, Gitman & Schvartsman 140

7.3 Three Other Equivalent Solution Forms 141

7.3.1 Schwinger's Proper-time Propagator 141

7.3.2 The $m_e^2 - i\epsilon$ Prescription and Continuation from Euclidean Time 142

7.4 Discussion 144

7.4.1 The Result 144

7.4.2 Conditions on the External Field 144
7.4.3 Mathematical Assumptions 146

8 Conclusion **149**

A The Quantum Effective Action in a Background Field **155**

B A Toy Model for the Correction Factor **158**

C Pair-Production in a Temporal Sauter Pulse **160**

D The Feynman-Cauchy Problem from FGS **163**

E Complex Fourier Analysis **165**

F The ± Components of a Source Supported on Finite Time **169**

G The Time-Translation Operator of the Dirac Equation **171**

Bibliography **172**

List of Figures

3.1 Maxwell-Boltzmann and Maxwell-Jüttner distributions. 58

3.2 General temperature-dependent prefactor to relativistic correction factor of collisional rates. 61

3.3 $P[\sigma]$ for excitation and ionisation. 62

3.4 Ratios of collisional ionisation, recombination and excitation rates when special relativity is accounted for against when it isn't. 66

4.1 Approximation and numerical calculation of thermal Breit-Wheeler pair-creation rate. 71

4.2 Next-to-leading-order contributions to Breit-Wheeler 74

4.3 Spectrum of photon energies contributing to Breit-Wheeler in a black-body. . . . 75

4.4 Energy spectrum of pairs created by Breit-Wheeler in a black-body. 76

5.1 Log-log plot of $f_{\mathrm{S}}(\lambda')$ 93

5.2 Example spectra of particles produced by Sauter pulses. 96

5.3 Example bump-sections of the black-body fitted to Sauter pulses. 97

5.4 Histograms of Sauter pulse parameters fitted to black-body field. 97

5.5 Histograms showing variation of local pair-production rate in black-body. 100

5.6 Comparison of particle creation rates in a black-body field calculated by different methods. 101

5.7 Energy spectrum of particles produced by black-body field. 103

C.1 Particle production rate in a temporal Sauter pulse external field over the locally-constant field estimate, $\gamma = 0$ 162

Important Symbols and Notation

Mathematical Notation

$\mathbb{R}$	The real numbers.
$\mathbb{R}^{\pm}$	Open $\pm$ve half-lines.
$\mathbb{C}$	The complex numbers.
$\mathbb{R}^{3\oplus 1}$	Lorentz spacetime.
$\mathrm{Li}_n(x)$	Polylogarithm of order n
$E_1(x)$	Exponential integral.
K_n	Modified Bessel function of the second kind.
$\mathcal{H}$	Hilbert space.
$\sigma(\hat{O})$	Spectrum of operator $\hat{O}$.
$\mu_{\hat{O}}$	Spectral measure of the operator $\hat{O}$
$\langle a, b\rangle$	Functional a acting on function b.
$\mathcal{H}_{\hat{O}}$	Representation of a Hilbert space in which $\hat{O}$ is diagonal.
$\mathcal{H}^a_{\hat{O}}$	The generalised eigenspace of $\mathcal{H}_{\hat{O}}$, on which $\hat{O}$ acts as multiplication by a.
$\delta(x)$, $\delta^{(n)}(x)$	Dirac delta function in 1 or n dimensions (respectively).

Basic Physical Quantities

t	Time.

$\mathbf{x}$, $\mathbf{y}$	Position 3-vectors.
x, y, z	3-vector coordinates or position 4-vectors, $= (tc, \mathbf{x})$, $(tc, \mathbf{y})$, $(tc, \mathbf{z})$.
v	Speed.
V	Volume (of cavity).
$A_\perp$	Area (of cavity) transverse to field direction.
$\mathcal{T}$	Duration of scattering event.
T	Temperature.
p	Probability or momentum.
E	Electric field strength or energy.
A_μ	Electromagnetic 4-potential, $= (A_0/c, \mathbf{A})$.
a_0	Peak electrostatic potential.
τ	Proper time.
$F_{\mu\nu}$	Electromagnetic field tensor.
t_{in}, t_{out}	Times of the start and end of the quantum process (respectively).
β	$= 1/(k_B T)$.
θ	Mass-normalised temperature, $= k_B T/(m_e c^2)$.
η	Mass-normalised energy, $= E/(m_e c^2)$.
$N_{\text{subscript}}$	Particle production rate per unite time or total particle number.
$n_{\text{Subscript}}$	Pair-creation rate per spacetime volume, or particle density per spatial volume
U	Total energy.
u	Energy density.

General Quantum Mechanics

$\hat{H}$	Hamiltonian operator.

$\hat{H}_0$	Free part of the Hamiltonian operator.
$\hat{H}_I$	Interaction part of the Hamiltonian operator
$\mathcal{L}$	Lagrangian density.
$\hat{\mathcal{H}}$	Hamiltonian density.
$\hat{U}$	Time-evolution operator.
$Z[J]$	Partition functional.
$\hat{\rho}$	Density matrix operator.

Thermal and Statistical Mechanics

η_T	Mass-normalised threshold energy of reaction.
f_{MJ}, f_{MJ}	Maxwell-Boltzmann and Maxwell-Jüttner distributions (respectively).
$r(\eta_T, \theta)$	Reaction rate per ion.
σ	Cross-section, standard deviation or spectrum (when it has an operator argument).
$R(\eta_T, \theta)$	Correction factor for collisional rate.
υ_γ or υ_0	energy normalised by temperature.
υ, $\boldsymbol{\upsilon}$	4-momentum and 3-momentum normalised by temperature (respectively).
X	Temperature-normalised position 4-vector.
$\boldsymbol{\mathcal{E}}(X)$, $\mathcal{E}_{\boldsymbol{\upsilon},r}$	Temperature-normalised electric field, as function of space or as amplitude of frequency-space mode.
$\rho_\hbar$	Density of states in temperature-normalised momentum-space.
Z	Partition function.
β_{c}, $\tilde{\beta}_{\mathrm{c}}$	Dimensionless constant of proportionality between characteristic inverse timescale and lengthscale (respectively) of the black-body field and temperature.

The Dirac Equation and QED

γ^μ	Dirac gamma matrices.
$G_{ll'}(x,y),\ \hat{G}$	A Green's function of the Dirac equation (sometimes with bispinor indices suppressed).
$J(x)$	Driving source for the Dirac equation, or classical source of the quantum theory (sometimes equivalent definitions).
$\hat{\psi}_l(x)$	Fermion field operator. H and S subscripts indicate Schrödinger and Heisenberg picture.
$\mathcal{H}_{\text{P.T.}}$	Hilbert space of square-integrable bispinor spacetime profiles. "P.T." stands for "proper-time", as it is used for the proper-time quantum mechanics.
$\mathcal{H}_{\text{S.T.}}$	Hilbert space of square-integrable bispinor spatial profiles. "S.T." stands for "spacetime", as it is used for quantum mechanics on spacetime.
$\hat{\mathscr{H}}_m$	Hamiltonian of the spacetime Dirac equation with mass m (subscript sometimes suppressed when $m = m_e$).
${}_{\pm}\varphi_\alpha(x),\ {}^{\pm}\varphi_\alpha(x)$	Eigenbasis of the Dirac Hamiltonian at start time and end time (respectively) with $\pm$ve energy.
$\hat{a}_\alpha,\ \hat{b}_\alpha$	Annihilation operators of electrons and positrons (respectively).
$\lvert 0, t_{\text{in}}\rangle,\ \lvert 0, t_{\text{out}}\rangle$	Schrödinger-picture fermion vacua at the start and end time (respectively).
$\lvert 0, \text{in}\rangle,\ \lvert 0, \text{out}\rangle$	Heisenberg-picture fermion vacua at the start and end time (respectively).
c_V	Zeroth-order vacuum persistence amplitude.
$S^c(x,y)$	"Causal propagator" of the Dirac equation in an external field.

$G(\,^{\xi}\!\mid_{\chi})_{\alpha\beta}$	Diagonal blocks of a matrix representation of the retarded propagator of the Dirac equation in mixed in/out bases.
γ_{K}, $\tilde{\gamma}_{\mathrm{K}}$	Temporal and spatial Keldysh parameters (respectively).
ω_c, k_c	Characteristic inverse time and lengthscale (respectively).
λ'	Dimensionless parameter characterising the Sauter pulse, $= ea_0/(K\hbar)$.
κ_0, $\kappa_\perp$	Energy and transverse momentum normalised by the peak electromagnetic potential (respectively).
$\epsilon_r(\mathbf{k})$	Polarisation vector, where $r = 1, 2$.
${}_{\pm}\mathcal{H}^m_{\mathrm{S.T.}}$, ${}^{\pm}\mathcal{H}^m_{\mathrm{S.T.}}$	Subspaces of $\mathcal{H}_{\mathrm{S.T.}}$, spanned by the $\pm$ve energy eigenvectors of the Dirac Hamiltonian $\hat{\mathscr{H}}_m$ at the start or end time, respectively.
${}_{\pm}\hat{P}^m$, ${}^{\pm}\hat{P}^m$	Projection operators onto these subspaces.
${}_{\pm}f_l(\mathbf{x})$, ${}^{\pm}f_l(\mathbf{x})$	Functions belonging to these subspaces (bispinor index sometimes suppressed).
$(a,b)_{\mathrm{S.T.}}$, $(a,b)_{\mathrm{P,T}}$	(For any a, b) Hilbert-space product on $\mathcal{H}_{\mathrm{S.T.}}$ and $\mathcal{H}_{\mathrm{P.T.}}$ (respectively). S.T. subscript is suppressed in chapter 6.
$\hat{H}_{\mathrm{P.T.}}$	Proper time Hamiltonian.
λ	Eigenvalue of $\hat{H}_{\mathrm{P.T.}}$.
$\hat{\Pi}$	$= \gamma^i(\partial_i + ieA_i)$.

Physical and Mathematical Constants

α	Fine structure constant, $\approx 1/137$.
$\hbar$	Reduced Planck's constant, $\approx 1.055 \times 10^{-34}$ Js.
c	Speed of light, $\approx 2.998 \times 10^{8}$ ms^{-1}.
k_B	Boltzmann's constant, $\approx 1.381 \times 10^{-23}$ JK^{-1}.
m_e	Mass of the electron, $\approx 9.110 \times 10^{-31}$ kg.

ϵ_0	Vacuum permittivity, $\approx 8.854 \times 10^{-12}$ $\mathrm{C^2 J^{-1} m^{-1}}$.
e	Elementary charge or Euler's number, $\approx 1.602 \times 10^{-16}$ C or ≈ 2.718.
E_S	Schwinger limit, $\approx 1.132 \times 10^{18}$ $\mathrm{J C^{-1} m^{-1}}$.
r_e	Classical electron radius, $\approx 2.818 \times 10^{-15}$ m.
γ_E	Euler-Mascheroni constant, ≈ 0.577.
A_G	Glaisher-Kinkelin constant, ≈ 1.282.

A Note on Units and Abbreviations

This thesis uses two different systems of units. In all chapters but 6 and 7, SI units are used. In chapters 6 and 7, $\hbar = c = 1$ natural units are used instead.

Chapter 1

Introduction

A thermal system in full or partial equilibrium at temperature T may produce free electrons and positrons, either by freeing electrons from an available bound state (such as within an ion), or by creating electron/positron pairs from the vacuum. This thesis is concerned with the dynamics of this process as temperature approaches and greatly surpasses the scale of the electron rest energy, $k_B T \sim m_e c^2$, where m_e is the electron rest mass and T is the free fermion temperature. If the process is slow enough, it is possible that the freed electrons and positrons can simply escape. If not, we expect there to eventually be overall equilibrium, and therefore for there to be no net thermal production of electrons or positrons. The process of particle creation can, in this context, be useful either to study the process of equilibration, or the state of equilibrium, by studying the conditions necessary for it to be balanced by the reverse rate.

This latter case is the situation supposed in Chapter 3, which examines a partially ionised plasma. This consists of a gas of both free electrons and ions, the collision of which can lead to ionisation, excitation, recombination or de-excitation. Usually these rates are calculated using the Maxwell-Boltzmann distribution for the free electrons, which assumes classical (Newtonian) dynamical motion of the electrons. This becomes insufficient as temperature approaches the electron rest mass, as then a substantial proportion of electrons approach relativistic velocities. Chapter 3 presents "correction factors" to account for the effect of relativistic motion of the free electrons for ionisation and excitation rates. We can then use equilibrium requirements between the bound and free electrons to extend this to a correction factor for the de-excitation and recombination rates.

Chapter 4 looks at the creation of electron-positron pairs from the vacuum by two-particle collisions in a free photon gas, i.e. Breit-Wheeler pair-creation in a black-body field [4]. Here we have appropriately general expressions in the literature, but only as an infinite sum of integrals of special functions over an infinite domain, which must be calculated numerically in the general case [5]. We use the high-temperature, $k_B T \gg m_e c^2$ limit to reduce this to a simple analytical expression. The argument amounts to a demonstration that one can use the high-energy limit of the Breit-Wheeler cross-section for the high-temperature rate. It is found that the leading term contains the logarithmic factor, so the result is given for the leading two terms, which scale as $c \log\left(k_B T/(m_e c^2)\right) \cdot (k_B T/(\hbar c))^4$ and $c\,(k_B T/(\hbar c))^4$. The logarithmic factor is curious; it is the only factor in the high-temperature limit which contains the electron rest mass, and prevents us formally treating the high-temperature limit as the zero-mass limit (since the logarithm would diverge).

This is a straightforward implementation of equations developed for application at lower temperatures in a new context. When we enter a higher energy regime, though, the formalisms that served well in the low-energy regime may become less useful. In quantum electrodynamics, in particular, low-energy and low-intensity scattering processes are well understood by taking the lowest, or lowest few, terms of the perturbative expansion. This is what the Breit-Wheeler pair-creation rate represents. At higher energies and intensities, though, where the standard perturbative expansion begins to break down, it becomes less clear which approximations are valid, or which approaches to the same problem are appropriate.

Chapter 5 applies to the same physical problem, of pair-creation by a black-body field in the $k_B T \gg m_e c^2$ limit, an alternative mechanism of particle creation by light: the Schwinger mechanism. This is named after Schwinger's calculation of the rate of pair-creation by a constant, homogeneous electric field [6]. Unlike Breit-Wheeler, it is *nonperturbative*, which means it cannot by calculated to any order in perturbation theory. This means that it cannot be imagined as occurring by processes composed of successive photon/fermion interactions. The physical reason for this can be appreciated by considering that it is a zero-frequency process, and hence, by energy conservation, cannot be mediated by any finite number of photons. Formally, the Schwinger mechanism is calculated by considering the electromagnetic field as an

"external classical field", rather than as an ensemble of photons, and as such can be generalised to external fields varying in space and time. In this general case the relationship between external field and perturbative methods is often unclear. There is a formal sense in which the choice between calculating pair-creation using Breit-Wheeler or using external fields is a choice between different Hilbert-space bases for the electromagnetic field. This framing of the issue ignores the fact, though, that both methods involve their own approximations and assumptions, neglecting effects which may be larger or smaller in specific instances. Therefore in specific applications one method or the other, both or neither, may be expected to give accurate predictions of observable quantities.

The background field method is most accurate when the electromagnetic field is in a "coherent state", and most of its applications are to this context (or a similar context where the field is in something like a coherent state, though maintained by external current sources). However, it can in principle be extended to an arbitrary quantum state of the electromagnetic field using the fact that the coherent states provide a complete basis for the quantum electromagnetic field states [7–9]. The choice between coherent states and photon-number states is a choice of basis. In the case of the black-body field, the coherent state basis is especially viable as an alternative to the photon basis because, it transpires, both bases diagonalise the density matrix, and hence one can do "classical statistical mechanics" in terms of both of them [9]. This means that one can assign a classical probability $1 \geq p \geq 0$ of the black-body being observed with either a definite number of photons or in a definite coherent state, and calculate statistical quantities, such as expectation values, using the formulae of classical statistical mechanics with these probabilities. The probability of the electric field being found in a particular coherent state even has a very simple mathematical form in momentum space: the amplitude at every mode follows a Gaussian. In principle it is therefore possible to calculate Schwinger particle production by assigning a particle production rate to every coherent field profile the black-body might be found in, then averaging these weighted by the probabilities.

The first part of the results presented in chapter 5 is the formal expression of the particle-production rate in terms of the coherent states of the black-body field, together with a description of a numerical procedure for a representative sampling of spatiotemporal profiles.

This involves some subtlety in moving from momentum space to real space. This can be done precisely. To get beyond this and calculate pair-production rate in the sampled fields is difficult, though, since there do not exist practical methods for calculating Schwinger particle-creation in an entirely general external field. A way forwards is to represent the sampled field profiles by simpler fields, for which the calculation of particle production rates is tractable.

The second part of the results presented in chapter 5 demonstrates how this can be done. We first generate a large sample of local spatial profiles of the black-body field, projected onto a single spatial axis. We then fit these local spatial field profiles to Sauter pulse $E(x) = E_0 \operatorname{sech}^2(Kx)$ "bump" fields by least-squares regression, therefore essentially representing the black-body field by a large set of Sauter-pulse parameters (specifically, their magnitude E_0 and inverse lengthscale K). There exists an analytic expression for the pair-creation rate in the Sauter pulse [10], so we can simply total the creation rate from all these Sauter pulses and divide by length for the overall rate. An important part of our procedure is that, by exploiting the correct limits, the scaling of the pair creation rate with temperature can be derived as a simple quartic $c\,(k_B T/(\hbar c))^4$ factor analytically. The numerical method can therefore be carried out independent of temperature, and returns a temperature-independent prefactor. Using this method we calculate a greater rate of pair creation than Breit-Wheeler by a factor of about 10 in the important regime. As an estimate to the pair-creation rate of the black-body treated as an ensemble of external fields, this involves many approximations and assumptions: that the black-body field produces pairs as if locally constant in time and transverse spatial dimensions; that the pair-creation rate is formed of a sum of independent contributions from local "bumps" of order the thermal wavelength; and it entirely neglects the magnetic field. Together, these considerations severely restrict how strong conclusions we can draw from the results of our model, though we argue that our result gives some reason to believe that an accurate external-field calculation would return a substantially higher result than Breit-Wheeler.

The rest of the thesis, chapters 6 and 7, continues the interest in QED in a strong external background field, and also continues the interest in comparing different methods meant to achieve the same ends. Specifically, it focuses on demonstrating the equivalence of different formal approaches to QED in an external field. Chapter 6 is interested in Feynman's demon-

stration that one can calculate scattering amplitudes in the theory of electrons and positrons in an external field by solving the homogeneous Dirac equation, as a $\mathbb{C}$-valued "single-particle" equation with a peculiar choice of boundary condition [11]. One must solve the equation not with a specified starting profile, nor ending profile, but with the positive-energy component of the solution specified at the start time, and the negative-energy component of the solution specified at the end time. His derivation relies on treating the external field perturbatively, though. Chapter 6 provides a nonperturbative demonstration of this result, valid for a wider range of applied fields. It does so using the "Bogoliubov transformation" formalism of external field QED, therefore showing equivalence between this and Feynman's application of the Dirac equation as a single-particle "Schrödinger-like" wave equation.

Chapter 7 is a more substantial piece of work. Most important physical quantities calculated using QED in an external field can be thought of, as in regular QED, as calculated using sums of Feynman diagrams. The main difference between QED with and without an external field is the fermion propagator used. In Feynman diagrams, this is the "fermion line" representing the propagation of electrons or positrons from one point to another [12]. Mathematically, it is a Green's function of the Dirac equation. In the case of regular QED without an external field, it is a Green's function of the regular homogeneous Dirac equation,

$$(i\gamma^\mu \hbar\partial_\mu - m_e c)G_0(x,y) = -\delta^4(x-y), \tag{1.1}$$

while for QED in an external field it is a Green's function of the Dirac equation coupled to an external field,

$$(i\gamma^\mu(\hbar\partial_\mu + ieA_\mu) - m_e c)G(x,y) = -\delta^4(x-y). \tag{1.2}$$

There are many different formalisms used in external field QED, whose equivalence is not always clear when the external field is such as might create particles. Most of this ambiguity between different formal approaches to external field QED can be reduced to ambiguities in their definitions of the fermion propagators. Therefore, a demonstration that their expressions for fermion propagators are equivalent is sufficient to demonstrate that the whole formal approaches

are equivalent. This is why the demonstration, in Chapter 7, that four different definitions of fermion propagators in use in the external field QED literature are equivalent, is important.

The demonstration proceeds by considering the propagators in their capacity as solvers of the inhomogeneous Dirac equation: as operators that, given a source profile, return solutions of the inhomogeneous Dirac equation for that driving source, i.e. if

$$\psi_l(x) = \sum_{l'} \int d^4y \; G_{l,l'}(x,y) J_{l'}(y) \tag{1.3a}$$

then

$$(i\gamma^\mu(\hbar\partial_\mu + ieA_\mu) - m_e c)\psi(x) = -J(x). \tag{1.3b}$$

The propagators can therefore be defined by conditions on inhomogeneous Dirac equation solutions that they give. We demonstrate equivalence between the four propagators by demonstrating that all obey the "Feynman boundary condition", which essentially means that they propagate only positive-energy solutions into the future, and negative-energy solutions into the past. Especial focus is given to Schwinger's definition of the propagator using the "proper-time quantum mechanics". Schwinger defined a kind of "quantum mechanics" (taken here to refer purely to the mathematical system, devoid of physical interpretation) in which quantum states were represented by arbitrary wavefunctions over *spacetime*, rather than space, and therefore "time evolution" must occur with respect to a fifth parameter: "proper time", τ [6]. He worked in a variety of Dirac's bra-ket notation, and constructed the Green's function as an operator on this space as a formal algebraic expression containing the Dirac equation differential operator. Specifically, denoting spacetime profiles as ket-vectors with rounded brackets, $|a) \in \mathcal{H}_{\text{P.T.}}$, and defining the "proper-time Hamiltonian"

$$\hat{H}_{\text{P.T.}} := -i\gamma^\mu(\hbar\partial_\mu + ieA_\mu), \tag{1.4}$$

we can write the propagator relation as

$$\text{if} \quad |\psi) = \hat{G}|J) \quad \text{then} \quad (\hat{H}_{\text{P.T.}} + m_e c)|\psi) = |J). \tag{1.5}$$

Schwinger's definition of the causal propagator is

$$\hat{G} = i \int_0^\infty d\tau \; e^{-(i\hat{H}_{\text{P.T.}} + m_e c)\tau}. \tag{1.6}$$

One issue with Schwinger's method, inherent in his use of the bra-ket notation, is that it is not mathematically rigorous: states that are not square-integrable functions on space, such as delta functions and plane waves, are treated formally as if they are in the Hilbert space, and generally the distinct properties of unbounded operators are not accounted for [13]. It is therefore worthwhile to reformulate his prescription, keeping to well-defined spaces of functions on spacetime. Chapter 7 shows that, underlying Schwinger's definition of the Green's function is a relationship between differential equations: between the Dirac equation and inhomogeneous "proper-time Dirac equation",

$$(i\partial_\tau - \hat{H}_{\text{P.T.}})\psi(x;\tau) = -J(x;\tau). \tag{1.7}$$

Specifically, if we drive the proper-time differential equation with a source profile with arbitrary spacetime shape $J(x)$ but with plane-wave dependence on proper-time, frequency $-m_e c$, $J(\tau; x) = J(x)e^{im_e c\tau}$, and find the retarded response, then this will be a plane-wave of form $\psi(\tau; x) = \psi(x)e^{im_e c\tau}$, where $\psi(x)$ is a solution of the regular inhomogeneous Dirac equation which obeys the Feynman boundary condition. This process of getting from $J(x)$ to $\psi(x)$ - by first turning $J(x)$ into a 5D plane wave $J(x)e^{im_e c\tau}$, finding the solution to a 5D partial differential equation, then projecting this solution onto a fixed τ - can easily be shown to be equivalent to the operation of Schwinger's $\hat{G}$, though considerably better defined mathematically. The demonstration that four other propagators give solutions that obey the same boundary condition is performed more perfunctorily, without similar concern for using a more rigorous mathematical formalism than past authors. The task of putting Schwinger's proper-time quantum mechanics on an alternative, more rigorous mathematical footing, and of demonstrating the equivalence of the causal propagators, are two separate ends aimed at by the work, though we have used the former to achieve the latter.

The next chapter is devoted to theoretical background. This thesis covers a wide range

of topics, so the choice of background covered is necessarily selective. Most attention is given to QED in an external field, with a focus on its comparison to perturbative methods.

Chapter 2

Theoretical Background

Quantum Electrodynamics is the theory of the interaction of light and matter. Regular perturbative QED describes interactions between charged particles as occurring by the exchange of photons. The "perturbative expansion" for the probability of a process occurring is a series expansion essentially in the number of discrete particle interactions occurring to mediate the process. It is an asymptotic expansion: although any finite number of terms of the series converges as the interaction strength approaches zero (once renormalisation has been handled properly), the series does not converge for any finite interaction strength as more terms are added.

When we do QED in a background field, we treat some portion of the electromagnetic field as a classical background. Loosely, the particle and classical field descriptions of light are *complementary* (in Bohr's sense [14,15]), analogous to that between the position and momentum of point particles in non-relativistic quantum theory. The electromagnetic field may have a definite number of photons or a definite field profile, but may not have both at once: certainty in one necessitates uncertainty in the other. (A classical electromagnetic plane wave has both expected number of photons and the variance in the photons equal to $I/(\hbar\omega c)$, where I is the intensity and ω is the photon frequency.) The electrons and positrons are still treated as particles, though their interactions with the external field may be treated "exactly", in a sense. The complication is that their interactions *with each other* are still treated using radiative photon exchange. Loosely speaking, we may understand the perturbative expansion as a Taylor expansion about a "point". The background field acts as a shift of the point about

which we are expanding, which can be to a distant point that accounts for physics completely invisible to the perturbative expansion about the original point. The true values of physical quantities must still be reached via an expansion about this new point, though. Using the background field method without any superimposed photon exchanges is, therefore, in one sense a "nonperturbative" calculation beyond all orders of perturbation theory, though is in another sense a zeroth-order perturbative calculation. It is infinite order with respect to the standard physical vacuum, zeroth order with respect to the "new vacuum".

This issue, of the physical and mathematical relation between regular perturbative QED and QED in a background field, is explored in section 2.1. This is relevant background to the concerns of chapters 4 through 7. Sections 2.2 and 2.3 describe two important formal approaches to the area: the "Bogoliubov transformation method", which is used in chapters 5 through 7; and the "proper-time method", which is used in chapter 7. Section 2.4 explores one of the main physical predictions of the external field method, the Schwinger mechanism, relevant to chapter 5, giving a review of the literature on its generalisation to inhomogeneous fields in space and time. Section 2.5 touches on the relevant background for handling finite temperature fields, and particle creation in a thermal field, relevant to chapters 4 and 5.

2.1 What Does it Mean to do Quantum Electrodynamics with a Background Classical Field?

Quantum mechanics has involved external fields treated classically since its inception. It is implicit in the potential term of the Schrödinger equation, and was hence ubiquitous in most early applications of quantum mechanics. Dirac's early studies of the relativistic dynamics of electrons and positrons assume a classical electromagnetic field background [16, 17]. This had always, of course, existed side-by-side with a theory of quantised radiation, or the photon, dating back to Planck [18] and Einstein [19], and of "radiative transitions" these induced in electrons. The photon theory developed into a thoroughgoing quantum theory of the dynamical interaction of light and matter with the development of Quantum Electrodynamics with Dyson [20], Tomonaga [21], Feynman [11, 22, 23] and Schwinger [24–26] in the years 1946 to 1950.

This went on concurrently with treatment of Dirac's relativistic fermions with an external field, with notable contributions by Euler & Heisenberg [27] and Feynman [11]. The two were combined into a formalism which allowed fermion motion under a classical field with superimposed radiative photon interactions by Furry in 1951 [28]. There might seem, on the face of it, to be something strange and unsatisfactory about this: the classical and quantum conceptions of light are sitting in the same theory in awkward company. How do we understand this procedure?

Quantum electrodynamics is a quantum theory, which still essentially obeys the quantum postulates formalised by Dirac [29] and von Neumann [30] around the turn of the 1930s. The fundamental experimental quantities of quantum mechanics are transition amplitudes, $\langle\phi|\psi\rangle \in \mathbb{C}$, which represent the "probability amplitude" that a system prepared as a state $|\psi\rangle$ is observed as a state $|\phi\rangle$. These states are, mathematically, vectors in a Hilbert space (or a limit of a sequence of vectors in a Hilbert space [31, 32]), and the transition amplitude is their inner product. How do we relate this abstract system of mathematical objects to things we can prepare and observe in a laboratory or through a telescope? The traditional way of doing this is by the process of canonical quantisation, as formalised by Dirac [29, 33, 34]. (For a modern treatment see Ref [35].) We start with a Hamiltonian description of a classical mechanical experimental setup, which means giving the energy as a function of a set of canonical coordinates q and their conjugate momenta p. These coordinates are the "dynamical variables" which we expect to prepare, measure, to change over time. Equivalently, we can specify a Lagrangian, which is a function of the canonical coordinates and their time derivatives, related to the Hamiltonian by a Legendre transformation. The classical Lagrangian densities of QED without and with a background field are, respectively,

$$\mathcal{L}_{\mathrm{QED}}(\psi(x), A_\mu(x)) = -\frac{1}{4}F_{\mu\nu}F^{\mu\nu} + \bar{\psi}\left(c\gamma^\mu\left[i\hbar\partial_\mu + ieA_\mu\right] - m_e c^2\right)\psi \tag{2.1}$$

$$\tilde{\mathcal{L}}_{\mathrm{QED}}(\psi(x), A_\mu(x); A^{\mathrm{ext}}_\mu) = -\frac{1}{4}F_{\mu\nu}F^{\mu\nu} + \bar{\psi}\left(c\gamma^\mu\left[i\hbar\partial_\mu + ieA_\mu + ieA^{\mathrm{ext}}_\mu\right] - m_e c^2\right)\psi, \tag{2.2}$$

where $A_\mu(x)$ is the "dynamical", "quantised" field while A^{ext}_μ is the "external", "back-

ground" field. Note that

$$\begin{aligned}\mathcal{L}_{\mathrm{QED}}(\psi(x), A_\mu(x) + A^{\mathrm{ext}}_\mu) =& \tilde{\mathcal{L}}_{\mathrm{QED}}(\psi(x), A_\mu(x); A^{\mathrm{ext}}_\mu) + A^{\mathrm{ext},\mu}(x) j^{\mathrm{ext}}_\mu(x) \\ &+ \text{unimportant terms},\end{aligned} \tag{2.3}$$

where "unimportant terms" refers to terms constant in the dynamical field within the spacetime bulk volume, that can therefore be subtracted from the Lagrangian without changing the theory it represents, and

$$j^{\mathrm{ext}}_\mu(x) := \partial^\nu F^{\mathrm{ext}}_{\nu\mu}. \tag{2.4}$$

The quantisation procedure involves replacing classical observables with Hermitian operators. The eigenstates of the Hermitian operators are defined as quantum states which will, when observed, be measured as having their eigenvalue for the corresponding classical observable. This is the most direct way the quantisation procedure provides a physical interpretation of states in the Hilbert space. The idea of the background field is most easily understood through this approach to canonical quantisation. Say we have a classical theory of the electromagnetic field, $A_\mu(x)$. We can choose to divide this field up, $A_\mu(x) = A^{\mathrm{ext}}_\mu(x) + A'_\mu(x)$, and put all "dynamics" in $A'_\mu(x)$, i.e. to record the response of the field to whatever input we desire through variation of $A'_\mu(x)$. $A^{\mathrm{ext}}_\mu(x)$ would then be regarded as part of the "system", as "external", an aspect of the physical laws our dynamical variables obey. We are therefore free to quantise $A'_\mu(x)$ rather than $A_\mu(x)$. This would give us a quantum theory of $A'_\mu(x)$ with the classical background $A^{\mathrm{ext}}_\mu(x)$. Practically, since our perturbative quantum field theories rely on the quantum variables attaining only small values (relative to their interaction strength) to be accurate, it would make sense to choose $A^{\mathrm{ext}}_\mu(x)$ such that we expect $A'_\mu(x)$ to be as small as possible to get accurate results. This requires $A^{\mathrm{ext}}_\mu(x)$ to be both *large* and *certain*: the two important qualities of a classical variable. Setting $A^{\mathrm{ext}}_\mu(x)$ to obey equation 2.4 then returns the external-field Lagrangian. In this approach, in the case of a free field $\partial^\nu F^{\mathrm{ext}}_{\nu\mu} = 0$, QED with and without a background field are, formally, different quantum theories based on alternative choices of quantisation of the same classical theory, appropriate to different physical situations.

In the case $j_\mu^{\text{ext}} \neq 0$ then it involves an additional approximation, which will be discussed in more detail below.

This approach, though, is old-fashioned. Canonical quantisation does not hold such a central place in the modern approach to quantum mechanics, where we have sophisticated measurement theories to examine the relationship between quantum and classical from the quantum side, and strange theories of quantum particles, such as QCD, with no clear classical counterpart. The modern approach, in particle physics and field theory anyway, is not to start with a classical lab-bench situation and quantise, but to start with a fundamental universal physical theory, already quantum-mechanical, and particularise to the lab-bench. This means that quantisation no longer seems to provide a physical interpretation by such direct means.[1] From the modern perspective, we would like a relation between QED with and without the background field that works within the quantum theory: a way of deriving the two as special cases of the same fundamental quantum theory.

To show how to do this, we will need a bit of formalism. The most common sort of transition amplitude calculation needed to be done in QFT is the transition amplitude between states specified at different times, i.e. transition amplitudes of form $\langle \Psi_{\text{out}} | \hat{U}(t) | \Psi_{\text{in}} \rangle$, or quantities derived as some sort of limiting case of these, such as scattering matrix elements. The problem is that in the kind of theories that represent real interesting physics, these calculations are in general intractable. What is calculated instead are small derivative variations of a transition amplitude $|\Psi_{\text{in}}\rangle$ and $|\Psi_{\text{out}}\rangle$ chosen to be have particularly simple time-evolution. To do this, we first consider adjusting our quantum theory by introducing "classical sources", or a term of the Lagrangian of form $\sum_i J_i(x)\phi_i(x)$, where $\phi_i(x)$ are the quantum fields of the theory, and the i index runs over both particle species and Lorentz group representation indices. The

[1] It still does so by an indirect means, though. When we construct a "classical Lagrangian", it is a function of classical observables with specified transformation properties, including the geometrical transformations that correspond to movements of the observation frame. (In special relativity, the Poincaré transformations.) The quantisation procedure that maps Poisson brackets to commutators automatically maps "canonical transformations" to unitary Hilbert-space transformations which preserve their group structure. It is these symmetry transformations which in fact is what gives physical meaning to the identification of Hilbert-space vectors with observables. As Weinberg puts it, "the point of the Lagrangian formalism is that it makes it easy to satisfy Lorentz invariance and other symmetries: a classical theory with a Lorentz-invariant Lagrangian density will when canonically quantized lead to a Lorentz-invariant quantum theory." [36] This is the case even for theories, such as QCD, for which there are no situations where the "classical Lagrangian" can ever be profitably employed *as* a classical Lagrangian, to get predictions using the classical equations of motion. For this reason, the "classical Lagrangians" of the theories are still essential to discussions of the quantum theory.

transition amplitude from the fundamental in-state $|\Psi_{\text{in}}\rangle$ to the out-state $|\Psi_{\text{out}}\rangle$ is called the partition functional,

$$Z[J] := \langle\Psi_{\text{out}}|\,\mathrm{T}\{e^{-i\left(\int_{t=t_{\text{in}}}^{t=t_{\text{out}}} d^4x\,\hat{\mathcal{H}}+\sum_i J_i(x)\hat{\phi}_i(x)\right)}\}\,|\Psi_{\text{in}}\rangle\,. \tag{2.5}$$

In most instances, the out-states and in-states $|\Psi_{\text{out}}\rangle$ and $|\Psi_{\text{in}}\rangle$ are taken to be the lowest energy state, which can be set to zero energy, and we take $t_{\text{in}} \to -\infty$ and $t_{\text{out}} \to \infty$. In this case, we can just formally sum over all possible boundary states at the infinite times, and project onto the 0-energy in-state and out-state by introducing a small imaginary time (which takes all states with finite positive energy to zero in the infinite future and past). In this way the specification of the in and out states is often somewhat obscure in the literature, transmuted as it is into the formal specification of the "deformation of the time contour into the complex plane", or similar. An exception to this generality is the literature on strong-field QED, where we must think more carefully about how we define these "vacuum" states.

The actual experimental quantities are the n-point correlation functions, $G(x_1, ..., x_n)$. (These are related to scattering matrix elements by the LSZ formula [37].) These represent statistical correlations between local observations of quantum fields. They are functional derivatives of the partition functional, $Z[J]$,

$$G(x_1, ..., x_n) = \frac{1}{Z[0]}\frac{\delta^n Z[J]}{\delta J(x_1)...\delta J(x_n)}. \tag{2.6}$$

Usually we are interested in the physics of a theory without classical sources, so the derivatives are taken around $J \equiv 0$. The standard peturbative scheme involves expressing correlation functions of the full quantum field theory in terms of the sum of a series of correlation functions of the "free" theory. This procedure is most conveniently performed by construction of a set of "Feynman rules" for the evaluation of Feynman diagrams. The partition functional, with a particular source profile, represents a single transition probability from one state to another. What it is easy to regard as making up the physical content of a quantum field theory - the Feynman rules, the properties of the particles, the scattering amplitudes between particles - are, more precisely, properties of a kind of tangent space of a particular transition probability,

usually that between the vacuum and the vacuum. Here, then, is a sense in which two different "theories", with different Feynman rules and non-commensurate particle definitions, emerge as special cases of one fundamental theory: by picking different $|\Psi_{\text{in}}\rangle$, $|\Psi_{\text{out}}\rangle$, and a classical source distribution.

QED in a background field bares precisely this relation to regular QED. To be more specific, we need to adapt a foundational result of the "background field method" [38–41] slightly: just enough to explicitly account for non-trivial $|\Psi_{\text{in}}\rangle$ and $|\Psi_{\text{out}}\rangle$. This formalism was developed in the practical context of the symmetry breaking of the electroweak field, where large "background fields" are in fact the lowest energy state of the theory, and hence we can expect particles on top of the physical vacuum to represent expansions around a non-trivial background [42, 43]. The result is given in terms of the "quantum effective action" functional, $\Gamma[\bar{\phi}]$. This is defined as a functional of the *expected* field, $\bar{\phi}_i(x) := \langle\Psi_{\text{out}}|\hat{U}^\dagger(t,t_{\text{out}})\hat{\phi}_i(\mathbf{x})\hat{U}(t,t_{\text{in}})|\Psi_{\text{in}}\rangle$, whose variations around the physical value produce a set of "one-particle irreducible" Green's functions, which are entirely equivalent in their information content to the regular Green's functions (one set can be derived from the other). $\Gamma[\bar{\phi}]$ is therefore a straightforward alternative to $Z[J]$. Note that specifying $\bar{\phi}$ implicitly specifies a classical source profile J and vice versa: it is assumed that both can be written as functionals of the other. It can be shown that

$$\frac{\delta\Gamma}{\delta\bar{\phi}(x)} = J(x). \tag{2.7}$$

If we consider $J(x)$ as a fixed part of the experimental situation, then this is a differential equation that the expected field must obey, in addition to boundary conditions imposed by $|\Psi_{\text{in}}\rangle$ and $|\Psi_{\text{out}}\rangle$.

Define $\tilde{\Gamma}[\tilde{\phi}, B; |\Psi_{\text{in}}\rangle, |\Psi_{\text{out}}\rangle]$ as the quantum effective action between $|\Psi_{\text{in}}\rangle$ as an in-state, $|\Psi_{\text{out}}\rangle$ as an out-state, B as the background field and $\tilde{\phi}$ as the expected observed field state. The space of ket-vectors are here to be thought of as defined in terms of the field basis: a ket-vector corresponds to a probability amplitude of being observed as having each particular spatial field profile. Here we take the "theory in a background field" to mean that, if the action of the original theory is $S[\phi]$, the action of the theory in a background is $\tilde{S}[\phi; B] := S[\phi + B]$. The arguments of Ref [40, 41] are adapted in Appendix A to show that

$$\tilde{\Gamma}[\tilde{\phi}, B; |\Psi_{\text{in}}\rangle, |\Psi_{\text{out}}\rangle] = \Gamma[\tilde{\phi} + B; \hat{D}[B(t_{\text{in}})] |\Psi_{\text{in}}\rangle, \hat{D}[B(t_{\text{out}})] |\Psi_{\text{out}}\rangle], \tag{2.8}$$

where $\hat{D}[B]$ is the "displacement operator" for the fields, which can be defined on eigenstates of the field operators

$$\hat{D}[\psi] |\phi\rangle = |\phi + \psi\rangle . \tag{2.9}$$

Setting $J \equiv 0$, we find

$$\left.\frac{\delta\tilde{\Gamma}[\psi, B; |\Psi_{\text{in}}\rangle, |\Psi_{\text{out}}\rangle]}{\delta\psi}\right|_{\psi=\tilde{\phi}} \equiv \left.\frac{\delta\tilde{\Gamma}[\psi, 0; \hat{D}[B(t_{\text{in}})] |\Psi_{\text{in}}\rangle, \hat{D}[B(t_{\text{out}})] |\Psi_{\text{out}}\rangle]}{\delta\psi}\right|_{\psi=\tilde{\phi}+B} \equiv 0. \tag{2.10}$$

There is a subtlety in how to interpret the notation. Physically, the same quantum field profile in the theories with different background fields signify different physical states. The ket-vectors, defined as a probability amplitude attached to each quantum field profile, therefore also represent different quantum states in different background fields. The point of the above deduction is that $|\Psi_{\text{in}}\rangle$, in the theory with a background field, and $\hat{D}[B(t_{\text{in}})] |\Psi_{\text{in}}\rangle$ in the theory without, represent the same physical state. Specifically, if $|\Psi_{\text{in}}\rangle$ and $|\Psi_{\text{out}}\rangle$ are formally the vacuum state, then the background-field theory formally defined as being between the vacuum and vacuum, is physically a theory between field states defined as displacement operators acting on the vacuum.

The theories are different by a relabelling of the field - a shift in coordinates - and by a change of the in and out states, much like we found from considerations of old-fashioned canonical quantisation. However, once we expand perturbatively, we expect to require small expected fields for accurate results. We will therefore expect more accurate results if we can choose B close to the expected field of the theory, i.e. the solution to equation 2.7. We might even find physics entirely invisible to the formalism without a background field, due to the limitations of the perturbation expansion.

Note that $\hat{D}[B(t)]$ does not in general commute with the time-evolution operator, unless we are dealing with a theory of non-interacting free fields. Therefore if $|\Psi_{\text{out}}\rangle$ is the time-

evolution of $|\Psi_{\text{in}}\rangle$, $\hat{D}[B(t_{\text{out}})]\,|\Psi_{\text{out}}\rangle$ is not necessarily the time-evolution of $\hat{D}[B(t_{\text{in}})]\,|\Psi_{\text{in}}\rangle$, and vice versa. This introduces complications to interpretations of our results. Part of the benefit of focusing on perturbations about the physical vacuum is that we cannot describe time-evolution of general states. In the usual scattering theory the vacuum time-evolution isn't entirely trivial, but the *free* vacuum's time-evolution is, so vacuum dynamics can be handled within the perturbative scheme somewhat easily. In external-field QED something similar is usually done: the photon out-state is chosen to be the time-evolution of the photon in-state *to zeroth order of perturbation theory*, such that vacuum dynamics can be studied perturbatively. If we cannot perform a simplifying manoeuvre along these lines, it is possible simply to define $|\Psi_{\text{out}}\rangle = \hat{U}(t_{\text{out}}, t_{\text{in}})\,|\Psi_{\text{in}}\rangle$. This leads to (for instance) expectation values of operators that look like $\langle\hat{O}(t)\rangle = \langle\Psi_{\text{in}}|\,\hat{U}^{\dagger}(t_{\text{out}}, t_{\text{in}})\hat{U}(t_{\text{out}}, t)\hat{O}\hat{U}(t, t_{\text{in}})\,|\Psi_{\text{in}}\rangle$. This time evolution that goes from t_{in} to t_{out} and back again is known as the "Keldysh contour", and leads to the distinctive doubling of the fields in the path integral formulation of the Schwinger-Keldysh "real time" formalism [44,45]. This has had especial success in applications to perturbations around thermal equilibrium [46, 47]. It is often used in external-field QED, though is not needed in this thesis.

So, QED in a background field is QED between two different in and out electromagnetic field states - almost. When applying the above discussion to QED in a background field there are two complications to consider. First, our discussion proceeded by defining the action in the background field as $\tilde{S}[\phi; B] := S[\phi + B]$, but we know from equation 2.3 that, for the Lagrangian used in for QED in a background field, this is only the case for an external field that obeys the free-field Maxwell equations. If it does not, then we find that the background field is equivalent to a background classical source, $j^{\text{ext}}_{\mu}(x)$, which for whatever reason can be approximated as "separated" from the dynamics of the system (since the source couples only to the background field, not to the dynamical field). Even accepting this "well separated" approximation as physically comprehensible (and there are surely difficulties when one starts examining the dynamics of the vacuum), one might well think that saying that imposing a classical background field is equivalent to imposing classical sources isn't much of a theoretical advance: they both seem similarly problematic to interpret. The advantage, if there is one, of the classical source profiles is that they can be seen as the *only* mysterious feature in the theory.

Indeed, it might be possible to replace the idea of preparation and observation of Hilbert space states with sources, since we can turn the vacuum into any state with sources, and portray every interaction of experimental equipment with the quantum system as occurring via the classical sources. This is the perspective of Schwinger's "source theory" [48].

The second complication is that there is often reason to select $|\Psi_{\text{in}}\rangle$ and $|\Psi_{\text{out}}\rangle$ as different from the formal vacuum, such that they are not simply related to the physical vacuum by $\hat{D}[B]$. As is discussed in the next section, most of the literature does implicitly use the formal vacuum for their *photon* vacua, but use something different for their *fermion* "vacua" in the presence of an applied electromagnetic background.

2.2 The Bogoliubov Transformation Method

The most comprehensive approach to QED in a background field is that known as the "Bogoliubov transformation method". This was developed as an approach to zero-order processes (without radiative interactions) largely by Nikishov in the years 1969-74 [10, 49–51]. It was extended to the full QED shortly afterwards, with the basic theory being worked out primarily by Gitman and Fradkin in the years 1976-81 [52–57], with applications and extensions by them and others [58–63]. We shall refer to this work as due to "FGS" after the authors of the book that summarises this work [12], and whose specific formulations we will use.

This method is arguably the most natural way to show how solutions of the Dirac equation are involved in external-field QED. These were originally introduced by Dirac, where they were treated as wavefunctions in the manner of Schrödinger-equation solutions in non-relativistic QED. Issues involved with the negative-energy solutions were solved by postulating the existence of the "Dirac sea" [17]. This is the idea that in the vacuum state all negative-energy solutions are occupied, and positrons are "holes" in the sea. This picture has problems: it is unclear how the infinite energy of the full sea should be treated; the formalism was developed for an external electromagnetic potential treated perturbatively, which leaves as a significant open question how we should treat the interactions of the sea; this approach fails utterly for bosons. Nonetheless, in the restricted model of non-interacting spin-1/2 fermions in an external field, the Dirac sea picture is mathematically equivalent to the QFT interpretation,

and sometimes provides the clearest way of interpreting certain phenomena and expressions. We shall make use of it twice in this chapter.

2.2.1 Formal Summary

The approach is centred on the bispinor field operator. In a background field $A_\mu(x)$ the Heisenberg-picture operator obeys the Dirac equation,

$$(i\gamma^\mu(\hbar\partial_\mu + ieA_\mu(x))) - m_e c)\hat{\psi}_{\mathrm{H}}(x) = 0. \tag{2.11}$$

This can be written in the Hamiltonian form,

$$(i\hbar\partial_t - \hat{\mathscr{H}}(x))\hat{\psi}_{\mathrm{H}}(x) = 0, \quad \hat{\mathscr{H}}_{m_e} := -(i\hbar c\gamma^0\gamma^i\partial_i - \gamma^0\gamma^\mu ceA_\mu - m_e c^2\gamma^0). \tag{2.12}$$

We call $\hat{\mathscr{H}}$ the "Dirac Hamiltonian". In the Schrödinger picture, we can write the field operator in terms of some function basis[2]. Two useful bases to use are the instantaneous eigenstates of the Hamiltonian at the in and out times, defined

$$\begin{aligned} \hat{\mathscr{H}}(t_{\mathrm{in}})\,{}_{\pm}\varphi_{l,\alpha} &= {}_{\pm}\epsilon_\alpha\,{}_{\pm}\varphi_{l,\alpha} \\ \hat{\mathscr{H}}(t_{\mathrm{out}})\,{}^{\pm}\varphi_{l,\alpha} &= {}^{\pm}\epsilon_\alpha\,{}^{\pm}\varphi_{l,\alpha}, \end{aligned} \tag{2.13}$$

which are assumed to be orthonormal. We assume that the Hamiltonian at both times has an energy gap, and therefore can define the eigenstates such that ${}_{+}\epsilon_\alpha$, ${}^{+}\epsilon_\alpha > 0$ and ${}_{-}\epsilon_\alpha$, ${}^{-}\epsilon_\alpha < 0$. A basis of the bispinor function space then defines a set of operators, specifically

$$\begin{aligned} \hat{\psi}_{\mathrm{S},l}(\mathbf{x}) &= \sum_\alpha {}_{+}\varphi_{l,\alpha}(\mathbf{x})\hat{a}_\alpha(t_{\mathrm{in}}) + {}_{-}\varphi_{l,\alpha}(\mathbf{x})\hat{b}^\dagger_\alpha(t_{\mathrm{in}}) \\ &= \sum_\alpha {}^{+}\varphi_{l,\alpha}(\mathbf{x})\hat{a}_\alpha(t_{\mathrm{out}}) + {}^{-}\varphi_{l,\alpha}l,\alpha(\mathbf{x})\hat{b}^\dagger_\alpha(t_{\mathrm{out}}). \end{aligned} \tag{2.14}$$

It will also be useful to define the Heisenberg-picture vacuum states,

[2]FGS do not specify what function space this ought to be a basis of exactly. FGS do not pretend to mathematical rigour, and to my knowledge no other author has made any substantial attempt to translate their work into rigorous terms.

$$|0,\text{in}\rangle := \hat{U}(0,t_{\text{in}})\,|0,t_{\text{in}}\rangle\,, \quad |0,\text{out}\rangle := \hat{U}(0,t_{\text{out}})\,|0,t_{\text{out}}\rangle\,, \tag{2.15}$$

and the zeroth-order "vacuum persistence amplitude",

$$c_V := \langle 0,\text{out}|0,\text{in}\rangle = \langle 0,t_{\text{out}}|\,\hat{U}(t_{\text{out}},t_{\text{in}})\,|0,t_{\text{in}}\rangle\,. \tag{2.16}$$

This is the probability amplitude for the vacuum to remain a vacuum in the absence of photon production or exchanges. The basis operators of the field operator can then be used to define two vacuum states, by

$$\begin{aligned} \hat{a}_\alpha(t_{\text{in}})\,|0,t_{\text{in}}\rangle = \hat{b}_\alpha(t_{\text{in}})\,|0,t_{\text{in}}\rangle = 0 \quad \forall\,\alpha \\ \hat{a}_\alpha(t_{\text{out}})\,|0,t_{\text{out}}\rangle = \hat{b}_\alpha(t_{\text{out}})\,|0,t_{\text{out}}\rangle = 0 \quad \forall\,\alpha \end{aligned} \tag{2.17}$$

The "free" fermion Hamiltonian of the quantum-mechanical system (which accounts for interactions between fermions and the external field but does not include photon exchanges) can be written, neglecting infinite constant terms associated with the absolute energy of the vacuum,

$$\begin{aligned} \hat{H}_0(t_{\text{in}}) &= \sum_\alpha {}_+\epsilon_\alpha \hat{a}^\dagger_\alpha(t_{\text{in}})\hat{a}_\alpha(t_{\text{in}}) + |\,{}_-\epsilon_\alpha|\hat{b}^\dagger_\alpha(t_{\text{in}})\hat{b}_\alpha(t_{\text{in}}) \\ \hat{H}_0(t_{\text{out}}) &= \sum_\alpha {}^+\epsilon_\alpha \hat{a}^\dagger_\alpha(t_{\text{out}})\hat{a}_\alpha(t_{\text{out}}) + |\,{}_-\epsilon_\alpha|\hat{b}^\dagger_\alpha(t_{\text{out}})\hat{b}_\alpha(t_{\text{out}}). \end{aligned} \tag{2.18}$$

This means that the in and out vacua can be defined as, instantaneously, the lowest-energy states. Two important objects in their theory are the "causal propagator",

$$S^c(x,y) = -i\,\langle 0,\text{out}|\,T\{\hat{\psi}_H(x)\hat{\bar{\psi}}_H(y)\}\,|0,\text{in}\rangle\,c_v^{-1}. \tag{2.19}$$

and the vacuum current,

$$\mathscr{J}^\mu(x) := \langle 0,\text{out}|\,\hat{j}(x)\,|0,\text{in}\rangle\,, \quad \hat{j}(x) := \frac{e}{2}\{\hat{\bar{\psi}}_{\text{H}}(x),\hat{\psi}_{\text{H}}(x)\}. \tag{2.20}$$

Note that the vacuum current can be derived from the causal propagator,

$$\mathscr{J}^{\mu}(x) = \frac{ie}{2} \lim_{\epsilon \to 0^+} \operatorname{tr} \gamma^{\mu} \left(S^c(x+\epsilon, x) + S^c(x, x+\epsilon) \right), \tag{2.21}$$

where ϵ is here understood to be a positive vector parallel to the time axis. The Feynman rules for calculating Green's functions between the in and out vacua as here defined are, then, exactly the same as for regular QED, except that the fermion propagator is $S^c(x, y)$ rather than the regular Feynman propagator, and all diagrams carry a factor c_V. $S^c(x, y)$, unlike the Feynman propagator, can give "closed fermion loops", which essentially act as a background source $\mathscr{J}^{\mu}(x)$ for photons. c_V may be calculated from a few formulas. In terms of the causal propagator,

$$c_V = \exp\left[-\operatorname{Tr} \log \frac{S^c}{G_0^c} \right], \tag{2.22}$$

where G_0^c is the regular Feynman propagator of the free field. We also have

$$c_V = \det G(\,^{+}|\,_{+}) = \det G(\,^{-}|\,_{-}), \tag{2.23}$$

where the matrices $G(\,^{\pm}|\,_{\pm})$ are components of the retarded propagator of the Dirac equation, G_{R},

$$G(\,^{\xi}|\,_{\chi})_{\alpha\beta} := \sum_{l,l'} \int d^3\mathbf{x} d^3\mathbf{y}\; {}^{\xi}\varphi^{\dagger}_{l,\alpha}(\mathbf{x}) G_{\mathrm{R},l,l'}(t_{\mathrm{out}}, \mathbf{x}; t_{\mathrm{in}}, \mathbf{y})\, {}_{\chi}\varphi_{l',\beta}(\mathbf{y}). \tag{2.24}$$

and

$$G(^{\xi}|_{\chi})^{\dagger} := G(_{\chi}|^{\xi}). \tag{2.25}$$

Using these, it is also possible to derive

$$\langle 0, \mathrm{out}|\, a_{\beta}(\mathrm{out}) a^{\dagger}_{\alpha}(\mathrm{in})\, |0, \mathrm{in}\rangle\, c_V^{-1} = [G^{-1}(_{+}|^{+})]_{\beta\alpha} \tag{2.26a}$$

$$\langle 0, \mathrm{out}|\, b_{\beta}(\mathrm{out}) b^{\dagger}_{\alpha}(\mathrm{in})\, |0, \mathrm{in}\rangle\, c_V^{-1} = [G^{-1}(^{-}|_{-})]_{\alpha\beta} \tag{2.26b}$$

$$\langle 0, \mathrm{out}|\, b^{\dagger}_{\beta}(\mathrm{in}) a^{\dagger}_{\alpha}(\mathrm{in})\, |0, \mathrm{in}\rangle\, c_V^{-1} = [G(_{-}|^{+}) G^{-1}(_{+}|^{+})]_{\beta\alpha} \tag{2.26c}$$

$$\langle 0, \text{out}|\, a_\beta(\text{out}) b_\alpha(\text{out})\, |0, \text{in}\rangle\, c_V^{-1} = [G(_+|^+) G^{-1}(_+|^-)]_{\beta\alpha}, \tag{2.26d}$$

which represent, respectively, the "relative probability amplitudes" for the scattering of an electron from the α to the β state, the scattering of a positron from the α to the β state, the annihilation of an electron in the α state and a positron in the β state, and the creation of an electron in the β state and a positron in the α state. What equations 2.22 and 2.26 represent is the reduction of the problem of vacuum persistence, scattering, pair-creation and pair-annihilation to first order in the background field to finding the retarded and advanced Green's function, and hence to solving the retarded and advanced homogeneous Dirac equation.

2.2.2 Points of Interest

There are two points of interest worth emphasising. The first is simply to note that FGS have identified particular formal fermion vacua, which are physically the instantaneously lowest-energy states to zeroth order (i.e. accounting only for the kinetic energy of the fermions and their potential energy in the background, not their interactions). These formal vacua need not appear much like a vacuum in any other respect: indeed, they have a non-trivial "vacuum current", $\mathscr{J}^\mu(x)$. The electrons and positrons are defined with respect to this vacuum. To understand this process physically, consider that within a pair-creating external field, a particle's potential energy may be greater than their rest mass, and so removing an electron at rest may *increase* the energy of the system. At this point, how do we really distinguish between the annihilation of an electron and the creation of a positron? This does mean that interpreting "rate of particle creation" is somewhat subtle. An adiabatic transition between lowest energy states is *by definition* a transition in which no particles have been created, even if there has been a vast increase in the charge current. In the general case this would need to be considered when comparing particle production with and without background field methods, though in our application in chapter 5 the formal in and out vacua do not have any charge current.

The second point is that, as we have said before, this choice of vacua is entirely contained in the choice of Green's function for the Dirac equation (2.19). All quantities can be derived from it: the zeroth-order vacuum current by equation 2.21, vacuum persistence ampli-

tude by equation 2.22, and all higher-order quantities via the Feynman rules in which the causal propagator is used as the fermion propagator. This means in particular that the problem of finding the vacuum persistence probability can be reduced to the problem of solving the Dirac equation. This can be understood as essentially due to unitarity, as a kind of version of the spectral theorem: the probability of not producing particles is calculated from the probabilities of all alternatives. It can also be understood more specifically via the Dirac sea picture. Equation 2.23 can be seen as the probability that all negative energy states at the in-time remain negative energy states at the out-time, i.e. that the "sea" remains full, with the antisymmetric structure of the fermion outer product giving the structure of the determinant.

2.3 Proper Time

In the Schrödinger picture of single-particle quantum mechanics, states are described by wavefunctions, which are square-integrable functions on space. The space of these square-integrable functions is the Hilbert space. Operators act on this space, and the Schrödinger equation determines a path through the Hilbert space. The spatial position of the particle is represented by an operator, while its temporal position is a parameter. Space and time are, manifestly, handled differently in this formalism, which presents a problem if we want a quantum mechanical description of relativistic dynamics. Although eventually it was accepted that no fully consistent relativistic single-particle dynamics was possible, and a relativistic quantum mechanics was only achieved as a quantum field theory, attempts were made to achieve the relativistic single-particle quantum mechanics. One, explored by Fock [64] and Stueckelberg [65], is to define the Hilbert space as the space of square-integrable functions over *spacetime*. "Time evolution" must then occur with respect to some fifth parameter - the "proper time" - though of course the formal interpretation of this procedure is now more obscure. (We certainly can't "prepare" and "observe" a whole spacetime profile in the same way.) Time can can now be defined as an operator. Feynman discussed such an idea within the path integral [23, 66, 67], and in this context posited the so-called "Feynman-Stueckelberg interpretation" of the positron, that describes it as the electron "travelling backwards in time." For a review of this early work and of later developments that focused on the "physical significance" of the proper-time parameter,

see Ref [68].

Schwinger made significant use of the proper-time quantum mechanics in his derivation of the Schwinger mechanism [6]. He introduced it into the theory as a tool to calculate the causal propagator, $G(x, y)$, though in doing so implicitly used it to *define* the causal propagator. His expression for the causal propagator in an external field (1.6) has seen much use since, being generalised by DeWitt to account for curved spacetimes [69], and by later authors for the general gauge theory [70], as is reviewed Ref. [71]. These later authors formalised the prescription, invoked by Schwinger only *ad hoc* late in his calculations, that the mass ought to be taken with a negative imaginary component, reduced to zero after the action of the operator. Schwinger also used the proper-time formalism to calculate the "effective action", and the effective action approach to QED in a vacuum-destabilising field has continued to make heavy use of the proper-time method [72]. Further, the "string-inspired worldline formalism" [73–75] has had very wide application. The worldline formalism bears a striking resemblance to Schwinger's proper-time method, though is carried out with both Euclidean coordinate-time and Euclidean proper-time. Much of the work is focused on calculating effective actions in classical backgrounds, which has especially wide applicability since, under the right conditions, it can be identified with the "quantum effective action" and hence related to general Green's functions by equation 2.8. See Ref [76] for a novel axiomatic treatment of QED using the worldline approach. The worldline approach, combined with the concept of "instantons" [77], has had strong recent success in application to nonperturbative particle production in QED [78, 79], as will be discussed in the following section.

2.4 The Schwinger Mechanism

The Schwinger mechanism describes the phenomenon of an external, applied classical electromagnetic field creating electron-positron pairs. Named after Schwinger's 1951 calculation [6], he gave the formula for the vacuum persistence probability,

$$\begin{aligned} |c_V|^2 =& e^{-wV}, \quad w_S := \sum_n \frac{1}{n^2} \frac{(eE)^2}{4\pi^3 c\hbar^2} \exp\left(-\frac{\pi n E_S}{E}\right), \\ E_S :=& \frac{e\hbar}{m^2 c^3} \approx 10^{18}\,\mathrm{Vm}^{-1}. \end{aligned} \tag{2.27}$$

This corresponds to the pair creation rate per unit spacetime volume [49, 80]

$$n_{\mathrm{S}} = \frac{(eE)^2}{4\pi^3 c\hbar^2} \exp\left(-\frac{\pi E_S}{E}\right), \tag{2.28}$$

equal to the first term of Schwinger's sum for w_S[3]. The Schwinger mechanism is "completely nonperturbative", in the sense that it cannot be calculated by any sum of Feynman diagrams. Mathematically, this is clear from the appearance of an essential singularity in the interaction strength, $\exp(-a/e)$ (for some $a > 0$). The perturbative expansion is an asymptotic series expansion in e, but the term $\exp(-a/e)$ has no asymptotic approximation but the trivial,

$$\exp(-a/e) \sim 0, \quad e \to 0^+. \tag{2.29}$$

The Schwinger mechanism therefore seems to describe an effect which is always, necessarily neglected by the perturbative approximation scheme. Continued interest in the quantity is, in large part, motivated by the fact that it is one of very few quantitative non-perturbative predictions of QED. Due to the size of the Schwinger limit E_S it has not yet been experimentally observed, nor discerned in astronomical data.

As explained at the start of this chapter, perturbation theory is still needed to calculate the production process precisely. The Schwinger mechanism is calculated assuming that the electron-positron pairs do not themselves interact with each other or produce photons. We can be more specific with the approximation that the Schwinger mechanism makes, though; as a calculation of the pair-production rate or the vacuum persistence probability it is a calculation

[3]Note that it is still not uncommon in the literature, following Schwinger, to describe w_S rather than n_{S} as the pair creation rate. This interpretation is plausible, as it follows from the assumption that each infinitesimal region of spacetime produces pairs independently [81]. But this assumption is flawed, as explored originally by Nikishov [49]. The main physical issue is that more time is needed to "accelerate" the modes produced at higher energies, so we cannot think of all modes being produced equally, independently, by all spacetime points. In Cohen & McGady's phrase, "To the extent that the natural way to characterize modes is in momentum space, there are very large temporal correlations in pair creation." [80] It is possible to construct a rigorous notion of "local creation rate" using the worldline concept, though the creation rate at a point still causally depends on the field in the surrounding spacetime region [82].

to "first loop order", since any higher-interaction-order processes that affect the production of pairs (such as the exchange of a photon between the produced particles) necessarily introduces another momentum loop. The Schwinger mechanism can be heuristically understood as a "tunnelling" process, akin to the tunnelling of a particle through a potential barrier [81]. The "Dirac sea picture" makes this idea clearest: if you describe the vacuum as a sea of occupied negative-energy states, then the Schwinger mechanism can be seen as particles "tunnelling" from negative-energy states into positive energy states. The barrier is given by their rest energy, which can be overcome by separating the particles by a wide enough distance, d, that their potential energy in the external field is larger than their energy, $d \geq p_0/(eE)$. (A similar semiclassical logic also gives a requirement for the duration of the applied field: to produce particles of momentum p_x in the direction of the applied field, the field must persist for a time, T, long enough for the particle to accelerate to that momentum, $T = p_x/(eE)$ [83].)

Physically, the process of pair-creation in QED and ionisation of an atom or a metal by light are closely related. Both describe incident electromagnetic radiation which induces a transition from a "bound" low-energy fermion state to a continuum of free-particle fermion states which are separated from the bound state by an energy gap, whether that gap corresponds to the ionisation energy of the material or the rest energy of the electron-positron pair. The distinction between Schwinger particle production and low-order perturbative particle production, such as the Breit-Wheeler process [4], is therefore precisely analogous to the distinction between ionisation by classical light waves and photons considered by Einstein in his treatment of the photoelectric effect [19]. This includes the contrast between dependence on the amplitude and frequency of the incident light. Indeed, this can be understood as the physical origin of the breakdown of perturbation theory when describing the Schwinger mechanism: since it is a time-independent process, it is zero-frequency, and hence it must be mediated by an infinite number of zero-energy photons. In the modern approach, Breit-Wheeler and the Schwinger mechanism, analogously to photo-ionisation and field-ionisation, are two different mechanisms by which particle creation can happen, appropriate to two different quantum states of the electromagnetic field: two high-energy photons, or a constant electric field. Both are calculated with different approximations, appropriate to contrasting preparations of the electromagnetic

field. They are conceptualised very differently, and have contrasting physical properties.

There exist generalisations of both particle creation mechanisms which can reduce the contrast between them, though. In particular, we can consider an electromagnetic field that varies in space and time. The theoretical study of the Schwinger mechanism in more general fields was initiated by Nikishov & Narozhyni in 1969 [10, 49, 50], as the earliest work in the development of the Bogoliubov transformation formalism described in section 2.2. As described there, the method involves finding solutions of the Dirac equation. Field configurations for which the Dirac equation is exactly solvable, for which we therefore have explicit closed-form expressions for creation rates of particular particle states, were largely solved around this time[4]. These consist of a small extension of Schwinger's result to a constant homogeneous electric and collinear magnetic field [49, 84, 85]; the Sauter pulse "bump" in both space [10] and time [50]; the "T-constant" temporal top-hat [86, 87]; the electric field oscillating sinusoidally in time [88, 89]; and a superposition of a collinear constant electric and magnetic field and a plane wave propagating along the direction of the field [90–93]. Much more recently, exact solutions have also been found for a top-hat spatial field (i.e. the ideal capacitor) [94], an inverse-square spatial field [95], and for a variety of time-dependent fields: exponential decay [96]; exponential "peak" [97, 98]; a "composite" electric field, or a "smoothed" top-hat [99]; an inverse-square bump [100]; and a bespoke "asymmetric" bump [101]. For a modern overview of exact temporally-varying solutions see Ref [102], and for spatially-varying see Ref [103].

In addition to these exact solutions of the Dirac equation, analysis of homogeneous time-varying fields using what was called the "imaginary time method" - essentially a form of semiclassical WKB approximation - was performed [104–107]. This is appropriate in the weak-field, slow-varying regime, where $E_0 \ll E_S$ and $\omega_\mathrm{c} \ll m_e c^2/\hbar$, where ω_c is the characteristic temporal frequency and E_0 the field strength. Berezin & Itzykson [107] in particular found an expression for the pair creation rate that depended on the "Keldysh parameter",

$$\gamma_\mathrm{K} := \frac{m_e c \omega_\mathrm{c}}{e E_0}. \tag{2.30a}$$

[4]Some numerical work may still be needed to get other quantities of interest, such as integration over particle state creation rates to get a total creation rate, but this is trivial compared to what is needed in non-solved cases.

When $\gamma_{\mathrm{K}} \ll 1$, we are in the "tunnelling regime" of strong, low-frequency fields, and pair-creation proceeds as if by the constant-field Schwinger mechanism (2.28) at every spacetime point. When $\gamma_{\mathrm{K}} \gg 1$ we are in the "multiphoton regime" of weak, fast-varying fields, and pair-creation proceeds largely by the simultaneous absorption of the smallest number of photons energetically permissible. The parameter is named as such because a precisely equivalent result exists for the ionisation of matter by incident coherent radiation, as first derived by Keldysh [45], in which context it has had a long history of both experimental and theoretical success [108].

The fact that an external field can ionise or pair-create by photon absorption ought not surprise. As described in section 2.1, QED in a free-field background is equivalent to QED with a coherent input state. This coherent wave state can be written as a linear superposition of photon states of the same frequency. Keldysh's result shows, in the abstract Hilbert-space language, that in the $\gamma_{\mathrm{K}} \gg 1$ regime the coherent plane wave's ionisation/particle-production is dominated by a single component in the photon-basis. As γ_{K} gets smaller more components contribute, until in the $\gamma_{\mathrm{K}} \ll 1$ regime infinite components make substantial contribution and it becomes impossible to form a qualitative description in terms of the photons.

As developed in this period, the main prospective areas of application for the Schwinger mechanism, where electric fields might be strong enough, were the electric fields of super-heavy nuclei [109, 110] and pulsars [85, 111]. (The latter being a much more straightforward application of the theoretical work considered here.) There was also a substantial interest, stemming from cosmology, due to the analogy between the Schwinger mechanism and particle creation by an intense gravitational field, such as around black holes, reviewed in Refs [112,113]. Theoretical investigation into the Schwinger mechanism has been reinvigorated more recently by the advent of modern high-power laser systems, like the X-ray free electron systems such as European XFEL and Linac Coherent Light Source (LCLS), or optical systems based on chirpsed pulse amplification [114] such as the Extreme Light Infrastructure (ELI4) or the High Power laser Energy Research facility (HiPER). Such systems bring strong-field QED processes within experimental reach (see e.g. Refs [115, 116] for reviews).

Modern theoretical study is therefore in large part focused on calculating pair-production rates for more realistic, and hence more complex, electromagnetic fields, with a focus on shapes

and parameter regimes relevant to the laser-field context. (Though other applications are also of interest, such as the mathematically equivalent hypothetical creation of magnetic monopoles by a strong magnetic field beyond the standard model [117].) Much early work focused on the laser-field application used "quantum kinetic methods", centred on the quantum Vlasov equation [118–120]. These are limited to spatially homogeneous electric fields. First used in early studies estimating the possibility of using X-ray [121, 122] and optical [123] lasers, where the electric field was modelled as a simple sinusoidal oscillation, the method has been extended to wavepackets [124–127], and then to superpositions of wavepackets with different frequencies [128], including "chirps" effects [129]. Numerical integration of the Dirac equation can also be used, with no *in principle* restriction of homogeneity, and indeed has found especial use in the $1 + 1$ dimensional problem of two linearly-polarised wave-packets travelling towards each other [130–133], although other field shapes varying in space [134], time [135] or both [136–139] have been examined. The "Wigner formalism" [140, 141], related to the quantum kinetic approach [142], has also found use in wavepackets varying both in space and time [143], but has found especial use applied to *rotating* fields [144–149], though these have also been studied by integration of the Dirac equation [150, 151] and semiclassical WKB-like methods [152, 153].

Indeed, since the laser-field situation is within the regime of the applicability of semiclassical methods ($E_0 \ll E_S$, $\omega_c \ll m_e c^2/\hbar$), these have had much application to the problem as well. Traditional WKB and "instanton" methods were applied to one-dimensional spatial variation of collinear electric and magnetic fields [154–156]. (See also Ref [157] for extension to more general inhomogeneity.) These methods were used to derive the "dynamically-assisted Schwinger mechanism" [158]. The original paper studies two homogeneous temporal-sauter-bumps, one much smaller and faster than the other, and shows that the pair creation rate is enhanced dramatically compared to both fields independently. Since this apparently provides a mechanism for detecting the Schwinger mechanism with much weaker field strengths than otherwise needed, it has been much much-studied since [159–168].

Semiclassical methods have also seen much success when combined with the "worldline formalism" mentioned at the send of section 2.3. The instanton is a solution to the classical "Euclidean" equations of motion, and the idea of particle creation by instantons is a fairly

straightforward generalisation of the application of the WKB approximation to quantum tunnelling through a barrier [77]. The novelty of the "worldline instanton" is that this formal approximation scheme is utilised in (a version of) the "proper-time quantum mechanics". This method has been used to give a generalisation of Berezin & Itzykson's Keldysh parameter result to cover both oscillating and sauter-pulse bump-profiles in both space and time [78, 79], where we write the spatial Keldysh parameter as

$$\tilde{\gamma}_{\mathrm{K}} := \frac{m_e c^2 k_{\mathrm{c}}}{e E_0}, \tag{2.30b}$$

where k_{c} the characteristic spatial frequency. In both cases $\gamma_{\mathrm{K}}, \tilde{\gamma}_{\mathrm{K}} \to 0^+$ corresponds to an approach to the constant-field regime, where the field creates as if "locally constant". When $\tilde{\gamma}_{\mathrm{K}} \geq 1$, though, the field simply ceases to create particles, with no equivalent to the multiphoton regime. Worldline instantons have been extended to cover fields that vary in two or three spatial dimensions [169], and have been used in studies of the dynamically-assisted Schwinger mechanism [160, 170, 171]. There are also numerical methods based on the worldline approach [82].

2.5 Thermal Theory

The black-body field is the electromagnetic field held at thermal equilibrium. Quantum mechanics began with Planck's study of the black-body in 1901 [18], with the *ad hoc* proposition that modes of the electromagnetic field could only have energies equal to positive integer multiples of their frequency times a constant, h. With Einstein's development [19], this became the proposition that we should think of the electromagnetic field as composed of a number of photons at each frequency. It is a curious feature of Planck's treatment that it requires such little alteration of classical statistical mechanics: that we can assign the probability of photon states being occupied a probability according to Boltzmann's factor $\propto e^{-E/(k_B T)}$, and calculate observable quantities according to the formulas of statistical mechanics. This feature of Planck's treatment has survived all developments since.

The feature is curious because although both quantum mechanics and statistical me-

chanics contain notions of a system being able to be observed in alternative states when observed, they have very different properties. Most pertinently, there exists *interference* between the different possibilities in quantum mechanics: if something has a finite chance of occurring by two different processes, it may have zero chance of occurring when both are possible. Nonetheless, it seems to be possible to think of a thermodynamic system as being composed of a classical statistical ensemble of microstates *if* we use the energy eigenstate basis. The now-accepted formalism for coping with both these notions of possibility together is the "density matrix" operator, $\hat{\rho}$ [172–174]. The density operator for a system at equilibrium can be written formally as

$$\hat{\rho} = e^{-\hat{H}\beta}, \quad \beta := \frac{1}{k_B T}. \tag{2.31}$$

In this formalism, Planck's usage of classical statistics is justified by the fact that the energy eigenstate basis is orthogonal, and that it diagonalises the density matrix.

2.5.1 General Thermal Quantum Field Theory

The simplicity of Planck's treatment owes to the fact that he can treat the electromagnetic field as "free", hence the modes as non-interacting, and hence, formally, the field as an ensemble of simple harmonic oscillators. The full formalism of quantum electrodynamics is needed when we introduce interactions between the electromagnetic field and the fermion field. There are a number of formal systems developed to adapt the perturbative Feynman-diagram QFT to the thermal context (see e.g. Refs [46,47]). Consider the expectation value of an operator $\hat{O}$ in the density matrix formalism,

$$\langle \hat{O} \rangle = \mathrm{Tr}[\hat{O}\hat{\rho}] \quad = \frac{1}{Z} \sum_{\alpha} \langle \alpha | \, \hat{O} e^{-\hat{H}\beta} \, | \alpha \rangle \, . \tag{2.32a}$$

There are two elements to formulating the Feynman rules to calculate this (and similar) quantities. The first is to recognise that the trace sum is, formally, identical to taking the expectation value between peculiar $|\Psi_{\mathrm{in}}\rangle$ and $|\Psi_{\mathrm{out}}\rangle$, as in equation 2.5. The second is to recognise that the density operator acts as a time-evolution operator for imaginary time

$t = i\beta$. Combined, this means that we can handle expectation values in the equilibrium system by a Feynman-diagram expansion. The Hamiltonian can be split into a non-interacting and interacting component, $\hat{H} = \hat{H}_0 + \hat{H}_I$, with non-interacting dynamics handled within an imaginary-time propagator,

$$G(\tau) := \frac{1}{Z} \sum_{\alpha} \langle \alpha | \hat{O} | \alpha \rangle e^{-E_{0,\alpha}\tau}, \tag{2.32b}$$

where we have here assumed that the α basis is diagonal in the free Hamiltonian. The influence of interactions can then be calculated according to a Feynman-diagram expansion. Note that the influence of the non-interacting thermal background (the α sum) is absorbed into the propagator in exactly the same way as the influence of the external field background is accounted for in the causal propagator (2.19) in external-field QED. This is the "imaginary-time formalism". The "real-time formalism" can provide an extension to include real time-evolution (owing to small deviations from equilibrium), and hence involves a non-trivial time-evolution "contour" which goes along both the real and imaginary axes of the complex plane [175].

In more physical terms, what we are doing here is calculating properties of the equilibrium system by first assuming a system of non-interacting particles. We then account for the influence of interactions perturbatively. "Imaginary time-evolution" physically amounts to the reduction in probability of states occurring due to having higher energy, as designated by their Boltzmann factor. Feynman diagrams used for calculating imaginary time-evolution therefore represent, physically, how particle interactions alter states' energy, and hence their Boltzmann factor.

The issue with this picture is that for many important physical quantities, the perturbative expansions that result do not provide series for which the first few terms provide an adequate approximation, reducing in size as the series goes on. Therefore sophisticated "resummation" schemes need to be used to generate valid approximations. Generally, different schemes are appropriate for observables of different order of momentum. For "hard" four-momenta, $p \sim k_B T$ and $p^2 \sim (k_B T)^2$, the naïve scheme described above is appropriate. For "soft" momenta, $p \sim \sqrt{\alpha} k_B T$, the "hard thermal loop" scheme is appropriate [176]. At "ultra-soft" $p \sim \alpha k_B T$ [177–179] or "lightcone" $p^2 \sim \alpha k_B T$ [180, 181] scales further adjustments are

needed.

2.5.2 Pair Production by the Black-Body Field

Thermal particle production occurs when a quantum field is heated to a high temperature and it starts producing particles. There is an approximation implicit in this definition, that the Hamiltonian that we use to define the quantum field system at equilibrium is modified so as not to include the relevant particle production mechanism: otherwise, it would be necessary to consider the thermal quantum field and the produced particles as a single thermal system at equilibrium, and the expected particle number would have to be constant. Current study of thermal particle production has been largely restricted to situations where this approximation is very good, such as Breit-Wheeler production of electrons and positrons by the electromagnetic field at temperatures much lower than the electron rest mass [5]; the emission of photons from a small volume of quark-gluon plasma of type created in high-energy heavy-ion collisions [182, 183]; the production of cold dark matter after "reheating" in early universe cosmology [184–187]; and the production of "Majorana neutrinos" by the electroweak plasma to explain the emergence of baryon/anti-baryon asymmetry in the early universe [181].

In all these cases the "external coupling" that produces the matter is weak enough that the equilibriation of the produced particles with the thermal field can be safely neglected for long periods. But this strict requirement doesn't need to be satisfied for there to be reason to be interested in the phenomenon. All that is strictly needed for the concept to make sense is for the rate of particle production to be substantially less than the rate of the reactions that equilibrate the thermal field. Then, a sufficiently rapid heating of the thermal field can produce disequilibrium even in the high-temperature limit. The rate of thermal particle production can then be used to study the process of equilibration between the thermal field and the field of produced particles.

In chapters 4 and 5 we consider the process of pair-creation by a black-body field described, like Planck's, as a free field, though we examine the high-temperature $k_B T \gg m_e c^2$ limit. Only the opposite limit has been previously studied, developed for examining high-energy astrophysical phenomena, such as supernovas [188] and galactic nuclei [189], and has also more

recently found application in the study of potential burning plasmas in the laboratory [190–192]. The use of the free Hamiltonian to define the equilibrium photon field implies two differences, or approximations, compared to the equilibrium QED field: first, there are no real fermions present (the sum over α in equations 2.32 is restricted to states with no fermions); second, the photon states are free, and only interact in order to create fermions. The first approximation means that the pair-creation rates calculated are only likely to hold good if the photon and fermion fields start far from equilibrium, and will only hold good for the early stages of equilibration. The second approximation is more difficult. At least in the case of Breit-Wheeler, it is a coherent first-order perturbative approximation, and since we can expect Breit-Wheeler to largely be mediated by hard photons we have some reason to think this is meaningful. (Though this is discussed at the end of chapter 4.) In the case of the Schwinger mechanism there is less clear justification for it, beyond the fact that the theoretical tools to go beyond this assumption have not been developed. This issue is discussed in chapter 8.

Chapter 3

Free Electron Relativistic Correction Factors to Collisional Excitation and Ionisation Rates in a Plasma

When calculating rates of collisional excitation and ionisation the free electrons in a plasma are usually taken to follow the Maxwell-Boltzmann distribution [193]. This means that they are treated classically, and hence is valid as an approximation when both quantum mechanical and relativistic effects are insignificant. The quantum mechanical degenerate limit has been well studied and correction factors to excitation and ionisation rates accounting for quantum effects have been calculated in some detail [194, 195]. The relativistic limit has been comparatively neglected. There are, though, good reasons to pay attention to it: in the context of laboratory plasmas Tabak [196] predicts that burning D plasmas in ICF could reach bulk reduced temperatures of up to $\theta = 0.31$ ($\theta = k_B T/(m_e c^2)$), and Xenon and Krypton dopants (which should remain only partially ionised up to such temperatures) are regularly included in ICF as diagnostics [197, 198] . In the astrophysical context, the intracluster medium can reach temperatures above $\theta = 0.04$ [199]. Depending, of course, on the accuracy needed, relativistic corrections could be significant in both cases.

The main correction to be made when accounting for relativistic effects is to replace the Maxwell-Boltzmann distribution,

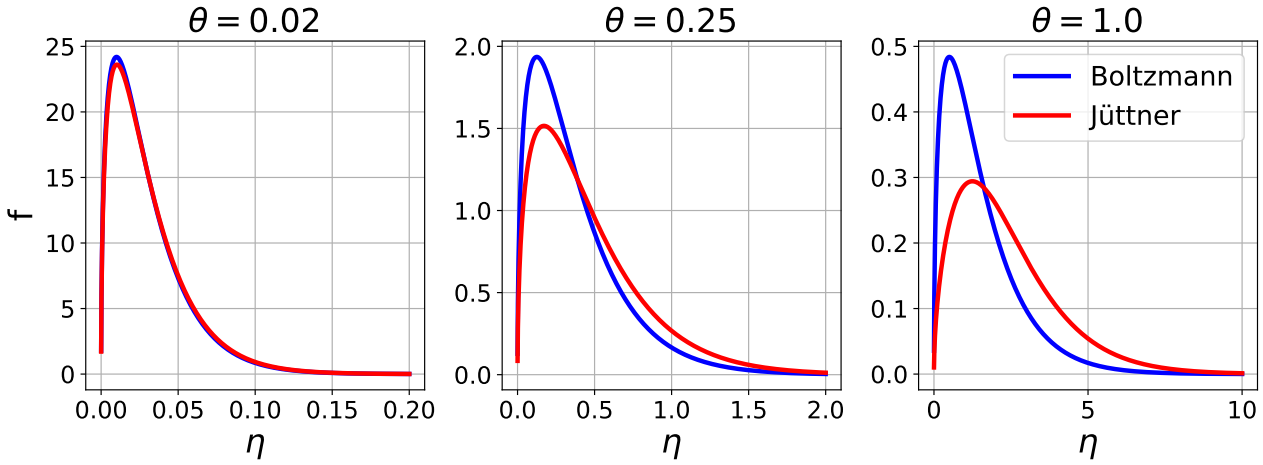

Figure 3.1: Maxwell-Boltzmann and Maxwell-Jüttner distributions plotted against reduced kinetic energy for a range of temperatures. Classically, energy is everywhere quadratic in momentum, while relativistically it becomes linear at high momentum. Therefore the density of energy states in phase space is classically suppressed at high momentum while relativistically it approaches a constant, so the normalised classical distribution is, compared to the relativistic, skewed towards low energies.

$$f_{\mathrm{MB}}(\eta,\theta) = 2\sqrt{\frac{\eta}{\pi}}\theta^{-\frac{3}{2}}e^{-\frac{\eta}{\theta}}, \tag{3.1}$$

(written here in terms of $\eta = E_K/(m_e c^2)$, the reduced electron kinetic energy) with the Maxwell-Jüttner [200] distribution,

$$f_{\mathrm{MJ}}(\gamma,\theta) \equiv \frac{\gamma^2 v}{c\theta K_2(1/\theta)}e^{-\frac{\gamma}{\theta}} \tag{3.2}$$

where $\gamma = 1/\sqrt{1-(v/c)^2} = \eta + 1$ and K_2 is the modified Bessel function of the second kind. The two are plotted in figure 3.1 for several temperatures. The Maxwell-Boltzmann distribution is recovered from the Maxwell-Jüttner in the expected classical limits $\theta \to 0$ and $\gamma \to 1$. Previous authors [201–203] have used these distributions to find a simple generic "relativistic correction factor" to excitation and ionisation rates based on the ratio of free electron partition functions (see Sect. 2, equation 3.11). In this chapter we develop more sophisticated correction factors by considering simple cross-sections for excitation and ionisation due, respectively, to Van Regemorter [204] and Lotz [205]. We also use detailed balance to extend these results to de-excitation and three-body recombination rates.

3.1 Calculation of Rates

3.1.1 Method

A collisional rate per electron per ion can be written in the form, keeping the cross section and energy distribution general,

$$r(\eta_T, \theta) = \int_{\eta_T}^{\infty} \sigma(\eta/\eta_T) f(\eta, \theta) v(\eta) d\eta. \tag{3.3}$$

where $v(\eta)$ is the velocity, $f(\eta, \theta)$ is the probability of finding a given electron at energy η, η_T is the threshold energy for the transition and $\sigma(\eta/\eta_T)$ is the cross section of the ions for the relevant collision reaction with the free electrons, which we are treating as a function of η/η_T (as is the case for most simple empirical or semi-empirical formulas for the ionisation or excitation cross-sections). It has the property $\sigma(x < 1) = 0$.

The rate of collision per free electron for the two cases is then

$$r_{\mathrm{MB}}(\eta_T, \theta) = \int_{\eta_T}^{\infty} \sigma(\eta/\eta_T) v_c(\eta) f_{\mathrm{MB}}(\eta, \theta) d\eta, \tag{3.4}$$

$$r_{\mathrm{MJ}}(\eta_T, \theta) = \int_{\eta_T}^{\infty} \sigma(\eta/\eta_T) v_r(\eta) f_{\mathrm{MJ}}(\eta, \theta) d\eta, \tag{3.5}$$

where we are using the r and c subscript on the velocity to denote, respectively, the relativistic and classical expressions for velocity in terms of kinetic energy. The quantity we want to calculate is the correction factor due to relativity,

$$R(\eta_T, \theta) \equiv \frac{r_{\mathrm{MJ}}(\eta_T, \theta)}{r_{\mathrm{MB}}(\eta_T, \theta)}. \tag{3.6}$$

For the relativistic case

$$f_{\mathrm{MJ}}(\eta, \theta) v_r(\eta) = \frac{2ce^{-\frac{1}{\theta}}}{\theta K_2(\frac{1}{\theta})} (\eta + \frac{1}{2}\eta^2) e^{-\frac{\eta}{\theta}}. \tag{3.7}$$

where $\gamma = 1/\sqrt{1 - (v/c)^2} = \eta + 1$. For the classical case

$$f_{\mathrm{MB}}(\eta,\theta)v_c(\eta) = 2c\sqrt{\frac{2}{\pi}}\theta^{-\frac{3}{2}}\eta e^{-\frac{\eta}{\theta}}. \tag{3.8}$$

Therefore the correction factor (3.6) can be written

$$R(\eta_T,\theta) = \Theta(\theta)\cdot\left[1+\frac{\theta}{2}P[\sigma;\frac{\eta_T}{\theta}]\right] \tag{3.9}$$

where we have defined the functional, using the substitution $z = \eta/\theta$,

$$P[\sigma;\frac{\eta_T}{\theta}] \equiv \frac{\int_{\eta_T/\theta}^{\infty} z^2\sigma(z\frac{\theta}{\eta_T})e^{-z}dz}{\int_{\eta_T/\theta}^{\infty} z\sigma(z\frac{\theta}{\eta_T})e^{-z}dz} \tag{3.10}$$

and the temperature-dependent prefactor is given by

$$\Theta(\theta) \equiv \sqrt{\frac{\pi}{2}}\left[\frac{\sqrt{\theta}e^{-\frac{1}{\theta}}}{K_2(\frac{1}{\theta})}\right] = \frac{Z_{\mathrm{MB}}(\theta)}{Z_{\mathrm{MJ}}(\theta)} \tag{3.11}$$

where $Z_{MB/MJ}$ is the partition function for a single free particle in the classical/relativistic case, defined as

$$Z_{MB/MJ}(\theta) = V\int_{\mathbb{R}^3}\exp(-\eta_{c/r}(\mathbf{p})/\theta)d^3\mathbf{p}, \tag{3.12}$$

with V the volume and c/r subscripts denoting classical/relativistic expressions for energy in terms of momentum. Note that Θ has been identified by previous authors [201–203] as a "relativistic correction factor" and has an asymptotic expansion [206]

$$\Theta(\theta)^{-1} \sim 1+\frac{15}{8}\theta+\frac{105}{128}\theta^2+\mathcal{O}(\theta^3), \quad \theta\to 0. \tag{3.13}$$

which, as can be seen in figure 3.2, is a good enough approximation for our uses. This correction factor is of far more general use: it is derived from the normalisation factors of the distributions, so will arise from the ratio of the expectation values of any quantity taken over the Maxwell-Jüttner distribution divided by that quantity averaged over the Maxwell-Boltzmann distribution.

Note also, from $\int_b^\infty z^n g(z)dz \geq b\int_b^\infty z^{n-1}g(z)dz$, where $g(z)$ is any everywhere positive function on $z\geq 0$, we get $P \geq \frac{\eta_T}{\theta}$. Therefore we have

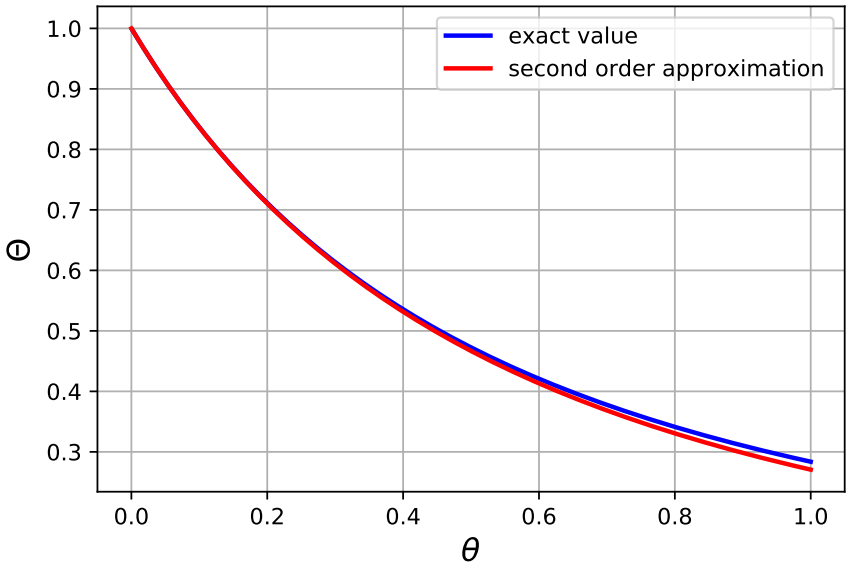

Figure 3.2: General temperature-dependent prefactor to relativistic correction factor of collisional rates. Both the exact value and second-order approximate value are plotted, showing very little difference between the two.

$$R(\theta, \eta_T) \geq \Theta(\theta) \cdot \left[1 + \frac{\eta_T}{2}\right] \tag{3.14}$$

for any cross section and all values of θ and η_T.

3.1.2 Excitation Rate

Our aim is to derive approximate generic correction factors, dependent on ion species only through the single parameter of threshold energy. We must therefore use a cross section which is a function of only η_T and η. For the excitation rate we use the Van Regemorter [204] cross section which for our purposes, if we set the gaunt factor equal in both cases, amounts to

$$\sigma_{VR} \propto 1/\eta. \tag{3.15}$$

Note that we use the classical expression for its energy dependence as the formula was calculated using non-relativistic quantum mechanics. Attempting to adjust the energy dependence of this expression to account for relativity would anyway only give higher-order errors which, given the broad approximations already inherent in using such simple cross sections,

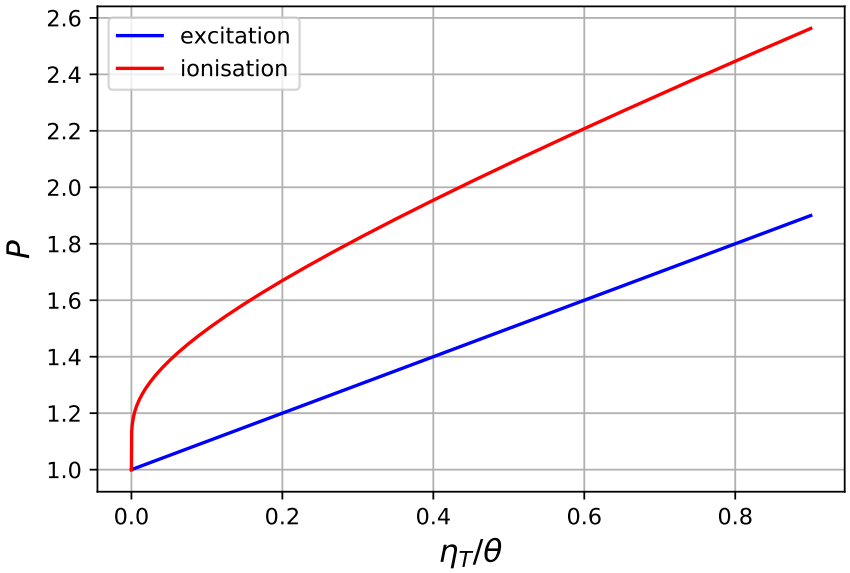

Figure 3.3: $P[\sigma]$ for excitation and ionisation using, respectively, Van Regemorter's and Lotz' simple expressions for the cross section.

can be neglected. Including this in equation 3.10 gives

$$P[\sigma_{VR}] = 1 + \frac{\eta_T}{\theta}. \tag{3.16}$$

This is plotted in figure 3.3.

3.1.3 Ionization Rate

For the ionisation rate we use an empirical formula due to Lotz [205],

$$\sigma_L(x) \propto \frac{\ln(x)}{x}. \tag{3.17}$$

This gives

$$P[\sigma_L] = \frac{e^{-\frac{\eta_T}{\theta}} + E_1(\frac{\eta_T}{\theta})}{E_1(\frac{\eta_T}{\theta})} = 1 + \frac{e^{-\frac{\eta_T}{\theta}}}{E_1(\frac{\eta_T}{\theta})} \tag{3.18}$$

where $E_1(x) = \int_x^\infty \frac{e^{-t}}{t} dt$ is the exponential integral. This is plotted in figure 3.3.

3.2 De-excitation and Recombination Rate Corrections

De-excitation and recombination rates can be calculated from excitation and ionisation using two requirements of equilibrium. The first is the principle of detailed balance, which enforces the requirement that an equilibrium state is constant in time. This gives the reverse rate as proportional to the forwards rate with a ratio that depends on the reactant number densities. The second is that the electrons be distributed between free and bound states in the proportion that maximises total entropy, which is equivalent (under constant temperature and volume) to the minimisation of the Helmholtz free energy, which is in turn equivalent to the maximisation of the total canonical partition function. This affects the reverse rate by determining the reactant number densities. Changing the free electron physics by accounting for relativistic effects changes the free electron partition function, and therefore changes the relative entropy of states that have different free electron number, and therefore changes which distribution of the fixed total electron number between the free and bound states maximises the entropy.

This does not apply to excitation processes because the free electron number doesn't change. This means that relativistic corrections to the de-excitation rate enter only through its proportionality to excitation, and therefore excitation and de-excitation are corrected by the same factor. Ionisation and recombination do change free electron number, so for recombination rates a further correction from adjustments to the free electron entropy is needed. The entropy-maximisation requirement for relative occupation of different ionisation states can be expressed by the general Saha equation [207, 208]

$$\frac{n_{i+1}n_e}{n_i} = 2Z(\theta)\frac{g_{i+1}}{g_i}\exp\left(-\frac{\eta_{i+1}-\eta_i}{\theta}\right), \tag{3.19}$$

where n_i, g_i and η_i are, respectively, the density, degeneracy and reduced energy of ions in the i'th ionisation state and n_e is the electron density, and Z is the appropriate free particle partition function. Using this with detailed balance ($n_{i+1}t = n_i r$ with t the recombination rate and r the ionisation), the ratio of recombination rates in the relativistic to classical cases is given

$$\frac{t_{\mathrm{MJ}}}{t_{\mathrm{MB}}} = \frac{n_e^{MJ}}{n_e^{MB}} \cdot \frac{Z_{\mathrm{MB}}(\theta)}{Z_{\mathrm{MJ}}(\theta)} \cdot \frac{r_{\mathrm{MJ}}}{r_{\mathrm{MB}}} = \Theta(\theta)^2 \cdot \left[1 + \frac{\theta}{2} P[\sigma; \frac{\eta_T}{\theta}]\right]. \tag{3.20}$$

3.3 Conclusion

In this section we have calculated approximate correction factors for ionisation and excitation rates due to collision with free electrons in a plasma to account for special relativity. We have done this by assuming the Van Regemorter expression for the excitation, $\sigma_{VG}(x) \propto 1/x$, and the Lotz expression for the ionisation cross section, $\sigma_L(x) \propto \ln(x)/x$. We then used the Saha equation to extend these results to recombination rates. These correction factors are given, in summary,

$$R(\theta, \eta_T) = \begin{cases} \sqrt{\frac{\pi}{2}} \left[\frac{\sqrt{\theta} e^{-\frac{1}{\theta}}}{K_2(\frac{1}{\theta})}\right] \cdot \left[1 + \frac{\theta}{2}\left(1 + \frac{e^{-\frac{\eta_T}{\theta}}}{E_1(\frac{\eta_T}{\theta})}\right)\right] & \text{ionisation} \\ \frac{\pi}{2} \left[\frac{\sqrt{\theta} e^{-\frac{1}{\theta}}}{K_2(\frac{1}{\theta})}\right]^2 \cdot \left[1 + \frac{\theta}{2}\left(1 + \frac{e^{-\frac{\eta_T}{\theta}}}{E_1(\frac{\eta_T}{\theta})}\right)\right] & \text{recombination} \\ \sqrt{\frac{\pi}{2}} \left[\frac{\sqrt{\theta} e^{-\frac{1}{\theta}}}{K_2(\frac{1}{\theta})}\right] \cdot \left[1 + \frac{1}{2}\left(\theta + \eta_T\right)\right] & \text{excitation or de-excitation} \end{cases}. \tag{3.21}$$

These are plotted in figure 3.4 for some reasonable values of the threshold energy and temperature. Also plotted is the temperature-dependent prefactor $\Theta(\theta)$ given in equation 3.11, which has been identified by previous authors [201–203] as the "relativistic correction factor". It can be seen that our correction factors differ significantly from both this and unity. We also, in section 2.1, found a lower bound for the relativistic correction factor with complete applicability to any cross section.

Though the precise value of our correction is necessarily limited by the simple forms of the cross sections we have used, there is no reason to expect that the true ratio will be substantially closer to unity. Where we find a ratio far from unity, as seen in figure 3.4, it is safe to conclude that accounting for special relativity in the free electron mechanics is important.

The origin of the difference between our result and that of previous authors can be

appreciated through our demonstration that their correction factor, Θ, is equal to the ratio of partition functions. It is shown in Appendix B that if the move from Maxwell-Boltzmann to Maxwell-Jüttner involved only a change in Boltzmann factors of states that did not participate in the collisional process, then the inverse ratio of their partition functions would equal the desired ratio of their collisional rates. This explains both where Θ succeeds and fails as an approximation to the correction factor. For Θ to be both a successful and non-trivial approximation, a significant number of electrons in the distribution must be relativistic while the dominant contribution to the collision process comes from non-relativistic electrons. In our models, this is broadly the case when $\eta_T \ll \theta$. Θ utterly fails when η_T much surpasses θ, when the high-energy tail of the distribution dominates the collision process. Both this relative success and failure can be seen in figure 3.4. Note that this means that our work will be especially important as an improvement on previous authors' in the context of high-Z diagnostic dopants in plasmas, where it is desirable to monitor spectral emission energies greater than the thermal energy.

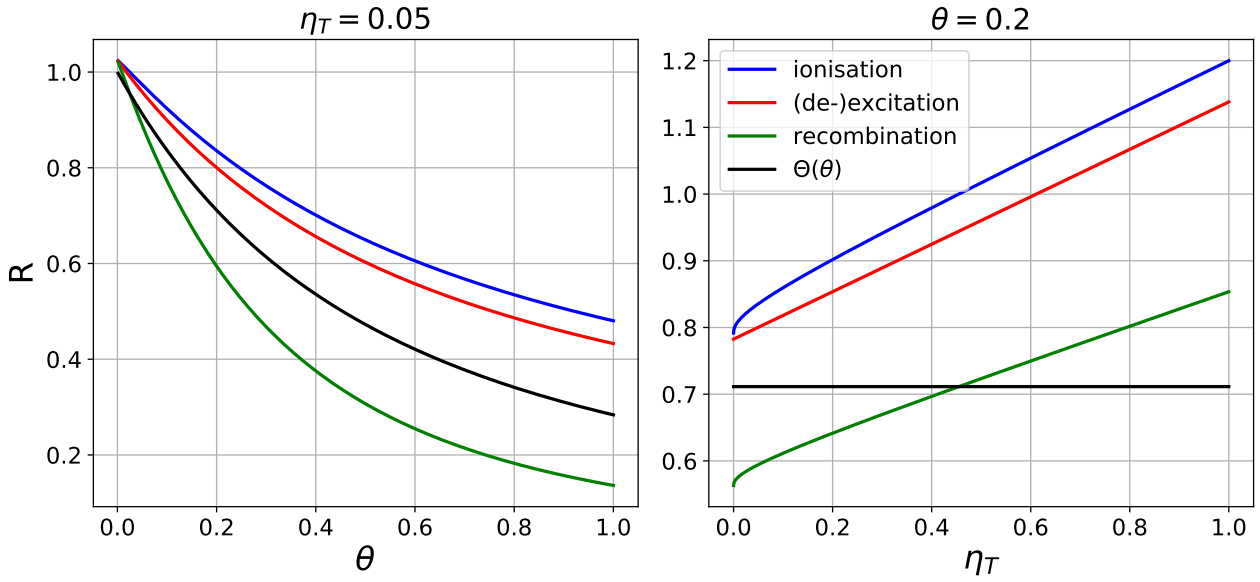

Figure 3.4: Approximations of the ratio of collisional ionisation, recombination and excitation rates when special relativity is accounted for against when it isn't, plotted with sensible values of the reduced threshold energy and reduced temperature. Ionisation and recombination rates are calculated using the Lotz cross section, excitation using Van Regemorter. The temperature-dependent prefactor Θ is also plotted independently.The values plotted are in regimes relevant to dopants in burning ICF plasmas: $\eta_T = 0.05$ is close to the first few ionisation energies of Krypton and Xenon [209], and $\theta = 0.2$ is in the range of burning plasma temperatures considered by Tabak [196].

Chapter 4

Breit-Wheeler Pair Production in a Black-Body Field at High Temperatures

4.1 Closed-Form Expression for the High-Temperature Limit

With sufficient energy, collisional processes don't need bound electrons available to set free from their bound states: electron-positron pairs can be created from the vacuum. One such process is by Breit-Wheeler, or the two photon $\rightarrow$ electron/positron pair scattering process. Weaver [5] expressed the rate of pair production by the Breit-Wheeler process in a Black-Body field as a sum of single integrals over special functions in 1976, which reduced to a simple expression in the low-temperature limit $k_B T \ll m_e c^2$, where T is the photon temperature and m_e is the electron rest mass. Weaver [5] gives the rate of two-photon interaction for a black-body radiation field as

$$
\begin{aligned}
n_{\mathrm{bb,BW}} &= \frac{c}{\pi^4\hbar^6}\int_0^\infty dp^* \int_0^\infty dp_1 \int_{(p^*)^2/p_1}^\infty dp_2 \; \frac{2(p^*)^3\sigma(p^*)}{(e^{cp_2/(k_BT)}-1)(e^{cp_1/(k_BT)}-1)} \\
&= \frac{4c}{\pi^4}\left(\frac{k_BT}{c\hbar}\right)^6 \sum_{n,l=1}^{\infty}\frac{1}{\sqrt{nl}}\int_0^\infty d\upsilon_\gamma \; \sigma\upsilon_\gamma^4 K_1(2\sqrt{nl}\upsilon_\gamma),
\end{aligned}
\tag{4.1}
$$

where $p_{1,2}$ are the lab-frame momenta of the photons, p^* is the centre-of-momentum momentum of either, K_n is the modified Bessel function of the second kind and

$$
\upsilon_\gamma = p^*c/(k_BT), \tag{4.2}
$$

The expression originates from an integration over two black-body photon distributions in momentum space, essentially by a two-particle version of equation 3.3. The sum over n, l corresponds to a sum over the photon occupation numbers of each mode. Jauch & Rohlich [210] give the Breit-Wheeler cross-section as

$$
\sigma(\phi) := \begin{cases} \pi r_e^2\phi^2\big[(2+2\phi^2-\phi^4)\cosh^{-1}(\phi^{-1}) \\ \qquad -(1+\phi^2)(1-\phi^2)^{1/2}\big], \qquad \phi<1\,, \\ 0, \qquad \phi\geq 1. \end{cases} \tag{4.3}
$$

$$
\phi := \frac{m_ec}{p_\gamma^*} = (\theta\upsilon_\gamma)^{-1}, \quad \theta := \frac{k_BT}{m_ec^2}. \tag{4.4}
$$

This chapter does not replace Weaver's expression, since it is already sufficiently general, but merely derives its high-temperature limit. This is worthwhile as it is only in the limits that the integral expression reduces to a closed-form expression. This has application in early-universe cosmology [211], where it could be used to study the equilibration of the fermion and photon fields. A simple expression could be especially useful where the pair-creation rate is used as a term in a differential equation to be solved, for instance as a source term in a Boltzmann transport equation [212]. Define

$$\sigma_0(\phi) := \pi r_e^2 \phi^2 \left[2\log(2\phi^{-1}) - 1\right] \tag{4.5}$$

$$\sigma_1 := \sigma - \sigma_0. \tag{4.6}$$

$\sigma \sim \sigma_0$ in the high-energy limit, and we will show that σ_0 acts as the effective cross-section in the high-temperature limit. σ_1 obeys

$$\sigma_1(\phi) = \mathcal{O}(\phi^4 \log(\phi)), \quad \phi \to 0^+. \tag{4.7}$$

We can write the dimensionless integral we need to approximate as

$$I := r_e^{-2} \int_{1/\theta}^{\infty} d\upsilon_\gamma \, \sigma \upsilon_\gamma^4 K_1(2\rho\upsilon_\gamma), \tag{4.8}$$

where $\rho := \sqrt{nl}$. Divide I into two parts,

$$I = I_0 + I_1 \tag{4.9}$$

$$I_{0,1} := r_e^{-2} \int_{1/\theta}^{\infty} d\upsilon_\gamma \, \sigma_{0,1}(\theta^{-1}\upsilon_\gamma^{-1}) \upsilon_\gamma^4 K_1(2\rho\upsilon_\gamma) \tag{4.10}$$

We have, first,

$$\begin{aligned} I_0 =& \frac{\pi}{\theta^2} \int_{1/\theta}^{\infty} d\upsilon_\gamma \, [2\log(2\theta\upsilon_\gamma) - 1] \upsilon_\gamma^2 K_1(2\rho\upsilon_\gamma) \\ =& \frac{\pi}{(2\rho)^3\theta^2} \Bigg[(-2\log\left(\rho\theta^{-1}\right) - 1) \int_{1/\theta}^{\infty} dy \, y^2 K_1(y) \\ &+ 2 \int_{1/\theta}^{\infty} dy \, \log(y) y^2 K_1(y) \Bigg], \end{aligned} \tag{4.11a}$$

where we have used the substitution $y = 2\rho\upsilon_\gamma$. Using

$$\int_{1/\theta}^{\infty} dy \, y^2 K_1(y) = 2 + \mathcal{O}(\theta^{-2}\log(\theta)) \tag{4.12a}$$

$$\int_{1/\theta}^{\infty} dy\; y^2 \log(y) K_1(y) = 1 - 2\gamma_{\mathrm{E}} + 2\log(2) + \mathcal{O}(\theta^{-2}\log(\theta)), \tag{4.12b}$$

where γ_{E} is the Euler–Mascheroni constant, this becomes

$$I_0 = \frac{\pi}{2\rho^3\theta^2}\left(\log(\theta) + \log(\frac{2}{\rho}) - \gamma_{\mathrm{E}}\right) + \mathcal{O}(\theta^{-4}\log(\theta)) \tag{4.13}$$

Next,

$$\begin{aligned} |I_1| &\leq r_e^{-2}\int_{1/\theta}^{\infty} d\upsilon_\gamma \left|\sigma_1(\theta^{-1}\upsilon_\gamma^{-1})\upsilon_\gamma^4 K_1(2\rho\upsilon_\gamma)\right| \\ &\leq \frac{1}{r_e^2(2\rho)^2\theta^3}\mathrm{Max}_{\phi\in(0,1)}\left(|\sigma_1(\phi)\phi^{-3}|\right)\int_0^{\infty} dy\; yK_1(y) \\ &= \frac{1}{r_e^2(2\rho)^2\theta^3}\mathrm{Max}_{\phi\in(0,1)}\left(|\sigma_1(\phi)\phi^{-3}|\right)\frac{\pi}{2} = \mathcal{O}(\theta^{-3}), \end{aligned} \tag{4.14}$$

where we know $\mathrm{Max}_{\phi\in(0,1)}\left(|\sigma_1(\phi)\phi^{-3}|\right)$ is finite from equation 4.7. Therefore $I = I_0 + \mathcal{O}(\theta^{-3})$ and hence

$$\begin{aligned} n_{\mathrm{bb,BW}} = \sum_{n,l=1}^{\infty} \frac{1}{(nl)^2}\frac{2r_e^2 c}{\pi^3}\left(\frac{m_e c}{\hbar}\right)^2\left(\frac{k_B T}{\hbar c}\right)^4 \Bigg[\log\left(\frac{k_B T}{m_e c^2}\right) \\ + \log\left(\frac{2}{\sqrt{nl}}\right) - \gamma_{\mathrm{E}} + \mathcal{O}\left(\frac{m_e c^2}{k_B T}\right)\Bigg] \end{aligned} \tag{4.15}$$

Using

$$\sum_{n,l=1}^{\infty}\frac{1}{(nl)^2} = \frac{\pi^4}{36}, \tag{4.16a}$$

$$\sum_{n,l=1}^{\infty}\frac{\ln(nl)}{(nl)^2} = -\frac{\pi^4}{18}\left(-12\log(A_{\mathrm{G}}) + \gamma_{\mathrm{E}} + \log(2\pi)\right) \tag{4.16b}$$

and defining

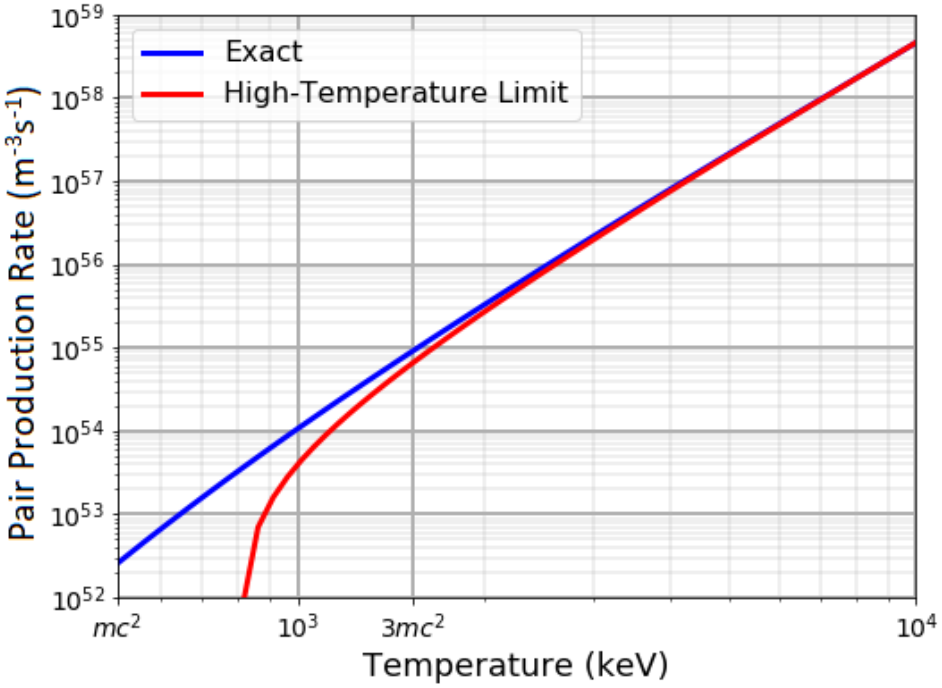

Figure 4.1: Approximation of thermal Breit-Wheeler pair creation rate plotting against numerical calculation, with n, l in equation 4.1 summed from 1 to 20, at which there is numerical convergence to precision visible on the graph. The approximation is seen to rapidly approach the exact result from below for $k_B T > 3 m_e c^2$.

$$\chi := \log(4\pi) - 12\log(A_{\mathrm{G}}) \approx -0.45403, \tag{4.17}$$

where A_{G} is the Glaisher-Kinkelin constant, this can be written

$$n_{\mathrm{bb,BW}} = \frac{\pi \alpha^2 c}{18} \left(\frac{k_B T}{\hbar c}\right)^4 \left[\log\left(\frac{k_B T}{m_e c^2}\right) + \chi + \mathcal{O}\left(\frac{m_e c^2}{k_B T}\right)\right]. \tag{4.18}$$

This approximation is plotted against a numerical calculation of the exact rate (4.1) in Figure 4.1, where it can be seen to be good for $k_B T > 3 m_e c^2$. Assuming a constant rate of pair production, no backwards rate, and free-field equilibrium density [211], this predicts equilibration of the fermion field in $\sim 2 \times 10^4\, \hbar/(k_B T[\log(m_e c^2/(k_B T)) + \chi])$. Since $k_B T/\hbar$ is the frequency scale of most particle reactants, this predicts equilibration over long timescales

compared to the quantum processes.

Quantities of a similar form have been found by other authors for similar quantities in high-temperature limits: the reverse process, i.e. the rate of pair annihilation in electrons and positrons in Maxwell-Jüttner distributions [213–215]; the rate of positron production in a plasma from electron and ion collisions [215]; the mean path of a high-energy non-thermal photon in a thermal bath [216]; and various quantities in an optically-thin relativistic plasma of finite size [217].

4.2 Discussion and Energy Spectrum

The logarithmic term might be surprising. The naïve expectation, on dimensional grounds, is that the thermally averaged cross-section for a two-particle collision at $k_B T \gg m_e c^2$ obeys $\langle \sigma \rangle \propto T^{-2}$ [211], which would give $n_{\mathrm{bb,BW}} \propto T^4$. This is based on the logic that, at temperature scales where the mass becomes irrelevant, temperature is the only appropriate energy-scale that can be chosen. But instead, as $m_e \to 0^+$, the rate diverges logarithmically. The high-energy process remains irrevocably coupled to the low-energy regime. To understand why, consider that the logarithmic divergence is inherited directly from the two-photon cross section, where it appears as a divergence in the virtual fermion propagator [210]. Specifically, the divergence is due to the possibility of Breit-Wheeler being mediated by the exchange of a real fermion of vanishing energy and momentum. The physics behind this is intuitive: in the zero-mass limit, a photon transforming into an electron of the same energy and momentum does not violate energy or momentum conservation. Therefore Breit-Wheeler needs involve only the exchange of a virtual fermion of vanishing energy and momentum. But in the zero-mass limit, this virtual fermion will be on the mass shell. Processes being mediated by real particles correspond to physical processes that can occur between widely-separated particles. We therefore have a clear physical picture for how the mass-scale remains relevant at high temperatures: photons in the thermal gas can interact to create electron-positron pairs which are separated by the length-scale of the inverse of the electron mass. This is in contrast to the "hard thermal loop" (HTL) paradigm [47, 176], where the dominant contribution to thermal quantities comes from the exchange of excitations with "hard" momenta $p \sim k_B T/c$. This is because we are dealing

with hard *external* momenta, while HTL assumes external momenta are soft, and because our virtual fermion propagator is not a thermal propagator, since we are formally examining a situation in which there is not a thermal fermion background

This absence of a fermion background is a major approximation made by equation 4.18 as a calculation of the physical pair production rate. If we are concerned with the equilibration of the fermion field with a rapidly heated photon field, then it will only hold good for a finite period of time. The other major approximation is that it is a lowest-order perturbative process. This could be problematic because we know that in a thermal context at high temperatures the perturbation expansion might not produce adequate results [47]. This is because at high temperatures, for soft momenta, the effective coupling constant scales with the temperature, which for temperatures much greater than $m_e c^2/k_B$ spoils the convergence of the perturbation expansion [218]. This problem is exacerbated by the fact that next-order corrections include a very large number of Feynman diagram contributions. To calculate probabilities to $\mathcal{O}(\alpha^3)$ (the next-leading-order after Breit-Wheeler) we must include Feynman diagrams with two, three and four interaction vertices, since amplitudes with two and four interaction vertices multiply when calculating a probability. Although at three interactions the only extra graphs considered are additional external photons, at four interactions a host of one-loop corrections are introduced: self-energy corrections on all propagators, vertex corrections and a one-particle-irreducible four-point vertex. (Examples are depicted in figure 4.2.) In general, in the theory of linear excitations about thermal equilibrium, we expect the perturbative expansion to only produce reasonable approximations in the regime of hard external momenta.

To determine whether Breit-Wheeler in a black-body field is a process largely involving hard momenta, we calculate two energy spectra associated with the production process. Defining the temperature-normalised lab-frame photon energies,

$$\upsilon_{a,b} = p_{a,b} c/(k_B T). \tag{4.19}$$

we can write Weaver's integral 4.1 (first line) as

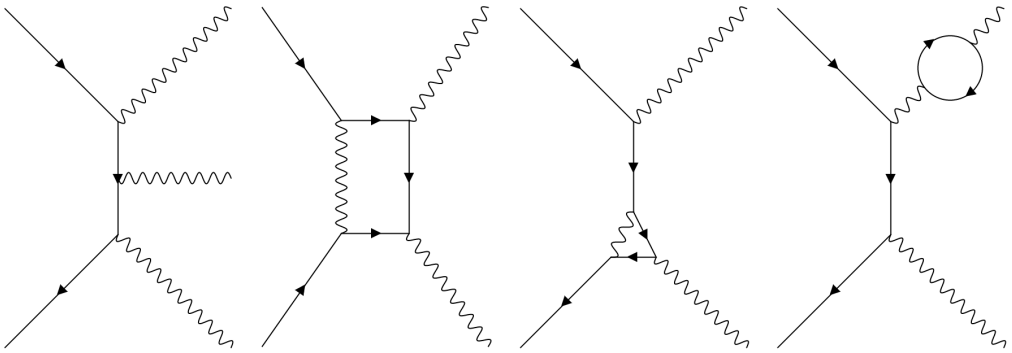

Figure 4.2: Examples of Feynman diagrams that contribute to Breit-Wheeler at next-to-leading-order. Specifically, from left to right, these are examples of an extra external photon, a one-particle-irreducible four-point vertex, a three-point vertex correction and a self-energy insertion.

$$\begin{aligned} n_{\mathrm{bb,BW}} &= \frac{2c}{\pi^4}\left(\frac{k_B T}{c\hbar}\right)^6 \int_0^\infty d\upsilon_\gamma \int_0^\infty d\upsilon_a \int_{\upsilon_\gamma^2/\upsilon_a}^\infty d\upsilon_b \, \frac{\upsilon_\gamma^3 \sigma(p^*)}{(e^{\upsilon_a}-1)(e^{\upsilon_b}-1)} \\ &= \frac{2c}{\pi^4}\left(\frac{k_B T}{c\hbar}\right)^6 \int_0^\infty d\upsilon_a \, F_1(\upsilon_a) \end{aligned} \tag{4.20}$$

where

$$F_1(\upsilon_a) := \int_0^\infty d\upsilon_\gamma \, \frac{\upsilon_\gamma^3 \sigma(p^*)}{e^{\upsilon_a}-1}\left(\frac{\upsilon_\gamma^2}{\upsilon_a} - \log\left[e^{\frac{\upsilon_\gamma^2}{\upsilon_a}}-1\right]\right). \tag{4.21}$$

This function is proportional to the contribution to the total particle production rate from collisions where the "first" photon has a particular energy. In the high-temperature limit, this will be equal to the energy distribution of produced electrons or positrons. It is plotted in figure 4.3, normalised for unit area under the curve. Alternatively, we could define the temperature-normalised total pair-energy,

$$\upsilon_T = \upsilon_a + \upsilon_b \tag{4.22}$$

we can write

$$n_{\mathrm{bb,BW}} = \frac{2c}{\pi^4}\left(\frac{k_B T}{c\hbar}\right)^6 \int_0^\infty d\upsilon_T \, F_2(\upsilon_T) \tag{4.23}$$

where

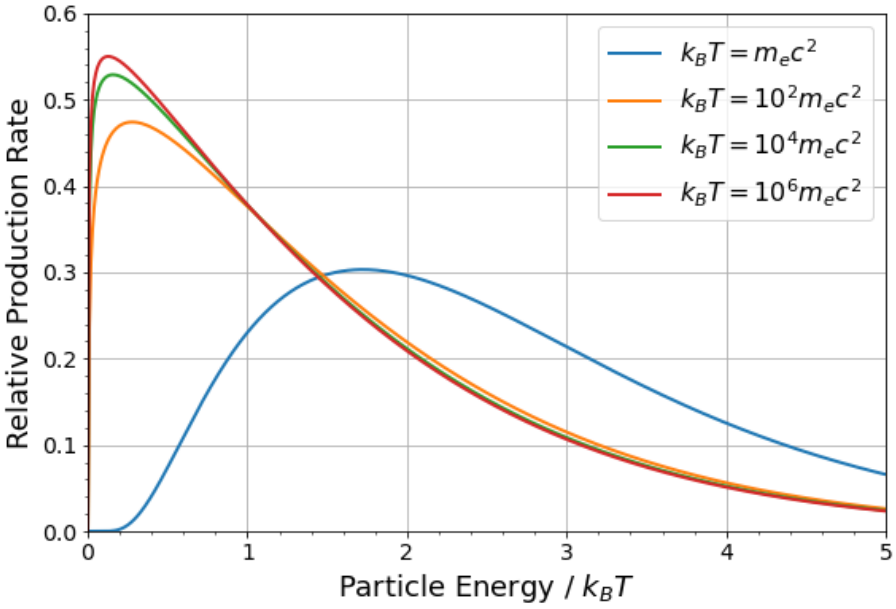

Figure 4.3: Contribution to total pair-production by Breit-Wheeler in a black-body made by photons of a given energy, normalised to unit area under the line. In the $k_BT \gg m_ec^2$ limit this is equal to the proportion of electrons or positrons produced at the given energy.

$$F_2(\upsilon_T) := \int_0^{\upsilon_T/2} d\upsilon_\gamma \, \frac{\upsilon_\gamma^3 \sigma(p^*)}{e^{\upsilon_T} - 1} \log\left(\frac{(1-e^{\upsilon_+})(e^{\upsilon_-} - e^{\upsilon_T})}{(1-e^{\upsilon_-})(e^{\upsilon_+} - e^{\upsilon_T})}\right), \qquad \upsilon_\pm := \tfrac{1}{2}(\upsilon_T \pm \sqrt{\upsilon_T^2 - 4\upsilon_\gamma^2}). \tag{4.24}$$

This function is proportional to the total energy of produced pairs. It is plotted in figure 4.4, normalised to unit area under the curve. Note that the significant difference in the shape of the two curves - beyond the scaling of the x-axis by a factor 2 - is due to the fact that a large number of reactions are between photons with significantly different energies.

Looking at the figures, especially figure 4.3, we can conclude that the majority of particles involved in the process are "hard", since there is greater area under the red curve to the right of 1 than to the left. We therefore have some reason to think of it as a meaningful quantity. This is only, strictly, though, an argument that the process *defined* as two photon → electron/positron pair is well-approximated by first-order Breit-Wheeler. There are other particle-producing scattering processes, which involve more particles in the in-state and/or the out-state, which this argument does not preclude being larger than Breit-Wheeler, and which could involve soft momenta. The argument is therefore for self-consistency: there is nothing in

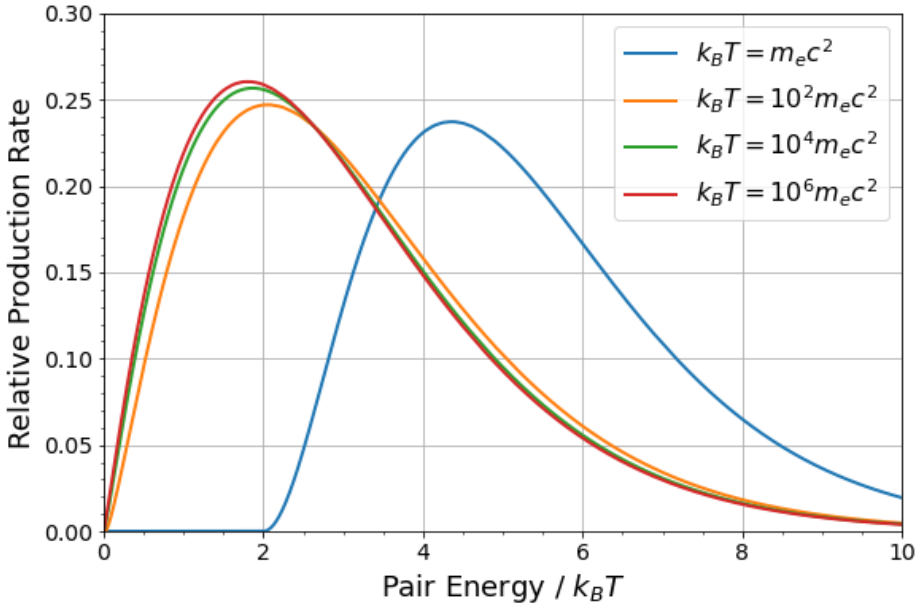

Figure 4.4: Proportion of pairs produced by Breit-Wheeler in a black-body with a given total energy, including kinetic and rest energy. Normalised to unit area under the curve.

the calculation *itself* that necessarily implies Breit-Wheeler is invalid as an approximation for the pair-creation rate. Other calculations could prove otherwise.

Even this moderate position is complicated, though, by the fact that we have just shown that the Breit-Wheeler is peculiarly coupled to the low-energy regime. To get a qualitative idea of the impact of the effects neglected, consider that one of the most important non-perturbative effects of a thermal background, that is introduced by a resummation procedure on the propagator, is to introduce a "thermal mass" to the constituent particles, $m_{\text{th}} := \mu k_B T/c^2$, where $\mu \sim \sqrt{\alpha}$ [47, 219, 220]. (Taking this to be the only thermal adjustment of the dispersion relations becomes a good approximation in the hard momentum regime.) Introducing this thermal mass as a correction to the fermion mass would induce us to replace equation 4.18 as $\mu k_B T \gg m_e c^2$ with

$$n_{\text{bb,BW}} = \frac{\pi \alpha^2 c}{18} \left(\frac{k_B T}{\hbar c}\right)^4 \left[-\log \mu + \chi + \mathcal{O}(\mu) + \mathcal{O}\left(\frac{m_e c^2}{\mu k_B T}\right) \right]. \tag{4.25}$$

It is therefore likely that under an appropriate resummation procedure the logarithmic

factor would approach a constant value as temperature increased past the point where the thermal mass of the electron exceeds its physical mass. Beyond this point the pair-production rate would simply grow with the fourth power of the temperature. As could be appreciated physically, it is the logarithm, which couples the process to the low-energy regime, which makes the thermal mass a leading-order effect. Corrections to external fermion propagators are subleading, as we would expect the corrections to the external photon propagators to be also. It is possible that the effects of a growing thermal fermion background in the process of equilibration could be included naturally in this formalism, by making the fermion thermal mass dependent on the background fermion density. Of course a much more substantial treatment would be needed both to rigorously justify this expression, since it is unclear whether the introduction of a thermal mass is really adequate to handle the interaction between the virtual fermion and the thermal background, and to use it, since the literature results for dispersion relations in a thermal background are restricted to the case of the fermion and photon field in equilibrium, where the notion of a particle creation rate has little meaning.

Chapter 5

The Schwinger Mechanism in a Black-Body Field

So far, both within this thesis and in the literature without, calculation of pair-creation by a black-body field has been restricted to first-order two-photon Breit-Wheeler [5]. The high-temperature limit of this rate was presented in the last chapter. There are three different categories of effects this neglects as an approximation: first, it neglects interactions with more than two input photons or more than one output pair; second, it is a lowest-order perturbative approximation for the two photon to electron/positron pair process; third, it assumes an entirely free field for the initial distribution. All these approximations can be seen as part of a first-order perturbative expansion of the total particle creation rate, with interactions in the definition of the equilibrium input state accounted for by imaginary time-evolution. An examination of Breit-Wheeler to higher loop order in the thermal QFT formalism is a task yet to be accomplished.

This chapter examines an alternative particle-creation mechanism: the Schwinger mechanism. As discussed in section 2.4, it is well established that "slowly-varying" applied fields produce particles according to Schwinger's expression at every point in space and time, i.e. as a "locally-constant field". This is called the "tunnelling regime". Multiple authors (most comprehensively in Ref [78, 79]) have found that the approach to this regime is governed by the dimensionless Keldysh parameters' (2.30) approach to 0.

It is straightforward to characterise the strength and frequency scale of the black-body field. It is clear from the energy density of the black-body field that the RMS electric field strength is

$$e\bar{E}_{bb} = \sqrt{\frac{4\pi^3\alpha}{15}}\frac{(k_B T)^2}{(\hbar c)}, \tag{5.1}$$

and from the peak frequency of the Planck spectrum, and the coherence properties of the black-body field [221–223], that the characteristic frequency scales of the black body field are

$$\hbar\omega_{c,\mathrm{bb}} = \beta_{\mathrm{c}} k_B T, \quad \hbar c k_{c,\mathrm{bb}} = \tilde{\beta}_{\mathrm{c}} k_B T, \tag{5.2}$$

where $\beta_{\mathrm{c}}, \tilde{\beta}_{\mathrm{c}}$ are a dimensionless constants of order of magnitude ~ 1. This gives

$$\gamma_{\mathrm{K,bb}} = \beta_{\mathrm{c}}\sqrt{\frac{15}{4\pi^3\alpha}}\frac{m_e c^2}{k_B T}, \quad \tilde{\gamma}_{\mathrm{K,bb}} = \tilde{\beta}_{\mathrm{c}}\sqrt{\frac{15}{4\pi^3\alpha}}\frac{m_e c^2}{k_B T}. \tag{5.3}$$

Therefore at temperatures $k_B T \gg m_e c^2$, both Keldysh parameters are very small. This argument suggests that the black-body field ought to be safely in the tunnelling regime, and hence ought to produce particles straightforwardly via the locally-constant Schwinger mechanism. This rate can be calculated from equations 5.1 and 2.28 as

$$n_{\mathrm{bb,LCS}} = \frac{\alpha c}{15}\left(\frac{k_B T}{\hbar c}\right)^4 \exp\left(-\sqrt{\frac{15}{4\pi\alpha}}\left[\frac{m_e c^2}{k_B T}\right]^2\right). \tag{5.4}$$

Taking the ratio of this with the $k_B T \gg m_e c^2$ limit of Breit-Wheeler pair production calculated in section 4, equation 4.18, gives

$$\frac{n_{\mathrm{bb,LCS}}}{n_{\mathrm{bb,BW}}} \sim \frac{6}{5\pi\alpha}\log\left(\frac{k_B T}{m_e c^2}\right) \approx 52\left(\log\left(\frac{k_B T}{m_e c^2}\right)\right)^{-1}, \quad k_B T \gg m_e c^2. \tag{5.5}$$

The rate of particle production calculated by the locally constant Schwinger mechanism would therefore far exceed the Breit-Wheeler rate well beyond the validity of QED.

However, the theoretical justifications for the Keldysh parameter result all use "semi-classical" approximation techniques, which are good when $E_0 \ll E_S, \hbar\omega_c \ll m_e c^2, \hbar k_c \ll m_e c$. This is the opposite regime to the black-body field as $k_B T \gg m_e c^2$. Examination of the "critical regime" $E_0 \sim E_S$ [224, 225], or numerical examination of a more general case [83], shows that other dimensionless parameters may also be important outside the semiclassical regime.

Therefore a more careful procedure is needed. There are two results given in this chapter. First, I present a method for calculating the pair-creation rate in a black-body field that treats the black-body as an ensemble of external fields. This is a formal result that is difficult to derive quantitative predictions from directly. The relationship between the particle production rate calculated by the normal perturbation expansion and by this formalism is equivalent to that between the calculation of particle production by perturbative expansion and the external-field formalism in a coherent field. As discussed in section 2.4, for oscillating fields in the weak-field regime, the Keldysh parameter was found to govern a transition between a fast-varying regime where the external field method gave a result entirely equivalent to the perturbative expansion, and a slow-varying nonperturbative regime where it represents an entirely different mechanism. In the general case, then, the external field can give both perturbative and nonperturbative contributions to pair-creation. It is therefore difficult, for a particular application, to say *a priori* what the relationship between the perturbation expansion and external-field calculation is precisely.

The second result is an estimate for the production rate from a statistical ensemble of one-dimensional Sauter pulse electric fields. This is constructed as a crude approximation to the formal external-field expression previously derived. The approximations are too substantial for the calculated rate to be taken seriously as an estimate, but it has significance as a demonstration of the principle of how the theoretical method could be made to yield results, and provides some motivation to believe that such a method would return a larger result than Breit-Wheeler.

5.1 Formalism for Treating the Black-Body Field as an External Field

The crucial equation we shall use is

$$n_{\mathrm{BB}} = \sum_{E(x)} P[E]n[E], \tag{5.6}$$

where n_{BB} is the total expected rate of particle production by the black-body field, $P[E]$ is the probability of the black-body field being found in a particular field configuration, and $n[E]$ is the rate of particle production by that particular field configuration. This use of a classical probability distribution over classical field states is justified in section 5.1.1. We can numerically estimate this sum using a Monte Carlo method, by generating a large set of fields with probabilities given by $P[E]$, i.e. producing a large sample of the distribution $P[E]$. This sampling can be done precisely, as is described in section 5.1.2. The calculation of the pair-creation rate in a black-body field can therefore be performed by calculating the pair-creation rate in a representative sample of electric field profiles. This cannot be done precisely, though, because there is no general precise method for calculating pair-creation rates in arbitrary external fields.

5.1.1 The Classical Probability Distribution over Classical Background Fields

The black-body field is the equilibrium thermal state of the free electromagnetic field. It is usually described in terms of a statistical distribution over the photon states. As discussed in section 2.5, this is because the photon states are the energy eigenstates of the free electromagnetic field, and these are an orthogonal basis which diagonalises the density matrix of the canonical ensemble. From this it follows that many statistical quantities can be calculated within quantum thermodynamics by assigning a *classical probability* (as against a quantum-mechanical probability amplitude) for the system to be found in each of its energy eigenstates, and using the formulas of classical statistical mechanics on these as if they were classical mi-

crostates.

Glauber and Sudarshan [7–9] have shown that the coherent states provide an overcomplete basis for the Fock space of electromagnetic field states, and that this can be used to diagonalise any density matrix with respect to a coherent-state basis. Because the coherent state basis is not orthogonal, though, the diagonal entries of the density matrix needn't be positive-definite, and so do not in all cases behave like a classical probability distribution. However, in the case of an equilibrium system, the diagonal entries *are* always positive, and in the case of taking the expectation value of a normal-ordered operator, it *does* behave like a classical probability distribution. This is shown in our case below. For the specific problem of calculating the expected rate of particle production by a black-body field, therefore, we are free to consider the black-body field as a classical probability distribution over either photon states or coherent field states.

We will now formally construct the problem. The main artificial element we introduce is that the electromagnetic field is free, and the electron-positron field in its vacuum state, until some initial time $t = t_{\text{in}}$ when we "switch on" the interactions. We therefore take the system to be represented at t_{in} by the density matrix

$$\hat{\rho}(t_{\text{in}}) = \hat{\rho}_{\text{BB}} \otimes |0\rangle_{\text{ee}} \langle 0|_{\text{ee}} \,, \tag{5.7}$$

where $\hat{\rho}_{\text{BB}}$ is the density matrix of the black-body field, $\otimes$ is the Kronecker product and $|0\rangle_{\text{ee}}$ is the vacuum state of the electron-positron system. The "ee" subscript labels states in the electron/positron Fock space. Take α to label some basis in which the density matrix is diagonal,

$$\hat{\rho}_{\text{BB}} = \sum_{\alpha} p_{\alpha} |\alpha\rangle_{\gamma} \langle \alpha|_{\gamma} \,. \tag{5.8}$$

The "γ" subscript labels states in the photon Fock space. Denote the expected number of electrons and positrons for a given input photon-state as

$$N(\alpha) := \langle \alpha|_{\gamma} \langle 0|_{\text{ee}} \hat{U}^{\dagger}(t_{\text{out}}, t_{\text{in}}) \hat{N} \hat{U}(t_{\text{out}}, t_{\text{in}}) |\alpha\rangle_{\gamma} |0\rangle_{\text{ee}} \,, \tag{5.9}$$

where $\hat{N}$ is the number operator for the electrons or positrons, and $\hat{U}$ is the time-evolution operator. We would like the expected number of particles produced by the black-body field to be written as a classical probability distribution,

$$N_{\mathrm{BB}} := \mathrm{Tr}[\hat{N}\hat{\rho}(t_{\mathrm{out}})] = \sum_{\alpha} p_{\alpha} N(\alpha), \tag{5.10}$$

which becomes 5.6 when divided by spatial volume. This formula is trivial to derive if the α-basis is orthogonal. If we want to calculate N_{BB} using standard perturbative techniques, then we take the α-basis to be the Fock-basis (which is orthogonal) and $t_{\mathrm{out}} - t_{\mathrm{in}}$ to be very large and hence approximate $\hat{U}(t_{\mathrm{out}}, t_{\mathrm{in}}) \approx \hat{U}(\infty, -\infty)$. We can then calculate $N(\alpha)$ using perturbative scattering theory, with the trace sum translated to a sum of Fock-state to Fock-state scattering amplitudes, with p_{α} given by the Boltzmann formula $p_{\alpha} = Z^{-1} \exp\left(-E_{\alpha}/(k_B T)\right)$.

We, though, will take the α-basis as the coherent state basis. α therefore represents a set of complex numbers, one for every mode of the electromagnetic field,

$$\alpha = \{\alpha_{\mathbf{k},r}\}_{\mathbf{k},r}, \quad a_{\mathbf{k},r} \in \mathbb{C},\ r = 1, 2. \tag{5.11}$$

Formally treating the number of modes as countable, the relationship between these quantities and the electric field is given

$$A_{\mu}(x) = \sum_{\mathbf{k},r} \sqrt{\frac{\hbar}{2\omega_{\mathbf{k}}\epsilon_0 V}} \left[\epsilon_r^{\mu}(\mathbf{k}) e^{-ik\cdot x} \alpha_{\mathbf{k},r} + \epsilon_r^{*\mu}(\mathbf{k}) e^{ik\cdot x} \alpha_{\mathbf{k},r}^{*}\right], \tag{5.12}$$

with some choice of polarisation basis $\epsilon_r^{\mu}(\mathbf{k})$. V is the volume of the cavity. As discussed in section 2.1, the external field formalism of QED in a background field A_{μ} is entirely equivalent to standard QED so long as the "vacuum" is interpreted as a coherent-field state,

$$|0\rangle_{A_{\mu}} := |\alpha\rangle_{\gamma}, \tag{5.13}$$

where "A_{μ}" as a subscript represents the photon Fock space of QED in an external background field. Within this framework QED in a background field neglecting photon interactions is a lowest-loop-order approximation to full QED. Defining the invertible operator,

$$f(\alpha) := \{e^{-i\hbar\omega_{\mathbf{k}}t}\alpha_{\mathbf{k},\lambda}\}, \tag{5.14}$$

we can therefore write

$$\begin{aligned} |\alpha, \text{out}\rangle\, |g(\alpha)\rangle_{\text{ee}} :=& \hat{U}(t_{\text{out}}, t_{\text{in}})\, |\alpha\rangle_\gamma\, |0\rangle_{\text{ee}} \\ =& \, |f(\alpha)\rangle_\gamma \left[\hat{U}_{A_\mu}(t)\, |0\rangle_{\text{ee}}\right] + \text{ higher loop terms}, \end{aligned} \tag{5.15}$$

where $\hat{U}_{A_\mu}$ is the time-evolution operator for non-interacting electrons and positrons in the classical background field A_μ and $t := t_{\text{out}} - t_{\text{in}}$. Ignoring the higher loop terms, this gives

$$\begin{aligned} N_{\text{BB}} &= \text{Tr}_\gamma \left[\sum_\alpha p(\alpha) N(\alpha)\, |f(\alpha)\rangle_\gamma \langle f(\alpha)|_\gamma\right] \\ &= \text{Tr}_\gamma \left[\sum_\alpha p(f^{-1}(\alpha)) N(f^{-1}(\alpha))\, |\alpha\rangle_\gamma \langle\alpha|_\gamma\right] = \sum_\alpha p(f^{-1}(\alpha)) N(f^{-1}(\alpha)). \end{aligned} \tag{5.16}$$

which by a change of variables in the sum returns the desired result, equation 5.6.

5.1.2 Numerical Generation of a Distribution of Local Black-Body Field Profiles

The probability $P[\mathbf{E}(x)]$ of finding the black-body field in a given field state has a simple expression in terms of the field's representation in Fourier space, since each mode is mathematically equivalent to a statistically independent simple harmonic oscillator. Formally assuming a countable set of cavity modes, we can write the probability of a field profile as [9]

$$P[\mathbf{E}(x)] = \prod_{\mathbf{k},r} \frac{1}{2\pi\sigma_{\mathbf{k}}^2} \exp\left(-\frac{|E_{\mathbf{k},r}|^2}{2\sigma_{\mathbf{k}}^2}\right), \quad \sigma_{\mathbf{k}}^2 = \frac{\hbar\omega_{\mathbf{k}}}{\epsilon_0 V(\exp(\hbar\omega_{\mathbf{k}}/(k_B T)) - 1)}, \tag{5.17}$$

where V is the volume of the cavity, $\omega_{\mathbf{k}}$ the frequency of a mode, and the $E_{\mathbf{k},r}$ are complex mode amplitudes related to the spatial field by

$$E_j(x) = \mathrm{Re}\left\{\sum_{\mathbf{k},r} \epsilon_{j,r}(\mathbf{k}) e^{-ik\cdot x} E_{\mathbf{k},r}\right\}. \tag{5.18}$$

The distribution of fields is, of course, temperature-dependent, but the dependence is of a simple sort that can be absorbed into a redefinition of scales. This is because of a symmetry in the black-body field, whereby scaling the temperature by a factor α is equivalent to scaling the lengthscale and Maxwell Tensor,

$$T \;\mapsto\; \alpha T \;\Leftrightarrow (x, F_{\mu\nu}) \;\mapsto\; (\alpha^{-1}x, \alpha^2 F_{\mu\nu}), \quad \alpha \in \mathbb{R}^+. \tag{5.19}$$

To take advantage of this symmetry, define the dimensionless quantities

$$X := \frac{k_B T}{\hbar}(t, \mathbf{x}/c) \tag{5.20a}$$

$$\upsilon := (\upsilon_0, \boldsymbol{\upsilon}) := \frac{\hbar}{k_B T}(\omega_{\mathbf{k}}, c\mathbf{k}) \tag{5.20b}$$

$$\mathcal{E}_{\boldsymbol{\upsilon},r} := \frac{\sqrt{\epsilon_0}\hbar^{3/2}c^{3/2}}{(k_B T)^2} E_{\mathbf{k},r} \tag{5.20c}$$

$$\boldsymbol{\mathcal{E}}(X) := \frac{\sqrt{\epsilon_0}\hbar^{3/2}c^{3/2}}{(k_B T)^2} \mathbf{E}(x). \tag{5.20d}$$

In terms of these, we can write the probability distribution for the dimensionless electric field,

$$P[\boldsymbol{\mathcal{E}}(X)] = \prod_{\boldsymbol{\upsilon},r} \frac{1}{2\pi\sigma_{\boldsymbol{\upsilon}}^2} \exp\left(-\frac{|\mathcal{E}_{\boldsymbol{\upsilon},r}|^2}{2\sigma_{\boldsymbol{\upsilon}}^2}\right), \quad \sigma_{\boldsymbol{\upsilon}}^2 := \frac{\upsilon_0}{(2\pi)^3 \rho_\hbar (e^{\upsilon_0} - 1)}, \tag{5.21}$$

where

$$\mathcal{E}_j(X) = \mathrm{Re}\left\{\sum_{\boldsymbol{\upsilon},r} \epsilon_{j,r}(\boldsymbol{\upsilon}) e^{-i\upsilon\cdot X} \mathcal{E}_{\boldsymbol{\upsilon},r}\right\}. \tag{5.22}$$

and $\rho_\hbar$ is the density of states in $\boldsymbol{\upsilon}$-space,

$$\rho_\hbar := \frac{(k_B T)^3 V}{(2\pi)^3 (\hbar c)^3}. \tag{5.23}$$

This gives the probability distribution for an electric field at any temperature through the equation 5.20d. Ultimately we are interested in the limit of the black-body cavity volume tending to infinity. The usual practice of taking the sum over $\boldsymbol{\upsilon}$-modes to an integral over all $\mathbb{R}^3$ in this limit is not valid in this case because the probability of a given magnitude and phase for each mode is independent, and hence the amplitudes of different $\boldsymbol{\upsilon}$ modes infinitesimally close together are uncorrelated. Therefore in the infinite-volume limit the mode amplitudes in general make functions that are discontinuous almost everywhere, so they are not Riemann-integrable.

The way forwards is to recognise that although the cavity volume tends to infinity, we are only interested in a finite spacetime region within it, say $U \subset \mathbb{R}^{3\oplus 1}$, for convenience centred on the origin. Within U, the $\boldsymbol{\upsilon}$-modes within a sufficiently small volume of $\boldsymbol{\upsilon}$-space centred on a given $\boldsymbol{\upsilon}$, $\delta\mathcal{T}_{\boldsymbol{\upsilon}} \subset \mathbb{R}^3$, are indistinguishable. We can therefore write

$$\mathcal{E}_j(X) = \mathrm{Re}\left\{ \sum_{\boldsymbol{\upsilon}\in P,r} \epsilon_{j,r}(\boldsymbol{\upsilon}) e^{-i\upsilon\cdot X} \bar{\mathcal{E}}_{\boldsymbol{\upsilon},r} \left[1 \; + \; \mathcal{O}\left(\mathrm{Max}_{X\in U, \boldsymbol{\upsilon}'\in\delta\mathcal{T}_{\boldsymbol{\upsilon}}} (X\cdot[\upsilon - \upsilon'])\right)\right] \right\}, \tag{5.24}$$

where P is a grid of points within accompanying volumes $\{\delta\mathcal{T}_{\boldsymbol{\upsilon}}\}_{\boldsymbol{\upsilon}\in P}$ that partition the total momentum-space, and

$$\bar{\mathcal{E}}_{\boldsymbol{\upsilon},r} := \sum_{\boldsymbol{\upsilon}'\in\delta\mathcal{T}_{\boldsymbol{\upsilon}}} \mathcal{E}_{\boldsymbol{\upsilon},r}, \tag{5.25}$$

The real and imaginary components of $\bar{\mathcal{E}}_{\boldsymbol{\upsilon},r}$ are both the sum of Gaussian random variables, and as such are themselves Gaussian random variables with standard deviation given by

$$\bar{\sigma}^2_{\boldsymbol{\upsilon}} = \sum_{\boldsymbol{\upsilon}'\in\delta\mathcal{T}_{\boldsymbol{\upsilon}}} \sigma^2_{\boldsymbol{\upsilon}'}. \tag{5.26}$$

There are $|\delta\mathcal{T}_{\boldsymbol{\upsilon}}|\rho_\hbar$ modes within $\delta\mathcal{T}_{\boldsymbol{\upsilon}}$. The probability distribution of dimensionless fields can therefore be written in terms of these coarse-grained modes as

$$
\begin{aligned}
P[\boldsymbol{\mathcal{E}}(X)] &= \prod_{\boldsymbol{\upsilon}\in P,r} \frac{1}{2\pi\sigma_{\boldsymbol{\upsilon}}^2} \exp\left(-\frac{|\bar{\mathcal{E}}_{\boldsymbol{\upsilon},r}|^2}{2\bar{\sigma}_{\boldsymbol{\upsilon}}^2}\right) \\
\bar{\sigma}_{\boldsymbol{\upsilon}}^2 &= \frac{|\delta\mathcal{T}_{\boldsymbol{\upsilon}}|\upsilon_0}{(2\pi)^3(e^{\upsilon_0}-1)}\left[1+\mathcal{O}\left(\mathrm{Max}_{\boldsymbol{\upsilon}'\in\delta\mathcal{T}_{\boldsymbol{\upsilon}}}(|\boldsymbol{\upsilon}'|-|\boldsymbol{\upsilon}|)\right)\right].
\end{aligned}
\tag{5.27}
$$

All that is needed is upper cutoffs to make P of finite size and this gives us a numerical method for generating a distribution of local spatial field profiles: mode amplitudes are generated as Gaussian random variables with standard deviation (5.27), and converted into a spatial profile with equation 5.24.

5.1.2.1 1D Longitudinal Projection

For reasons discussed in section 5.2, we will be interested in the longitudinal component of the electric field along a single spatial axis. To get this more efficiently, we can analytically sum over entire slices of $\boldsymbol{\upsilon}$-space of constant υ_z. To do so, first note that we can choose $\epsilon_{j,r}(\boldsymbol{\upsilon})$ such that

$$
\begin{aligned}
\boldsymbol{\epsilon}_1(\boldsymbol{\upsilon})\cdot\hat{\mathbf{z}} &= \frac{\upsilon_\perp}{\sqrt{\upsilon_z^2+\upsilon_\perp^2}} \\
\boldsymbol{\epsilon}_2(\boldsymbol{\upsilon})\cdot\hat{\mathbf{z}} &= 0,
\end{aligned}
\tag{5.28}
$$

where $\upsilon_\perp = \sqrt{\upsilon_x^2+\upsilon_y^2}$. The probability of a single $r=1$ mode to give an electric field of a certain strength in the z-component is a Gaussian with standard deviation $(\boldsymbol{\epsilon}_1(\boldsymbol{\upsilon})\cdot\hat{\mathbf{z}})\,\sigma_{\boldsymbol{\upsilon}}$. The probability of the z-component of the electric field for the modes of a given υ_z to take a given value is then a normal distribution with standard deviation given by equation 5.26 with the sum taken to an integral,

$$
\begin{aligned}
\bar{\sigma}_{\upsilon_z}^2 &= \delta\upsilon_z \int_{\mathbb{R}^2} d\upsilon_x d\upsilon_y\ (\boldsymbol{\epsilon}_1(\boldsymbol{\upsilon})\cdot\hat{\mathbf{z}})^2\rho_\hbar\sigma_{\boldsymbol{\upsilon}}^2 + \mathcal{O}(\delta\upsilon_z^2) \\
&= \delta\upsilon_z \int_0^\infty \pi d(\upsilon_\perp^2)\ \frac{p_\perp^2}{(2\pi)^3\sqrt{\upsilon_\perp^2+\upsilon_z^2}(\exp(\sqrt{\upsilon_\perp^2+\upsilon_z^2})-1)} + \mathcal{O}(\delta\upsilon_z^2) \\
&= \frac{\delta\upsilon_z}{(2\pi)^2}\int_{|\upsilon_z|}^\infty du\ \frac{u^2-\upsilon_z^2}{e^u-1} + \mathcal{O}(\delta\upsilon_z^2) \\
&= \frac{\delta\upsilon_z}{2\pi^2}\left(|\upsilon_z|\,\mathrm{Li}_2(e^{-|\upsilon_z|}) + \mathrm{Li}_3(e^{-|\upsilon_z|})\right) + \mathcal{O}(\delta\upsilon_z^2),
\end{aligned}
\tag{5.29}
$$

where $\mathrm{Li}_n(z) = \sum_{k=1}^\infty z^k/k^n$ is the polylogarithm of order n. This standard deviation is

used to generate a set of mode amplitudes $\{\bar{\mathcal{E}}_{\upsilon_z}\}_{\upsilon_z \in \upsilon_z}$, which give the longitudinal electric field along the z-axis by

$$\mathcal{E}(y_z) \cdot \hat{\mathbf{z}} = \sum_{\upsilon_z \in \upsilon_z} \bar{\mathcal{E}}_{\upsilon_z} e^{-i\upsilon_z y_z} \left[1 + \mathcal{O}\left(\frac{\delta \upsilon_z Y}{4} \right) \right]. \tag{5.30}$$

υ_z is 1D grid, including the origin, with spacing $\delta\upsilon_z$. $Y > 0$ is the length, even about the origin, of X-space that we choose to sample. Results presented in section 5.2.3 used $\delta\upsilon_z = 1 \times 10^{-5}$, $Y = 20$, and an upper-bound cutoff of $\upsilon_{\max} = 30$. (At which the standard deviation is reduced by a factor of about $\upsilon_{\max} e^{-\upsilon_{\max}} \approx 10^{-12}$ from the peak.) The greatest source of error in our simulation, therefore, ought to be the effect of coarse-graining momentum on the spacetime dependence of the modes, which by equation 5.30 should introduce an error factor of about 10^{-4} in field amplitudes.

There is a straightforward sanity check of our method based on the energy density, u_{bb} of the black-body field. In terms of the dimensionless units by equation 5.20d,

$$\begin{aligned} \frac{1}{6} u_{\text{bb}} &= \frac{\pi^2 (k_B T)^4}{90 (\hbar c)^3} = \frac{\epsilon_0}{2N} \sum_X |\mathcal{E}(X)|^2 \frac{(k_B T)^4}{\epsilon_0 (\hbar c)^3} \\ \Rightarrow \frac{1}{N} \sum_X |\mathcal{E}(X)|^2 &= \frac{\pi^2}{45} \approx 0.2193, \end{aligned} \tag{5.31}$$

where the sum is over all discrete y points sampled, and N is the total number of points sampled. The factor of 1/6 comes from the fact that we only expect the z-component of the electric field to account for one-sixth of the energy density. Our numerical model came to 0.2182, implying an error at this stage of $\sim 0.5\%$. The sum was over $N = 11907951$ sampled points.[1] Therefore, this error is about an order of magnitude higher than both the expected error inherent in random sampling of $\sim 1/\sqrt{N}$ times the standard deviation, and the coarse-graining error. This is perhaps an indication that the coarse-graining error is larger than the above big-$\mathcal{O}$ estimate suggests.

[1] This is the number of sampled X-points from 5000 sampled fields. The irregular number comes from the fact that the X-spacing is dictated by the FFT as $\delta X = \pi/\upsilon_{\max}$.

5.2 Pair-Creation Rate from a Statistical Ensemble of Sauter Pulses

There does not exist a practical method for calculating the rate of particle creation for an entirely general background field. With few exceptions, such as the plane wave, analytical results appropriate for our regime exist for electric fields and magnetic fields that exist separately from each other, point in one direction and vary only in time or only in one spatial dimension. Modern computationally-expensive numerical methods can extend to fields that vary in two spacetime dimensions [139]. The black-body fields vary in all four spacetime dimensions, and twist to point in all directions, though. This precludes precise calculation.

A possible way of proceeding is to try and represent the field profiles generated by the method of section 5.1 with simplified versions that capture some of their properties but which have calculable pair-creation rates. In the remainder of this chapter, the principle is demonstrated by a procedure for representing the black-body field as an ensemble of longitudinally-oriented spatial Sauter pulses.

The choice of spatial Sauter pulses is intended to capture the main effect likely to *suppress* particle production relative to a constant field of the same energy density. This is so that, when the result exceeds the Breit-Wheeler result (4.18), it provides evidence that the true value of the particle production rate calculated according to the procedure described in section 5.1 exceeds the low-order perturbative result in the high-temperature limit. This is because there is good reason to believe that the neglect of temporal variation of the electric field should be a strict underestimate of the pair-production rate: it is well-established in the semiclassical regime that the constant-field approximation underestimates particle production for fields varying only in time [78, 79, 107], and numerical calculations of fields varying in time and one spatial dimension around the critical strength $E_0 \sim E_S$ establish the same result [83, 139]. In Appendix C we show that this is the case for a temporal Sauter pulse field with parameters appropriate to a thermal field with $k_B T$ greater than $m_e c^2$.

Still, there are too many serious problems with the model as a representation of the black-body field to draw strong conclusions from this work. An important part of this model is

the idea that particle-production could be well-approximated by localised "bump" fields about the size of the thermal wavelength. This concept has two requirements: that the "formation length" [226] of the particle-creation process is smaller than the bump field; and that the particles produced in adjacent bumps add incoherently. The second requirement is supported by the coherence length and timescales of the black-body field being $\propto \hbar/(k_B T)$, with constant of proportionality of order of magnitude 1 [221–223]. The first requirement is more difficult to ascertain. Broadly, we expect the formation length to be of similar scale to the wavelength of produced particles, which it can be seen in figure 5.7 are largely between ~ 0.2 and 2 times the thermal wavelength. Ref [82] investigates the formation region with the worldline method, and associates it with the region occupied by the worldlines that form the dominant contribution to the pair-creation rate. Refs [78, 79] find, in the semiclassical regime, for small γ the worldline instanton paths are confined to spatial regions of similar size to the wavelength of the oscillating field. These results give some reason to believe the "local" production rate can give a reasonable estimate, but it is far from conclusively demonstrated. It especially relies on the debatable idea that at very high temperatures, when most particles are being produced with energies much greater than the rest mass, the Compton wavelength becomes an irrelevant scale.

The most egregious simplification of our model is that we treat the black-body field as a purely electric field, neglecting the magnetic field. The number of produced particles is a Lorentz-invariant quantity, and so the Schwinger mechanism is dependent on the Lorentz-invariants of the electromagnetic field [12], rather than the frame-dependent division between electric and magnetic components. The inclusion of the magnetic field can therefore quite radically suppress particle production. The extreme case is that of a travelling plane-wave, or crossed constant electric and magnetic fields of equal strength, which create no particles at all [6], since their Lorentz-invariants are everywhere zero. For the black-body field this is not the case: locally the electric and magnetic field components are neither necessarily of equal magnitude nor crossed. The profiles still obey the vacuum Maxwell equations, though, a feature that is removed entirely by our neglect of the magnetic field. In the comparable free-field situation of two counter-propagating laser pulses the magnetic field has been found to significantly suppress particle production [130–132].

Still, the model has interest in its own right, as a demonstration of the principle of the application of the method outlined in section 5.1, and as an effort to capture specifically the effects of the longitudinal spatial variation of the black-body field on its particle production. The argument proceeds as follows. In section 5.2.1 the particle-production rate in a spatial Sauter pulse fields with strength and frequency varying as in equations 5.1 and 5.2 is analysed. It is shown that these parameters put the black-body fields "between regimes" in an important sense. In section 5.2.2 we derive the energy spectrum of produced particles for the Sauter pulse in the appropriate limit. In section 5.2.3 we use the results from section 5.2.1 and 5.2.2 to construct the toy numerical model, and compare the result to that of chapter 4.

5.2.1 High-Temperature Limit of Nikishov's Sauter Pulse Result: Total Pair-Creation Rate

A Sauter pulse field has electrostatic potential and electric field given by

$$V(z) = -a_0 \tanh(Kz) \tag{5.32a}$$

$$E(z) = E_0 \operatorname{sech}^2(Kz), \tag{5.32b}$$

where $E_0 = ca_0K$. Nikishov [10] gives the expected number of created particles in a Sauter pulse external field,

$$N_{\text{Sauter}} = \frac{2A_\perp \mathcal{T}}{(2\pi)^2\hbar^3} \int_0^{k_{\perp,\max}} dk_\perp k_\perp \int_{-eac+\sqrt{k_\perp^2c^2+m_e^2c^4}}^{eac-\sqrt{k_\perp^2c^2+m_e^2c^4}} dk_0 \, \frac{w(\mathbf{k}, a_0, K)}{1 + w(\mathbf{k}, a_0, K)}, \tag{5.33}$$

where $A_\perp$ is the transverse area (i.e. in the two directions in which the field is uniform), and

$$w(\mathbf{k}, a_0, K) = \frac{\mu[(k_0 - ea_0c)/(2Kc\hbar) + \mu]}{\nu[-(k_0 + ea_0c)/(2Kc\hbar) - \nu]} \cdot \frac{1}{|C_1|^2}$$

$$
\begin{aligned}
C_1 &= \frac{\Gamma(1-2i\mu)\Gamma(2i\nu)}{\Gamma(-i\mu-i\nu+i\lambda')\Gamma(1-i\mu-i\nu-i\lambda')} \\
\mu &= \sqrt{(k_0-ea_0c)^2-k_\perp^2c^2-m_e^2c^4}/(2Kc\hbar) \\
\nu &= \sqrt{(k_0+ea_0c)^2-k_\perp^2c^2-m_e^2c^4}/(2Kc\hbar) \\
\lambda' &= \frac{ea_0}{K\hbar} \\
k_{\perp,\max} &= \sqrt{e^2a^2c^2-m_e^2c^4}.
\end{aligned}
\tag{5.34}
$$

The Keldysh parameter in this case is given by

$$
\tilde{\gamma}_{\mathrm{K}} = \frac{m_e c}{e a_0}. \tag{5.35}
$$

Using

$$
|\Gamma(iz)|^2 = \frac{\pi}{z\sinh\pi z}, \quad |\Gamma(1+iz)|^2 = \frac{\pi z}{\sinh\pi z}, \tag{5.36a}
$$

and defining

$$
\kappa_0 := k_0/(ea_0c), \quad \kappa_\perp := k_\perp/(ea_0) \tag{5.37}
$$

$$
a := \sqrt{(\kappa_0-1)^2-\kappa_\perp^2-\tilde{\gamma}_{\mathrm{K}}^2} \tag{5.38}
$$

$$
b := \sqrt{(\kappa_0+1)^2-\kappa_\perp^2-\tilde{\gamma}_{\mathrm{K}}^2} \tag{5.39}
$$

we get

$$
N_{\mathrm{Sauter}} = \frac{2A_\perp\mathcal{T}(ea_0)^3c}{(2\pi)^2\hbar^3}\int_0^{\sqrt{1-\tilde{\gamma}_{\mathrm{K}}^2}} d\kappa_\perp\kappa_\perp \int_{-1+\sqrt{\kappa_\perp^2+\tilde{\gamma}_{\mathrm{K}}^2}}^{1-\sqrt{\kappa_\perp^2+\tilde{\gamma}_{\mathrm{K}}^2}} d\kappa_0 \, \frac{w(\kappa,\lambda',\tilde{\gamma}_{\mathrm{K}})}{1+w(\kappa,\lambda',\tilde{\gamma}_{\mathrm{K}})}, \tag{5.40}
$$

where

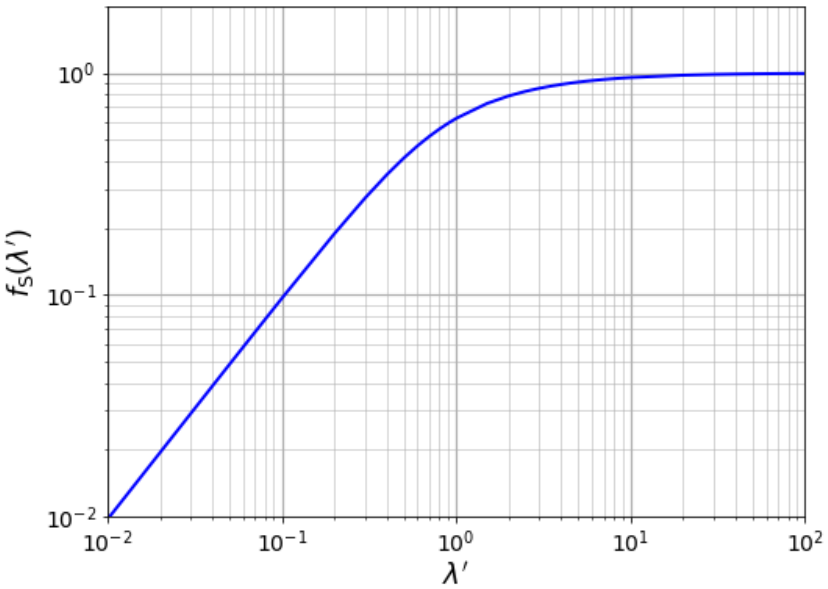

Figure 5.1: Log-log plot of $f_S(\lambda')$. Its approach to 1 signifies an approach to the high-strength constant-field limit.

$$w(\kappa, \lambda', \tilde{\gamma}_K) = -\frac{(\kappa_0 - 1 + a)(a + b + 2)\sinh(\pi\lambda' b)\sinh(\pi\lambda' a)}{(\kappa_0 + 1 + b)(a + b - 2)\sinh\frac{\pi\lambda'}{2}(a + b - 2)\sinh\frac{\pi\lambda'}{2}(a + b + 2)}. \tag{5.41}$$

Written in this form, we can clearly take the high-temperature limit by taking $\tilde{\gamma}_K \to 0^+$. Define

$$f_S(\lambda') := \frac{3\pi\lambda'}{2}\int_0^1 d\kappa_\perp \kappa_\perp \int_{-1+\kappa_\perp}^{1-\kappa_\perp} d\kappa_0 \, \frac{w(\kappa, \lambda', 0)}{1 + w(\kappa, \lambda', 0)}. \tag{5.42}$$

This is plotted in figure 5.1. We can therefore write

$$N_{\text{Sauter}} \sim \frac{A_\perp \mathcal{T}(eE_0)^2}{3\pi^3 c\hbar^2 K} f_S(\lambda'), \quad \tilde{\gamma}_K \to 0^+. \tag{5.43}$$

This approaches the locally constant field as $\exp(-\pi E_S/E_0) \sim f_S(\lambda') \sim 1$, and hence in the limit of $\lambda' \gg 1$ and $E_0 \gg E_S$. We therefore have two dimensionless parameters that determine the approach to the constant field case in the strong-field limit. One of these is the Keldysh parameter, and the other can be written, using equations 5.1 and 5.2,

$$\lambda' = \frac{eE_{\mathrm{bb}}}{c\hbar k_{c,\mathrm{bb}}^2} = \frac{1}{\tilde{\beta}_{\mathrm{c}}^2}\sqrt{\frac{8\pi^3\alpha}{15}}. \tag{5.44}$$

As T varies λ' is constant and of order of magnitude ~ 1. Looking at figure 5.1, it can be seen that $f_{\mathrm{S}}(\lambda')$ is quite fast-varying around $\lambda' = 1$. In a black-body field, though the scale is broadly characterised by λ', we expect particular "bumps" to vary chaotically in a reasonably large region around λ'. This means that we cannot get a sufficient characterisation of our black-body field merely by specifying a parameter regime. We are in the space between regimes, neither "fast-varying" nor "slow-varying", and the precise details of the spacetime fluctuations matter. We must therefore implement equation 5.43 using a numerical method.

5.2.2 High-Temperature Limit of Nikishov's Sauter Pulse Result: Energy Spectrum

To calculate the production rate at a specific energy, we exchange the order of integration in $f_{\mathrm{S}}(\lambda')$ in equation 5.43, and change the outer variable of integration to the kinetic energy,

$$E = (1 + \kappa_0)ea_0c \tag{5.45}$$

so that we can write

$$\begin{aligned} N_{\mathrm{Sauter}} =& \int_0^{2ea_0} dE\ \frac{dN_{\mathrm{Sauter}}}{dE} \\ \frac{dN_{\mathrm{Sauter}}}{dE} :=& \frac{2A_\perp \mathcal{T}(ea_0)^2}{(2\pi)^2\hbar^3} G(\kappa_0, \lambda'), \end{aligned} \tag{5.46}$$

where

$$G(\kappa_0, \lambda') := \int_0^{1-|\kappa_0|} d\kappa_\perp\ \frac{\kappa_\perp w(\kappa, \lambda', 0)}{1 + w(\kappa, \lambda', 0)}. \tag{5.47}$$

Three examples are plotted in figure 5.2. Since they are plotted normalised with respect to the total production rate, they are dependent only on λ'. The graphs can be interpreted as giving the distribution of electron or positron kinetic energy. The total kinetic energy of the pair is always equal to the potential difference across the pulse, $2ea_0c$. (For this reason the

graphs must be symmetric under the transformation $E \to 2ea_0 - E$.)

5.2.3 Using Sauter Pulses to Estimate Black-Body Pair-Production

5.2.3.1 Representing the Black-Body with a Distribution of Dimensionless Sauter Pulse Parameters

We have, as described in section 5.1.2, a large sample of one-dimensional electric fields generated by the black-body. We wish to estimate particle production of the black-body by representing these fields as spatial Sauter pulses. As a first step, in order for the sampled fields to better represent the full black-body, we multiply them by a factor of $\sqrt{3}$, so that the average electric field strength is correct. We then partition each of these one-dimensional field profiles into individual "bumps" based on where they cross $\mathrm{Re}\{\mathcal{E}\} = 0$. These are padded with some zero-values (equal to the half-width of the pulse) either side, then fitted to Sauter pulses by least-squares regression. This gives us, for every bump, the dimensionless peak electric field strength $\mathcal{E}_{0,j}$, dimensionless frequency scale $\upsilon_{\mathrm{S},j}$, and a dimensionless centre $X_{0,j}$ for each bump labelled by $j = 0, ..., J$, where J is the total number of bumps, which obey

$$\mathcal{E}_j(X) = \mathcal{E}_{0,j}\,\mathrm{sech}^2(\upsilon_{\mathrm{S},j}[X - X_{0,j}]). \tag{5.48}$$

Figure 5.3 demonstrates the principle with three examples of bumps and the Sauter pulses fitted to them. Bumps for which the least-squares does not converge, or converges to a pulse with error estimate > 1 or with inverse frequency scale $(\upsilon_{\mathrm{S},j})^{-1}$ less than four times the width of the bump, are discarded. This will introduce some bias but it should not throw off the results too badly since, as specified later, $\sim 95\%$ of bumps converge and pass this sanity check. We also store the width of each bump (not the fitted Sauter pulse), ΔX_j. This gives us a (sample of) a distribution of dimensionless Sauter pulse parameters, representative of the distribution of electric field profiles. Histograms of the two interesting parameters, $\mathcal{E}_0$ and υ_{S} are plotted in figure 5.4.

Note that, converted to dimensionless parameters, our black-body characteristic inverse lengthscale (5.2) becomes $\upsilon_{\mathrm{bb}} \approx 4.1\tilde{\beta}_{\mathrm{c}}$. The fact that $\tilde{\beta}_{\mathrm{c}}$ is order-of-magnitude ~ 1 is therefore

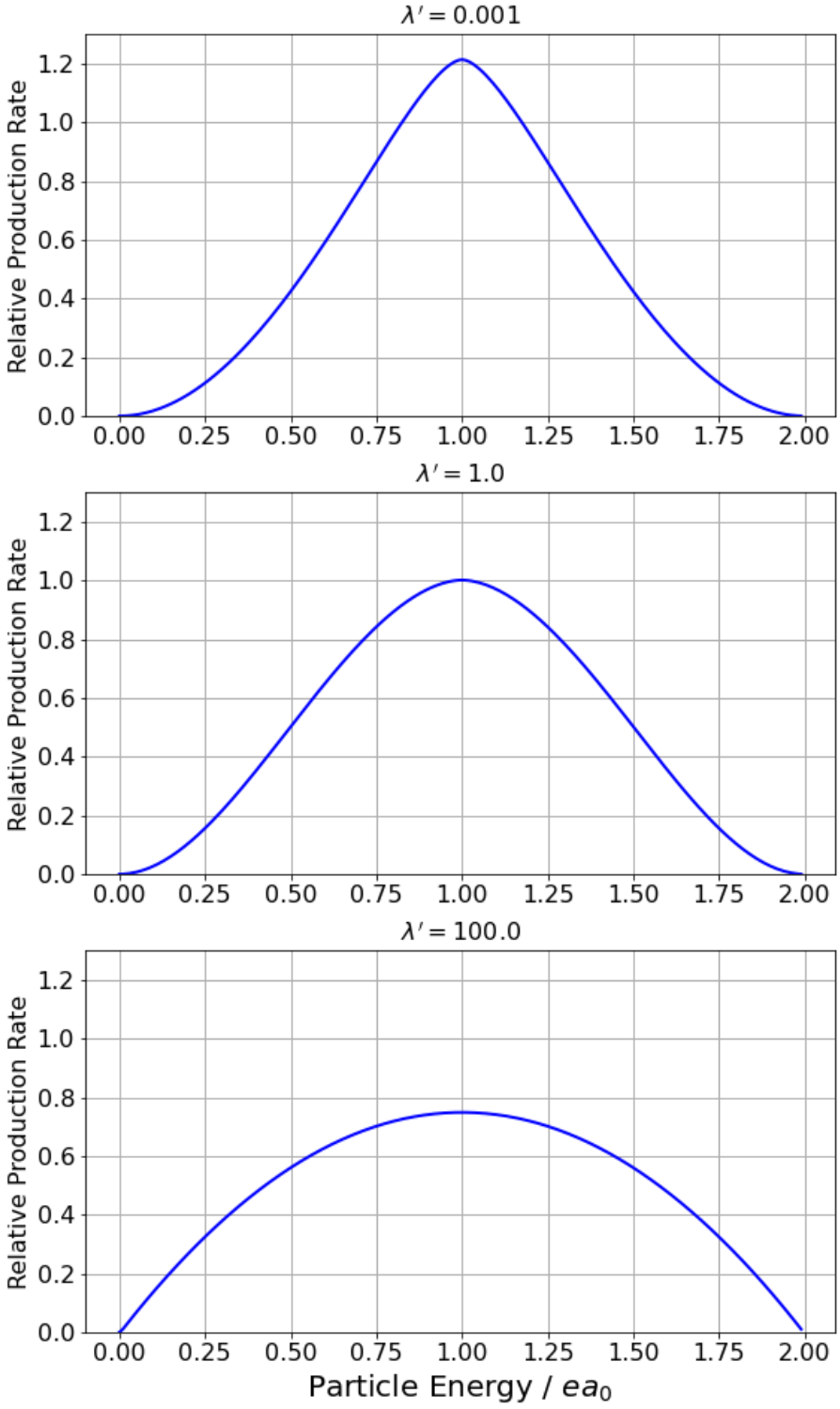

Figure 5.2: Energy distributions of produced electrons or positrons by a Sauter pulse in the $\tilde{\gamma}_{\mathrm{K}} \ll 1$ limit for three different values of λ'. Normalised so that total area under the graph=1.

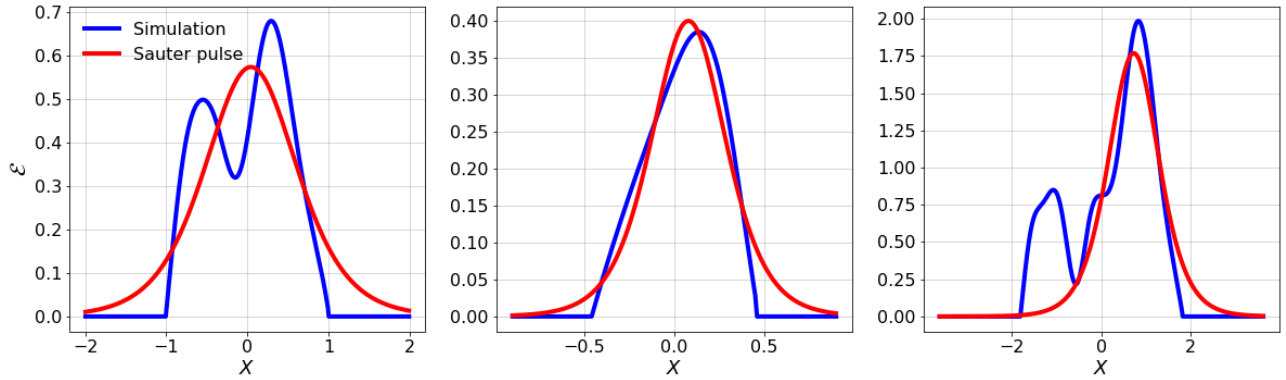

Figure 5.3: Three example "bumps", or portions of the 1D cross-section of the longitudinal electric field, in blue, with the Sauter pulses fitted to them by least-squares regression in red. These are all examples of curves where the fit was deemed good enough to include.

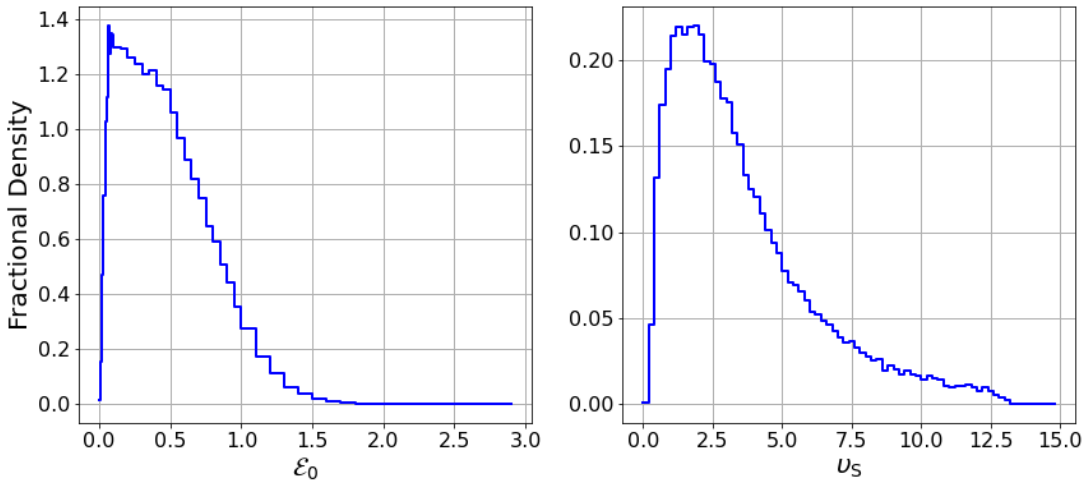

Figure 5.4: Histograms. Shows the distribution of the dimensionless Sauter pulse parameters generated by fitting Sauter pulses to the microscopic "bump" field profiles sampled from the black-body distribution.

verified in figure 5.4. A better sanity-check of our representation of the black-body field is performed by calculating the energy-density of the field represented by these Sauter pulses. For this we calculate the total energy per transverse unit area of all Sauter pulses in our sample,

$$\begin{aligned}\frac{1}{6}\frac{U_{\text{Sauter}}}{A_\perp} &= \cdot\frac{\epsilon_0}{2}\sum_j\int_{-\infty}^{\infty} dx\ |E_j(x)|^2 = \frac{(k_BT)^3}{2(\hbar c)^2}\sum_j\int_{-\infty}^{\infty} dX\ |\mathcal{E}_j(X)|^2 \\ &= \sum_j \frac{2|\mathcal{E}_{0,j}|^2}{3\upsilon_{\text{S},j}}\frac{(k_BT)^3}{(\hbar c)^2}.\end{aligned} \tag{5.49}$$

The factor of $1/6$ comes from the fact that we expect a single component of the electric field to account for a sixth of the total black-body energy. Dividing this by the total length,

$$L = \frac{\hbar c}{k_BT}\sum_j \Delta X_j, \tag{5.50}$$

we find

$$\frac{(\hbar c)^3}{(k_BT)^4}u_{\text{Sauter}} = \frac{4\sum_j |\mathcal{E}_{0,j}|^2/\upsilon_{\text{S},j}}{\sum_j \Delta X_j} \approx 0.57 \tag{5.51}$$

Comparing this to the figure from theory, from equation 5.31,

$$\frac{(\hbar c)^3}{(k_BT)^4}u_{\text{bb}} = \frac{\pi^2}{15} \approx 0.66, \tag{5.52}$$

we find agreement within order of magnitude, with our model giving an underestimate. This large dataset of dimensionless Sauter pulse parameters can be used to calculate both the total particle creation rate and the energy spectrum of produced particles.

5.2.3.2 The Particle Creation Rate

We can calculate a particle creation rate for every Sauter profile using equation 5.43, once we convert from the dimensionless quantities (5.20). Note that since λ' is temperature-independent it can be directly expressed in terms of the dimensionless parameters. Specifically,

$$ea_0c = \sqrt{4\pi\alpha}(k_BT)\frac{\mathcal{E}_0}{\upsilon_{\text{S}}}, \tag{5.53}$$

therefore

$$\lambda'_j = \sqrt{4\pi\alpha}\frac{\mathcal{E}_{0,j}}{(\upsilon_{\mathrm{S},j})^2}. \tag{5.54}$$

In terms of these quantities, the rate of particle production per unit transverse area per unit time (5.43) is

$$\frac{N_{\mathrm{Sauter},j}}{A_\perp \mathcal{T}} \sim \frac{4\alpha c}{3\pi^2}\frac{\mathcal{E}_{0,j}^2 f_{\mathrm{S}}(\lambda'_j)}{\upsilon_{\mathrm{S},j}}\left(\frac{k_B T}{\hbar c}\right)^3. \tag{5.55}$$

For the estimated rate per unit spacetime in the high-temperature regime we need to add the contributions of all bumps, and divide by their total width,

$$n_{\mathrm{bb,Sauter}} = \zeta\frac{4\alpha c}{3\pi^2}\left(\frac{k_B T}{\hbar c}\right)^4, \quad \zeta := \frac{1}{\sum_j \Delta X_j}\sum_j \frac{\mathcal{E}_{0,j}^2 f_{\mathrm{S}}(\lambda'_j)}{\upsilon_{\mathrm{S},j}}, \tag{5.56}$$

where ΔX_j is the dimensionless width of each bump. Running the program with 67910 iterations gave $J = 64424$ successful convergences of the regression fit that passed our sanity check, and gave

$$\zeta \approx 0.136. \tag{5.57}$$

This gives ratios to the constant-field Schwinger rate and the Breit-Wheeler rate

$$\frac{n_{\mathrm{bb,Sauter}}}{n_{\mathrm{bb,LCS}}} = \frac{20}{\pi^2}\zeta \approx 0.275 \tag{5.58a}$$

$$\frac{n_{\mathrm{bb,Sauter}}}{n_{\mathrm{bb,BW}}} = \frac{24}{\pi^3\alpha}\zeta\left(\log\left(\frac{k_B T}{m_e c^2}\right) + \chi\right)^{-1} \approx 14.4\left(\log\left(\frac{k_B T}{m_e c^2}\right) - 0.454\right)^{-1}. \tag{5.58b}$$

We therefore find that the Sauter pulse model predicts a suppression of particle production by about a factor of 0.3 relative to the constant-field Schwinger mechanism, which still puts it well in excess of Breit-Wheeler, by about a factor 14 just above the electron rest mass. This is plotted in figure 5.6. Breit-Wheeler overtakes the Sauter pulse model at about $k_B T \approx 2\times 10^6 m_e c^2 \approx 920$ GeV, which is well beyond the domain of applicability QED. (Among other problems, it is above the temperature of electroweak symmetry breaking [227].)

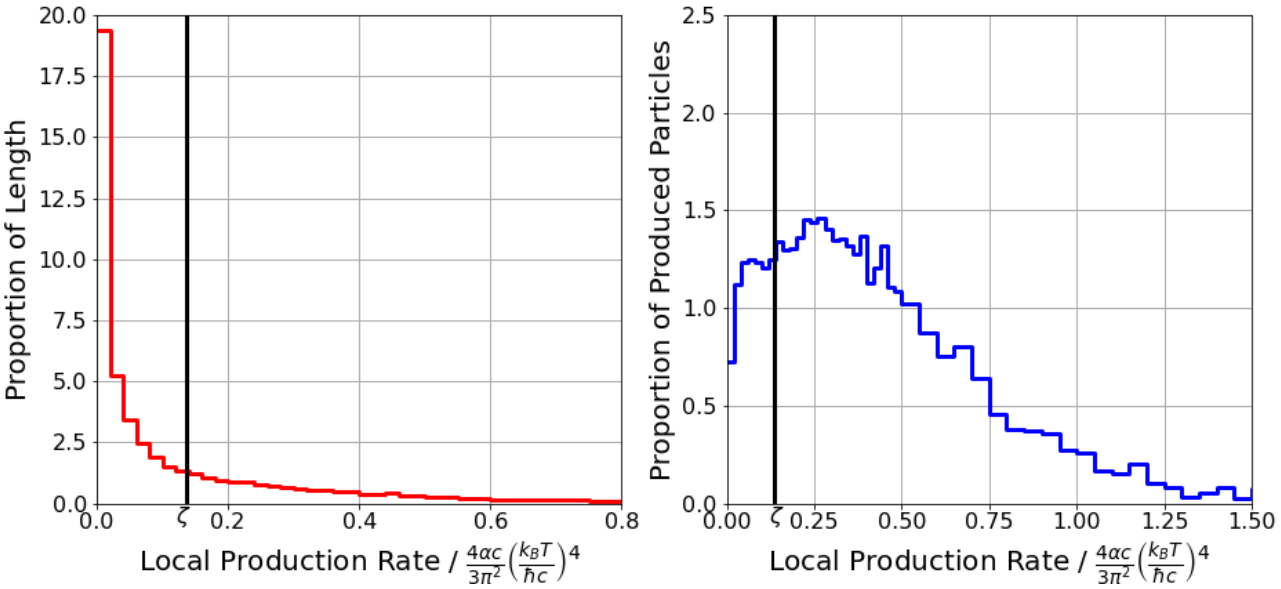

Figure 5.5: Histograms. On the x-axis is the local particle production rate, normalised to remove temperature scaling. The area under the left-hand graph is proportional to the length occupied by fields producing at the given local production rate. The area under the right-hand graph is proportional to the the contribution to the total production rate made by local fields producing at the given local production rate. The black-line gives the overall production rate. Notice that most of the field is producing at less than the overall rate (as most of the area under the left-hand graph is to the left of the black line), while most of the contribution to the overall rate is made by higher local production rates (as most of the area under the right-hand graph is to the right of the black line).

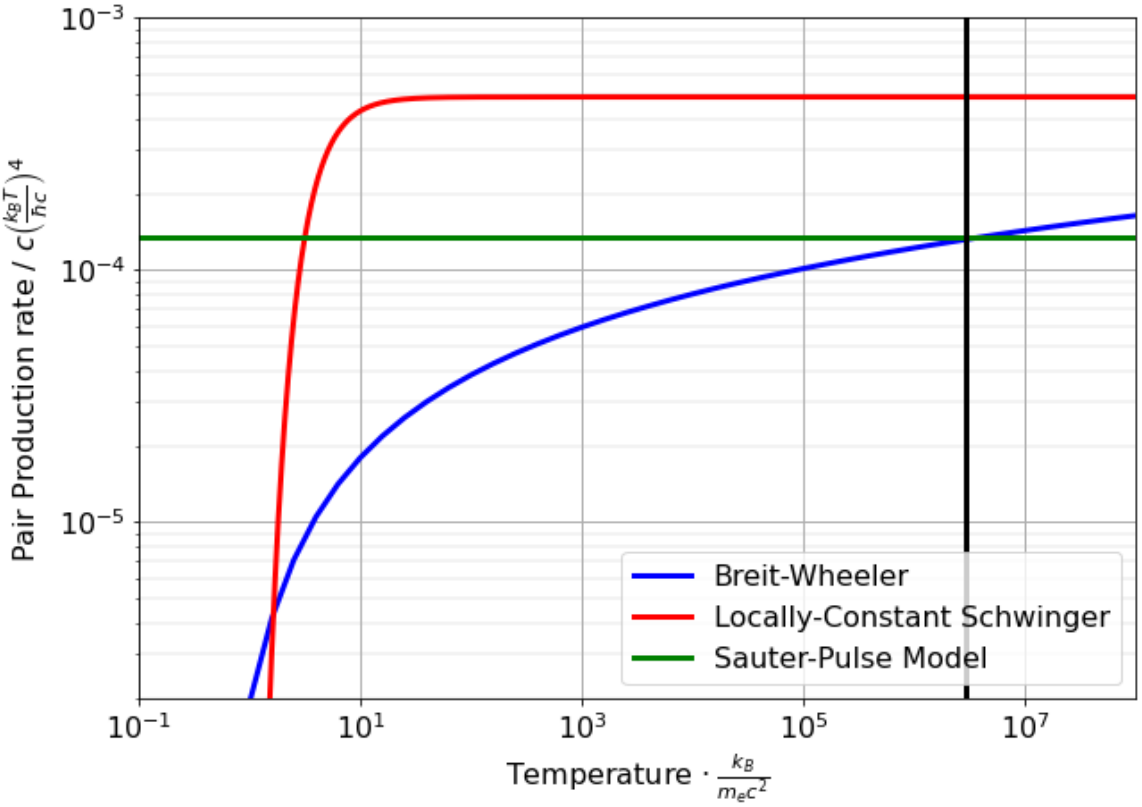

Figure 5.6: Log-log plot of different estimates of the rate of electron/positron pair production in a black-body fields for temperatures varying from below the electron rest mass to the muon rest mass. Note that quartic growth with temperature has been factorised out of the y-axis scale. The Sauter pulse model has a high-temperature assumption built in, so its value at $k_B T/(m_e c^2) < 1$ is unphysical. The Breit-Wheeler rate is calculated as a sum of numerical integrals. The black vertical line indicates where Breit-Wheeler meets the Sauter pulse model, at $k_B T \approx 2 \times 10^6 m_e c^2 = 920$ GeV. Note that the Sauter Pulse model, though here plotted over all temperatures, is only valid as an approximation at temperatures larger than the electron rest mass.

5.2.3.3 Breaking Down the Rate in Real Space and Momentum Space

Our model can give us more than simply the overall particle creation rate. Equation 5.56 is the total, spacetime-averaged rate, but our model gives us separate, "local" rates for each bump. It is interesting to ask: how spatio-temporally uniform *is* particle production? Figure 5.5 shows how the total rate is made up of contributions from widely varying local rates. We can see that most of the field is producing at less than the overall average rate, while most of the particle production is done by fields producing at a much larger rate than the overall. Therefore, we see that particle production occurs very unevenly, and most production happens in relatively small regions of unusually strong or persistent field.

It is also interesting to ask for some details of particle production in momentum space. To calculate the spectrum of produced particles, define the dimensionless particle energy, $\eta := \frac{E}{k_B T}$, and write equation 5.56 as

$$\begin{aligned} n_{\text{bb,Sauter}} &= \int_0^\infty d\eta \, \frac{dn_{\text{bb,Sauter}}}{d\eta} \\ \frac{dn_{\text{bb,Sauter}}}{d\eta} &:= \frac{2\alpha c}{\pi \sum_j \Delta X_j} \left(\frac{k_B T}{\hbar c}\right)^4 \sum_j \frac{\mathcal{E}_{0,j}^2}{\upsilon_{\text{S},j}^2} \; G\left(-1 + \eta \upsilon_{\text{S},j}/(\sqrt{4\pi\alpha}\mathcal{E}_{0,j}), \lambda'\right), \end{aligned} \tag{5.59}$$

where G is as defined in equation 5.47. This allows us to calculate the spectrum of produced particles numerically with the same sample of dimensionless Sauter pulse parameters used to calculate the total rate. The result is plotted in figure 5.7.

5.2.3.4 Discussion

Though, as discussed earlier, it can hardly be taken as conclusive, the results of section 5.2 suggest that the method outlined in section 5.1 will return a larger result than Breit-Wheeler. Why should this be the case? In section 4.2 we argued that it is self-consistent to imagine that Breit-Wheeler is a good approximation to the true pair-creation rate because the bulk of thermal Breit-Wheeler occurs via "hard" photons and fermions, and it is a well-established result that the standard perturbative expansion is legitimate in this case. There are two reasons we provided to mistrust the figure as an estimate for the total particle creation rate. First,

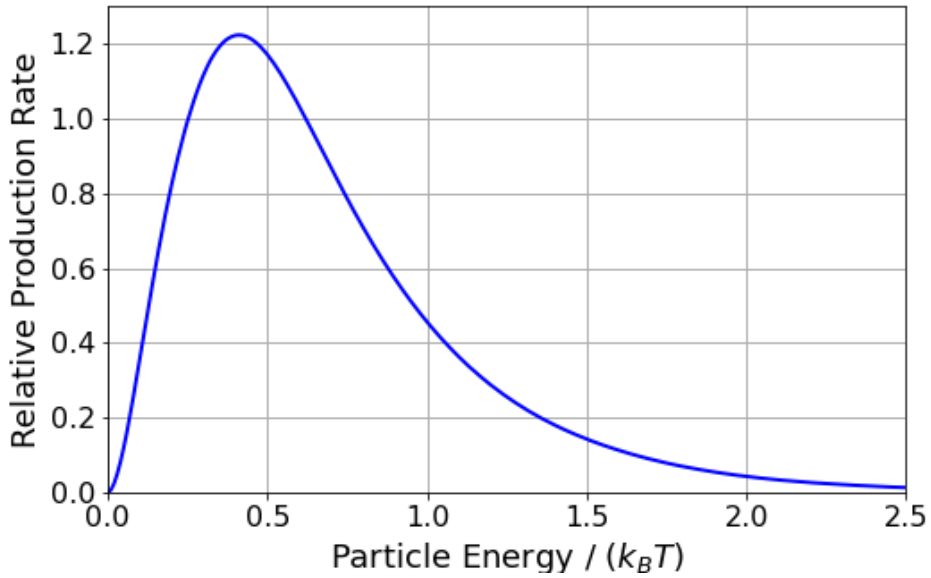

Figure 5.7: Energy distribution of produced electrons or positrons by the black-body field modelled as a statistical distribution of one-dimensional Sauter pulse bumps. Normalised to have unit area under the curve.

the coupling to the low-energy regime provided by the virtual fermion exchange allows thermal corrections to be leading order, which we showed would be likely to have the effect of suppressing the logarithmic growth with temperature. Second, there might be processes that involve soft momenta of either the colliding photons or produced particles (or both), for which the naïve perturbation expansion is known to be invalid. This second option provides a plausible way that Breit-Wheeler could underestimate particle production by an order of magnitude. It can be seen, by comparing figures 5.7 and 4.3, that the Sauter pulse calculation does indeed involve the production of softer fermions than Breit-Wheeler, but it is likely that the more significant effect would be from processes with a large number of soft input photons, which we know from the analysis discussed in sections 2.1 and 2.4 can be accounted for within the external field calculations.

The problem with this argument is, of course, that deep into this regime we really have no necessary expectation that the external field method will be any more of a sufficient estimate to the true value than Breit-Wheeler. It certainly doesn't capture *all* the relevant terms of the Feynman-diagram series: it does not include any virtual photons exchanged between the produced fermions, and it assumes that the black-body field is well approximated by the free-

field. Further work is needed to determine whether the external field method really captures all the most important physics for a good approximation, or whether it captures more than other schemes developed in thermal QFT. This issue is discussed further in Chapter 8.

Chapter 6

The Feynman-Cauchy Problem

In the previous two chapters we have compared two methods of calculating particle production in the black-body field: Breit-Wheeler, based on the standard perturbative expansion, and the Schwinger mechanism, based on QED in a vacuum-destabilising external field. In this chapter and the following, we focus on QED in a vacuum-destabilising external field, but shift to more abstract, general problems. QED in a vacuum-destabilising external field has less consensus in its formalism than regular perturbative QED. Multiple approaches have been developed whose equivalence (or otherwise) is not fully understood. These chapters are devoted to showing equivalence, under well-specified conditions, of different approaches to external-field QED while particles are being created. This chapter focuses on the relationship between solutions of the homogeneous Dirac equation and the problem of non-interacting fermions in an external field. The next, by extending to the inhomogeneous Dirac equation, can demonstrate equivalence between approaches to full interacting QED in an external field.

In 1929 Klein solved the problem of single-particle scattering at a potential step under the assumption that the Dirac equation was a wave-equation describing the time-evolution of the probability amplitude for the observation of a single particle, and found nonsensical quantities for the transmission and reflection coefficients [228]. This became known as "Klein's paradox", which was only ultimately resolved with the acceptance that the Dirac equation is not, and cannot be, wholly consistently treated as a relativistic Schrödinger equation, but is rather a "field equation" to be obeyed by an operator. Curiously, though, the quantities Klein calculated do have physical meaning. Hansen and Ravndal [229] show, by arguing from

classical analogy and from comparison with Nikishov's method, that the unphysical reflection and transmission coefficients can be used to calculate the rate of positron production.

Feynman, in his first of three major foundational papers of QED [11], does something similar. He considers the Dirac equation as a relativistic time-dependent Schrödinger equation in the context of a generic external field that acts for a finite time, but says it ought to be solved with strange boundary conditions: rather than giving a profile at an initial time or final time and propagating forwards or back, one ought to give the positive-energy component at the start time and the negative-energy component at the end time, and find the corresponding solution of the Dirac equation. This can then be used to calculate electron scattering, positron scattering, pair annihilation or pair creation, depending on the input states and inner products taken. Feynman, of course, fits this into the broader quantum field theory, such that the results are consistent [22, 23], but only with the external field interactions handled perturbatively. In particular, this allows him to define the solutions in terms of the free Hamiltonian: at every scattering event, positive-energy solutions with respect to the *free* Hamiltonian are propagated into the future, and negative-energy solutions with respect to the *free* Hamiltonian are propagated into the past. His boundary condition is therefore also defined with respect to the free Hamiltonian.

This chapter shows that Feynman's result holds in the nonperturbative case, with a field that may create particles and may still exist at the in and out times. This is done using the "Bogoliubov transformation" formalism described in section 2.2. As a practical mathematical result this is only a slight rephrasing of the FGS results, who have of course shown how all these quantities can be calculated using solutions of the Dirac equation. Pragmatically the difference is that they construct the Dirac equation solutions that satisfy the Feynman boundary condition out of retarded solutions, without stating the more direct derivation. More loosely, their highly formal method, of matrix manipulations of a basis state of solutions, obscures the connection with the single-particle Schrödinger mechanics.

Note that in this chapter and the following we use $\hbar = c = 1$ natural units, as against the rest of the thesis, where we use SI units.

6.1 Precise Statement of the General Result

We will first need to define a few objects. Define S as the manifold formed by attaching a bispinor to every point in space, $S = \mathbb{R}^3 \otimes \{0, 1, 2, 3\}$, and $\mathcal{H}_{\text{S.T.}}$ as the Hilbert space of square-integrable functions on it,

$$\mathcal{H}_{\text{S.T.}} \cong L^2(S, d^3x). \tag{6.1}$$

We will write the Hilbert-space product as

$$(f, g) := \sum_l \int d^3\mathbf{x}\, f_l^*(\mathbf{x}) g_l(\mathbf{x}), \quad (f, g)^* = (g, f). \tag{6.2}$$

Note that something like this Hilbert space is essentially implicit in FGS's work (section 2.2), though they do not strictly define it as a Hilbert space. Consider $\hat{\mathscr{H}}(t)$ defined in equation 2.12 as a time-dependent operator on $\mathcal{H}_{\text{S.T.}}$, and assume that it can partition $\mathcal{H}_{\text{S.T.}}$ into a positive and negative energy subspace[1]. In particular, we are interested in the partition between the positive and negative energy subspaces at the in and out times, t_{in} and t_{out}, which we write

$$\mathcal{H}_{\text{S.T.}} = {}_+\mathcal{H}^m_{\text{S.T.}} \oplus {}_-\mathcal{H}^m_{\text{S.T.}} = {}^+\mathcal{H}^m_{\text{S.T.}} \oplus {}^-\mathcal{H}^m_{\text{S.T.}}. \tag{6.3}$$

In the notation of FGS, ${}_\pm\mathcal{H}^m_{\text{S.T.}}$ is spanned by $\{{}_\pm\varphi_\alpha\}_\alpha$ and ${}^\pm\mathcal{H}^m_{\text{S.T.}}$ is spanned by $\{{}^\pm\varphi_\alpha\}_\alpha$. As an orthogonal bipartition of the subspace we can define projection operators ${}_\pm\hat{P}^m$ and ${}^\pm\hat{P}^m$, which map $\mathcal{H}_{\text{S.T.}} \to {}_\pm\mathcal{H}^m_{\text{S.T.}}$ and $\mathcal{H}_{\text{S.T.}} \to {}^\pm\mathcal{H}^m_{\text{S.T.}}$, respectively, and obey $\sum_\pm {}_\pm\hat{P}^m = \sum_\pm {}^\pm\hat{P}^m = 1$, $({}_\pm\hat{P}^m)^2 = {}_\pm\hat{P}^m$, $({}^\pm\hat{P}^m)^2 = {}^\pm\hat{P}^m$ and ${}_+\hat{P}^m\,{}_-\hat{P}^m = {}^+\hat{P}^m\,{}^-\hat{P}^m = 0$. The "*Feynman-Cauchy problem*" can be stated as follows

Definition (Feynman-Cauchy problem): Given a positive-energy spatial profile at the initial time, ${}_+f \in {}_+\mathcal{H}^m_{\text{S.T.}}$ and a negative-energy spatial profile at the final time, ${}^-f \in {}^-\mathcal{H}^m_{\text{S.T.}}$, find the spacetime profile $\psi(x)$ which satisfies three criteria: 1) its positive-energy component

[1]This is a weaker assumption than that made by FGS, but since we here still use FGS's results, it doesn't make much of a difference. The difficulty of defining an eigenbasis of $\hat{\mathscr{H}}$ is discussed in detail in chapter 7.

equals ${}_+f(\mathbf{x})$ at t_{in}, ${}_+\hat{P}^m\psi(t_{\text{in}}) = {}_+f$; 2) its negative-energy component equals ${}^-f$ at t_{out}, ${}^-\hat{P}^m\psi(t_{\text{out}}) = {}^- f$; and 3) it obeys the Dirac equation $(i\partial_t - \hat{\mathscr{H}}(x))\psi(x) = 0$. We assume that the solution to the Feynman-Cauchy problem is unique.

We have so far given only mathematical definitions. How do we relate these mathematical objects to physical quantum states? Feynman worked in the perturbative picture, with a field that acted for a finite time. He could therefore use the *free* Dirac Hamiltonian to define the $\pm$ partitions of $\mathcal{H}_{\text{S.T.}}$, with ${}_\pm\mathcal{H}^m_{\text{S.T.}} = {}^\pm\mathcal{H}^m_{\text{S.T.}}$. Then, ${}_+\mathcal{H}^m_{\text{S.T.}}$ is defined as the Hilbert space of electron wavefunctions, and ${}_-\mathcal{H}^m_{\text{S.T.}}$ the *conjugate* of the Hilbert space of positron wavefunctions. The complete multiparticle Fock space is then formed as the product of the Grassmann algebras[2] of both of these spaces. With this interpretation of the bispinor profiles, Feynman's result as given in Ref [11] can be stated as follows.

1. Say $\psi(x)$ is the solution to the Feynman-Cauchy problem with the output negative-energy component set to ${}^-f(\mathbf{x}) = 0$, with input positive-energy component ${}_+f(\mathbf{x})$. Then the inner product of the solution's positive-energy component at t_{out} with a given out-profile ${}^+g(\mathbf{x})$, $({}^+g, \psi(t_{\text{out}}))c_V$, gives the probability amplitude of the electron prepared with wavefunction ${}_+f(\mathbf{x})$ at t_{in} being observed as scattering to the wavefunction ${}^+g(\mathbf{x})$ at t_{out}. Also, the inner product of the solution's negative-energy component at t_{in} with a given in-profile ${}_-g(\mathbf{x})$, $({}_-g, \psi(t_{\text{in}}))c_V$, gives the probability amplitude of the electron prepared with wavefunction ${}_+f(\mathbf{x})$ and a positron prepared as the state with wavefunction ${}^+g^*(\mathbf{x})$ at t_{in} annihilating.

2. Say $\psi(x)$ is the solution to the Feynman-Cauchy problem with the input positive-energy component set to ${}_+f(\mathbf{x}) = 0$, with output negative-energy component ${}^-f(\mathbf{x})$. Then the inner product of the solution's positive-energy component at t_{out} with a given out-profile ${}^+g(\mathbf{x})$, $({}^+g, \psi(t_{\text{out}}))c_V$, gives the probability amplitude of the field creating a pair at t_{out} with the positron with wavefunction ${}^-f^*(\mathbf{x})$ and the electron with wavefunction ${}^+g(\mathbf{x})$. Also, the inner product of the solution's negative-energy component at t_{in} with a given in-profile ${}_-g(\mathbf{x})$, $({}_-g, \psi(t_{\text{in}}))c_V$, gives the probability amplitude of a positron prepared with wavefunction ${}_-g^*(\mathbf{x})$ at t_{in} being observed as scattering to the electron with wavefunction

[2]The Grassmann algebra is the algebra formed with the antisymmetric outer product.

${}_{+}f(\mathbf{x})$ at t_{out}.

Multi-particle scattering can be handled by considering antisymmetrised products of the chances of all appropriate combinations of single-particle scatterings, annihilations and creations.

6.2 Proof for a Vacuum-Destabilising External Field

This section proves this result for the case of a nonperturbative background field. The main difficulty, when compared with Feynman's perturbative method, is that we can no longer freely use the same "wavefunction" notion, as the bipartition of the space of spatial bispinor profiles into electron wavefunctions and positron conjugate wavefunctions is based on the free Hamiltonian. We will need a different way of identifying bispinor field profiles with electron and positron quantum states. To do so, we use FGS's definition of $\{\hat{a}^{\dagger}_{\alpha}(t_{\text{in}}), \hat{b}^{\dagger}_{\alpha}(t_{\text{in}})\}_{\alpha}$ (equation 2.14) as the creation operators of electrons in the energy eigenstates ${}_{+}\varphi_{\alpha}$ or positrons in the eigenstates ${}_{-}\varphi^{\dagger}_{\alpha}$. (And equivalently for the out-states.) We can construct a general electron state from the positive-energy eigenstates by

$$ {}_{+}f(\mathbf{x}) = \sum_{\alpha} {}_{+}f_{\alpha}\, {}_{+}\varphi_{\alpha}(\mathbf{x}), \quad {}^{+}f(\mathbf{x}) \;= \sum_{\alpha} {}^{+}f_{\alpha}\, {}^{+}\varphi_{\alpha}(\mathbf{x}), \tag{6.4} $$

and a positron by

$$ {}_{-}f(\mathbf{x}) = \sum_{\alpha} {}_{-}f_{\alpha}\, {}_{-}\varphi_{\alpha}(\mathbf{x}), \quad {}^{-}f(\mathbf{x}) \;= \sum_{\alpha} {}^{-}f_{\alpha}\, {}^{-}\varphi_{\alpha}(\mathbf{x}). \tag{6.5} $$

We can then define general basis-independent creation operators of the electron state $f(\mathbf{x})$ and the positron state $g(\mathbf{x})$ using equation 6.2, as $(\hat{\psi}_S, f)$ and $(f, \hat{\psi}_S)$, such that

$$ \langle 0, t_{\text{in}}| \left(\hat{\psi}_S,\, f\right) = \left(f, \hat{\psi}_S\right) |0, t_{\text{in}}\rangle = 0, \quad \text{if } f \in {}_{+}\mathcal{H}^{m}_{\text{S.T.}} \tag{6.6a} $$

$$ \left(\hat{\psi}_S,\, f\right) |0, t_{\text{in}}\rangle = \langle 0, t_{\text{in}}| \left(f, \hat{\psi}_S\right) = 0, \quad \text{if } f \in {}_{-}\mathcal{H}^{m}_{\text{S.T.}} \tag{6.6b} $$

$$ \langle 0, t_{\text{out}}| \left(\hat{\psi}_S,\, f\right) = \left(f, \hat{\psi}_S\right) |0, t_{\text{out}}\rangle = 0, \quad \text{if } f \in {}^{+}\mathcal{H}^{m}_{\text{S.T.}} \tag{6.6c} $$

$$(\hat{\psi}_S,\ f)\,|0, t_{\text{out}}\rangle = \langle 0, t_{\text{out}}|\,(f, \hat{\psi}_S) = 0, \quad \text{if } f \in {}^{-}\mathcal{H}^{m}_{\text{S.T.}}. \tag{6.6d}$$

These operators obey the anticommutation relations, $\forall\ f, g\ \in \mathcal{H}_{\text{S.T.}}$,

$$\{(\hat{\psi}, f), (\hat{\psi}, g)\} = \{(f, \hat{\psi}), (g, \hat{\psi})\} = 0 \tag{6.7a}$$

$$\{(g, \hat{\psi}), (\hat{\psi}, f)\} = (g, f). \tag{6.7b}$$

We shall therefore call, for instance, $(\hat{\psi}_S,\ {}_{+}f)$ the creation operator for an electron at t_{in} with wavefunction ${}_{+}f_l(\mathbf{x})$. It is easy to work out that this interpretation accords with the probabilities for measurements of energy and total charge, and for the overall expectation value of charge current. Whether we can attach the full interpretation of the probability amplitude for the spacetime observation of the particle to ${}_{+}f_l(\mathbf{x})$ would require further analysis. The formal difficulty of defining particle perturbations about a nontrivial "vacuum" with a nonzero expectation for the vacuum current which is not necessarily an eigenstate of energy or momentum, also creates interpretational difficulties about what it means to observe the position of a charged particle: how do we distinguish its measurement from that of the "vacuum"? Still, it is a natural generalisation of FGS's definitions, and it is the definition that allows a generalisation of Feynman's result.

With our definition of electron and positron wavefunctions in hand, we turn to a proof of the scattering amplitude formulae. First, we know that the solution to the operator equation of motion

$$i\partial_t \hat{A}(t) = [\hat{H}(t), \hat{A}(t)] \quad \text{and} \quad \hat{A}(t_0) = \hat{B}. \tag{6.8}$$

is unique and is given by

$$\hat{A}(t) = \hat{U}(t, t_0)\hat{B}\hat{U}^{\dagger}(t, t_0). \tag{6.9}$$

Next note that

$$\begin{aligned}[\hat{H}(t), (\hat{\psi}_S, f)] &= (-[\hat{H}(t), \hat{\psi}_S], f) = (\hat{\mathscr{H}}(t)\hat{\psi}_S, f) \\ &= (\hat{\psi}_S, \hat{\mathscr{H}}(t)f),\end{aligned} \tag{6.10}$$

where in the second equality we have used the Heisenberg-picture equation of motion to extract the Schrödinger-picture relation, specifically

$$\hat{U}(t)i\partial_t\hat{\psi}_H(x)\hat{U}^\dagger(t) = -[\hat{H}_S(t), \hat{\psi}_S(\mathbf{x})] = \hat{\mathscr{H}}\hat{\psi}_S(x)$$

(where we have put in an explicit subscript for the Schrödinger-picture Hamiltonian in this equation only), and in the second line we have used the fact that $\hat{\mathscr{H}}(t)$ is Hermitian in the $\mathcal{H}_{\text{S.T.}}$ product. Therefore

$$i\partial_t(\hat{\psi}_S, f(t)) = [\hat{H}(t), (\hat{\psi}_S, f(t))] \tag{6.11}$$

if and only if $f_l(x)$ obeys the Dirac equation, $i\partial_t f = \hat{\mathscr{H}} f$. Therefore

$$\hat{U}(t_2, t_1)(\hat{\psi}_S, f(t_1))\hat{U}^\dagger(t_2, t_1) = (\hat{\psi}_S, f(t_2)) \tag{6.12}$$

if and only if $f_l(x)$ obeys the Dirac equation on the region $t_2 \geq t \geq t_1$. Note in passing that this means that if $|\Psi(t)\rangle$ obeys the Schrödinger equation, then $(\hat{\psi}_S, f(t))\,|\Psi(t)\rangle$ does also. This is the most direct statement available that relates $\mathbb{C}$-valued solutions of the Dirac equation to full states in the field theory: we can "add" a solution of the Dirac equation on top of any other state-valued function of time, and preserve its obedience of the Schrödinger equation.

Define $f_{\text{in}}(x)$ as the solution to the Feynman-Cauchy problem that satisfies

$$ {}_+\hat{P}^m f_{\text{in}}(t_{\text{in}}) = {}_+f \tag{6.13a}$$

$$ {}^-\hat{P}^m f_{\text{in}}(t_{\text{out}}) = 0. \tag{6.13b}$$

Define $f_{\text{out}}(x)$ as the solution to the Feynman-Cauchy problem that satisfies

$$ {}_{+}\hat{P}^m f_{\text{out}}(t_{\text{in}}) = 0 \tag{6.14a} $$

$$ {}^{-}\hat{P}^m f_{\text{out}}(t_{\text{out}}) = {}^{-}f \tag{6.14b} $$

Define $\hat{U} := \hat{U}(t_{\text{out}}, t_{\text{in}})$ for the remainder of this chapter. Now consider the four quantities that Feynman says we can calculate using two solution of the Feynman-Cauchy problem.

1.) Electron scattering, with input profile ${}_{+}f$ and output ${}^{+}g$,

$$ \begin{aligned} \langle 0, t_{\text{out}}| ({}^{+}g, \hat{\psi}_S)\hat{U}(\hat{\psi}_S, {}_{+}f)\,|0, t_{\text{in}}\rangle &= \langle 0, t_{\text{out}}| ({}^{+}g, \hat{\psi}_S)\hat{U}(\hat{\psi}_S, f_{\text{in}}(t_{\text{in}}))\,|0, t_{\text{in}}\rangle \\ &= \langle 0, t_{\text{out}}| ({}^{+}g, \hat{\psi}_S)(\hat{\psi}_S, f_{\text{in}}(t_{\text{out}}))\hat{U}\,|0, t_{\text{in}}\rangle \\ &= ({}^{+}g, f_{\text{in}}(t_{\text{out}}))c_V - \langle 0, t_{\text{out}}| (\hat{\psi}_S, f_{\text{in}}(t_{\text{out}}))({}^{+}g, \hat{\psi}_S)\hat{U}\,|0, t_{\text{in}}\rangle \\ &= ({}^{+}g, f_{\text{in}}(t_{\text{out}}))c_V. \end{aligned} \tag{6.15a} $$

In the first line we can replace ${}_{+}f$ with $f_{\text{in}}(t_{\text{in}})$ because of equations 6.13a and 6.6b. In the second line we have used equation 6.12, in the third line we have used equations 6.7b and 2.16, and in the last line we have used equations 6.13b and 6.6c.

2.) Pair Annihilation, with input electron profile ${}_{+}f$ and positron profile ${}_{-}g$,

$$ \begin{aligned} \langle 0, t_{\text{out}}|\, \hat{U}({}_{-}g, \hat{\psi}_S)(\hat{\psi}_S, {}_{+}f)\,|0, t_{\text{in}}\rangle &= \langle 0, t_{\text{out}}|\, \hat{U}({}_{-}g, \hat{\psi}_S)(\hat{\psi}_S, f_{\text{in}}(t_{\text{in}}))\,|0, t_{\text{in}}\rangle \\ &= ({}_{-}g, f_{\text{in}}(t_{\text{in}}))c_V - \langle 0, t_{\text{out}}| (\hat{\psi}_S, f_{\text{in}}(t_{\text{out}})\hat{U}({}_{-}g, \hat{\psi}_S))\,|0, t_{\text{in}}\rangle \\ &= ({}_{-}g, f_{\text{in}}(t_{\text{in}}))c_V. \end{aligned} \tag{6.15b} $$

In the first line we can replace ${}_{+}f$ with $f_{\text{in}}(t_{\text{in}})$ because of equations 6.13a and 6.6b. In the second line we have used equations 6.7b, 6.12 and 2.16, and in the last line we have used equations 6.13b and 6.6c.

3.) Positron scattering, with input profile ${}_-g$ and output ${}^-f$,

$$\begin{aligned}\langle 0, t_{\text{out}}|\,(\hat{\psi}_S,\, {}^-f)\hat{U}({}_-g, \hat{\psi}_S)\,|0, t_{\text{in}}\rangle &= \langle 0, t_{\text{out}}|\,(\hat{\psi}_S,\, f_{\text{out}}(t_{\text{out}}))\hat{U}({}_-g, \hat{\psi}_S)\,|0, t_{\text{in}}\rangle \\ &= \langle 0, t_{\text{out}}|\,\hat{U}(\hat{\psi}_S,\, f_{\text{out}}(t_{\text{in}}))({}_-g, \hat{\psi}_S)\,|0, t_{\text{in}}\rangle \\ &= (f_{\text{out}}(t_{\text{in}}),\, {}_-g)c_V - \langle 0, t_{\text{out}}|\,\hat{U}({}_-g, \hat{\psi}_S)(\hat{\psi}_S,\, f_{\text{out}}(t_{\text{out}}))\,|0, t_{\text{in}}\rangle \\ &= (f_{\text{out}}(t_{\text{in}}),\, {}_-g)c_V.\end{aligned} \tag{6.15c}$$

In the first line we can replace ${}^-f$ with $f_{\text{out}}(t_{\text{out}})$ because of equations 6.14b and 6.6c. In the second line we have used equation 6.12, in the third line we have used equations 6.7b and 2.16, and in the last line we have used equations 6.14a and 6.6b.

4.) Pair creation, with output electron profile ${}^+f$ and positron profile ${}^-g$,

$$\begin{aligned}\langle 0, t_{\text{out}}|\,({}^+f, \hat{\psi}_S)(\hat{\psi}_S,\, {}^-g)\hat{U}\,|0, t_{\text{in}}\rangle &= \langle 0, t_{\text{out}}|\,(\,f_{\text{out}}(t_{\text{out}}), \hat{\psi}_S)(\hat{\psi}_S,\, {}^-g)\hat{U}\,|0, t_{\text{in}}\rangle \\ &= (f_{\text{out}}(t_{\text{out}}),\, {}^-g)c_V - \langle 0, t_{\text{out}}|\,(\hat{\psi}_S,\, {}^-g)\hat{U}(\,f_{\text{out}}(t_{\text{in}}), \hat{\psi}_S)\,|0, t_{\text{in}}\rangle \\ &= (f_{\text{out}}(t_{\text{out}}),\, {}^-g)c_V.\end{aligned} \tag{6.15d}$$

In the first line we can replace ${}^-f$ with $f_{\text{out}}(t_{\text{out}})$ because of equations 6.14b and 6.6c. In the second line we have used equations 6.7b, 6.12 and 2.16, and in the last line we have used equations 6.14a and 6.6b.

6.3 Discussion

Equation 6.15 gives the appropriate generalisation of Feynman's result. It shows how one can calculate the four rudimentary processes of electrons and positrons in an external field by solving the the Dirac equation with slightly peculiar boundary conditions, with a precise specification of how to interpret bispinor profiles as quantum mechanical states.

How original is this result? It is at the heart of Nikishov's method, developed and explained in FGS, that we solve the $\mathbb{C}$-valued Dirac equation in order to solve quantum elec-

trodynamics in an external field. Nikishov and FGS, though, use the retarded solutions of the Dirac equation, and assemble the the physical quantities from formal matrix manipulations of inner products of these results. That their results agree with ours is demonstrated in Appendix D (which is therefore also an alternative derivation of our result). Their method is formal and highly basis-dependent. This work, therefore, shows the continuity of their method with the single-particle Schrödinger equation interpretation of the Dirac equation far more clearly. As a practical calculational result, then, this work is only a rephrasing of well-established methods, unlikely to be important since the retarded solutions are more easy to calculate. But as a work of clarification of the relationship between different formalisms extant in the literature it is significant and new.

Chapter 7

Causal Propagators of the Dirac Equation

In this chapter we move from considering the homogeneous Dirac equation to the inhomogeneous Dirac equation. By doing this, we are able to study the propagator of the Dirac equation, since the propagator is a Green's function, which can be defined as a mapping from the space of source profiles to solutions to the inhomogeneous Dirac equation, as in equation 1.3. We specifically demonstrate that four different causal propagators used in the literature on quantum electrodynamics in a vacuum-destabilising external field are equivalent, under certain well-specified conditions and assumptions. As discussed in section 2.1, these propagators are essentially the only point of potential confusion between different approaches: they can be used to construct any quantity of interest using other mathematical objects and procedures which are, to within the mathematical precision one can expect of a quantum field theory, well-defined with wide consensus agreement. We restrict attention to the case that $J(x)$ is supported only on a finite time, between $t_{\text{in}} < 0$ and $t_{\text{out}} > 0$. (The assumption that such an operator defines the Green's function well is discussed in section 7.4.3.1.) We then impose the condition that before the time $t_{\text{in}} < 0$ and after time $t_{\text{out}} > 0$ there is no electric field, and that the gauge field is constant in time. This implies that it can be written with the following restricted dependencies,

$$A_\mu(x) = \begin{cases} (A_0^{\text{out}}, \mathbf{A}^{\text{out}}(\mathbf{x})), & t \geq t_{\text{out}} \\ (A_0^{\text{in}}, \mathbf{A}^{\text{in}}(\mathbf{x})), & t \leq t_{\text{in}}. \end{cases} \tag{7.1}$$

Under these conditions, it is possible to demonstrate that all propagators return solutions of the inhomogeneous equation that obey the "Feynman boundary condition", defined in section 7.1.2.3, where we also argue that such a condition uniquely specifies the solution.

Although this is the principle explicit result, much of the work is towards a different end. Section 7.1 is dedicated to a redefinition of Schwinger's proper-time quantum mechanics from scratch, with a re-derivation of the propagator 1.6. Schwinger formulated his proper-time quantum mechanics using Dirac's bra-ket notation, which does not account for the difficulties involved with unbounded operators and their continuous eigenbases [13]. This work applies formalisms to the proper-time quantum mechanics, such as von Neumann's direct integral [230], which have been applied in rigorous formulations of non-relativistic quantum mechanics to account for unbounded operators [31]. Our argument, though, is not a full rigorous proof, as through section 7.1 we make a number of mathematical assumptions. As discussed in section 7.4.3, these assumptions are the sort that implementations of the bra-ket formalism frequently make implicitly. We have chosen to use this formalism in the belief that it is an advance to make mathematical assumptions explicit which have previously been left implicit, as the more conventional physics formalism does. It therefore acts as an initial step towards formulating Schwinger's proper-time quantum mechanics in the rigorous terms that have been developed for regular quantum mechanics since he wrote. This is an alternative to the modern proper-time formulations based on the Euclidean path-integral discussed in section 2.3.

Demonstrating equivalence of our Green's function with Schwinger's propagator (1.6) is then trivial, as shown in section 7.3.1. In section 7.2 we demonstrate that solutions derived using FGS's causal propagator also obey the Feynman boundary condition, and in section 7.3.2 we demonstrate the same for solutions derived using two different varieties of analytic continuation from complexified parameters. We therefore demonstrate the equivalence of four different causal propagators, with caveats discussed in section 7.4.

The bulk section 7.1 is quite mathematical. To aid understanding, there is a short paragraph to the start of every subsection, describing in qualitative terms what will then be demonstrated mathematically, and providing some motivation for some of the choices of what is presented.

7.1 The Inhomogeneous Proper-Time Dirac Equation

7.1.1 Basic Definitions

The main result we are after is a relationship between solutions of two different inhomogeneous differential equations, the regular, "spacetime Dirac equation" (1.3b) and the "proper-time Dirac equation" (1.7). Solutions of these equations can be seen as paths in two different Hilbert spaces: solutions of the spacetime Dirac equation are time-dependent paths in the Hilbert space of bispinor spatial profiles, $\mathcal{H}_{\text{S.T.}}$, while solutions of the proper-time Dirac equation are proper-time-dependent paths in the Hilbert space of bispinor *spacetime* profiles, $\mathcal{H}_{\text{P.T.}}$.

Both the spacetime and inhomogeneous Dirac equations can be written in Hamiltonian form (i.e. as Schrödinger equations), with spacetime Hamiltonian written as $\hat{\mathscr{H}}_m$ and proper-time Hamiltonian as $\hat{H}_{\text{P.T.}}$. Our method to arrive at our main result relies, essentially, on using the eigenbases of these operators. (Specifically for the spacetime Hamiltonian, the eigenbases of $\hat{\mathscr{H}}_m^{\text{in/out}}$, or the Hamiltonian before the in-time and after the out-time.) The spectral theorem guarantees that there exists an orthogonal eigenbasis for any bounded Hermitian operator. The problem is that neither $\hat{\mathscr{H}}_m$ nor $\hat{H}_{\text{P.T.}}$ is necessarily either bounded or Hermitian. In this section we state the generalisation of the spectral theorem appropriate to unbounded Hermitian operators. In the following two sections we apply it to construct diagonal representations of the Hamiltonians by relating them to unbounded Hermitian operators.

Define M and S as the manifolds formed by attaching a bispinor to every point in spacetime and space, respectively,

$$M = \mathbb{R}^{3\oplus 1} \otimes \{0,1,2,3\}, \qquad S = \mathbb{R}^3 \otimes \{0,1,2,3\}. \tag{7.2}$$

We are interested in the Hilbert spaces defined by their representation as square-integrable functions on M and S,

$$\mathcal{H}_{\text{P.T.}} \cong L^2(M, d^4x), \quad \mathcal{H}_{\text{S.T.}} \cong L^2(S, d^3x), \tag{7.3}$$

where "P.T" stands for "proper-time" and "S.T." stands for "Spacetime". Denote the inner products on these spaces $(\varphi, \phi)_{\text{P.T.}}$ and $(\varphi, \phi)_{\text{S.T.}}$, respectively. There are three basic operators that we consider: the "proper-time Hamiltonian" operator $\hat{H}_{\text{P.T.}}$ on $\mathcal{H}_{\text{P.T.}}$ (1.4), and two operators on $\mathcal{H}_{\text{S.T.}}$,

$$\hat{\Pi}^{\text{in/out}} := \gamma^i(\partial_i + ieA_i^{\text{in/out}}) \tag{7.4a}$$

$$\hat{\mathscr{H}}_m^{\text{in/out}} := \gamma^0(m - i\hat{\Pi}^{\text{in/out}}) + eA_0^{\text{in/out}}. \tag{7.4b}$$

The operator (7.4b) is the Dirac Hamiltonian for times $t \leq t_{\text{in}}$ or $t \geq t_{\text{out}}$, since at these times the homogeneous spacetime Dirac equation with mass m can be written on elements of $C^1(\mathbb{R}; \mathcal{H}_{\text{S.T.}})$ as equation 2.12, with $\hat{\mathscr{H}} = \hat{\mathscr{H}}_m^{\text{in/out}}$.

In Sections 7.1.2 and 7.1.3 we construct representations of, respectively, $\mathcal{H}_{\text{S.T.}}$ and $\mathcal{H}_{\text{P.T.}}$ in which $\hat{\mathscr{H}}_m^{\text{in/out}}$ and $\hat{H}_{\text{P.T.}}$ are represented by multiplication operators. To do this, we use the "direct integral" version of the spectral theorem, as presented in e.g. Ref [31]. If $\hat{A}$ is a self-adjoint operator, then we denote its spectrum by $\sigma(\hat{A})$, its corresponding representation of the Hilbert space by $\mathcal{H}_{\hat{A}}$, and the unitary transformation from the abstract space to $\mathcal{H}_{\hat{A}}$ by $\hat{U}_{\hat{A}}$. The spectral theorem tells us that that there exists a measure, $\mu_{\hat{A}}$, on $\sigma(\hat{A})$, such that

$$\mathcal{H}_{\hat{A}} := \int_{\sigma(\hat{A})}^{\oplus} d\mu_{\hat{A}}(\alpha)\, \mathcal{H}_{\hat{A}}^{\alpha}. \tag{7.5a}$$

Note the "$\oplus$" written as an upper limit is the standard notation to denote that the integral is a "direct integral", which bares a similar relation to the direct sum of vector spaces that a regular integral bares to a regular sum. Elements $\varphi \in \mathcal{H}_{\hat{A}}$ are sections on the spectrum with values in the generalised subspaces, $\varphi(\alpha \in \sigma(\hat{A})) \in \mathcal{H}_{\hat{A}}^{\alpha}$. We write the product on these subspaces as $(a, b)_\alpha$, and the Hilbert space product is represented by

$$(\varphi, \phi) = \int_{\sigma(\hat{A})} d\mu_{\hat{A}}(\alpha)\ (\varphi(\alpha), \phi(\alpha))_\alpha. \tag{7.5b}$$

On this space, $\hat{A}$ is represented by a multiplication operator,

$$[\hat{A}\varphi](\alpha) = \alpha\varphi(\alpha). \tag{7.5c}$$

$\hat{\Pi}^{\text{in/out}}$ and $\hat{H}^2_{\text{P.T.}}$ are symmetric[1]. We assume that they are also self-adjoint, which means we assume that their domain equals the domain of their adjoint. This allows us to use the spectral theorem on them directly, and we then use their spectral representations to construct those of $\hat{\mathscr{H}}_m^{\text{in/out}}$ and $\hat{H}_{\text{P.T.}}$. The relationship between these representations is examined in sections 7.1.4 and 7.1.5. In section 7.1.6 these results are used to analyse the relationship between the solutions of the inhomogeneous spacetime Dirac equation (1.3b) and the inhomogeneous proper-time Dirac equation, defined on elements of $C^1(\mathbb{R}; \mathcal{H}_{\text{P.T.}})$ as equation 1.7. We use the convention that the same symbol is used to represent the same vector as it appears in different representations of the same Hilbert space, with the representation being distinguished by the argument of the vector, i.e. if a vector in the abstract space is written as $\varphi \in \mathcal{H}$ then

$$[\hat{U}_{\hat{A}}\varphi](\alpha) = \varphi(\alpha). \tag{7.6}$$

We will also write vectors in Hilbert spaces defined as direct sums, $\mathcal{H}_A \oplus \mathcal{H}_B$, as column vectors. The convention we use is that the top row of the column contains the vector in the space on the left side of the sum, i.e.

$$\psi = \begin{bmatrix} \phi \\ \varphi \end{bmatrix}, \quad \psi \in \mathcal{H}_A \oplus \mathcal{H}_B,\ \phi \in \mathcal{H}_A,\ \varphi \in \mathcal{H}_B. \tag{7.7}$$

[1] We use the term "symmetric" here as in the maths literature, to describe a property close to what physicists generally call "Hermitian". The term "Hermitian" is avoided to avoid confusion with the property of being "self-adjoint"; the usual physics vocabulary does not distinguish between the two properties.

7.1.2 A Representation of $\mathcal{H}_{\text{S.T.}}$ in which the Dirac Hamiltonian is Diagonal

---

We use equation 7.4 to construct the generalised eigenbasis of $\hat{\mathscr{H}}_m^{\text{in/out}}$ - or, more precisely, to construct the representation of the Hilbert space of spatial bispinor profiles, $\mathcal{H}_{\text{S.T.}}$, in which $\hat{\mathscr{H}}_m^{\text{in/out}}$ is diagonal. This is possible because $\hat{\Pi}^{\text{in/out}}$ is Hermitian, so we can use the spectral theorem on it. It is worth noting that $\hat{\mathscr{H}}_m^{\text{in/out}}$ is itself Hermitian *if* m is real. However, we must also consider the possibility that m is imaginary, in order for the solutions to provide a complete basis of *spacetime* profiles, as explained in section 7.1.3.

This diagonal representation allows us to do two important things. First, because at times $t < t_{\text{in}}$ and $t > t_{\text{out}}$ the Hamiltonian is constant, it commutes with the time-translation operator and so we can use its diagonal basis to define a time-translation operator for the spacetime Dirac equation with mass m at times $t < t_{\text{in}}$ and $t > t_{\text{out}}$. Second, we can define a bipartition of $\mathcal{H}_{\text{S.T.}}$ between positive and negative energy states for every mass. This allows us to define the "Feynman boundary condition" for any m as spacetime bispinor profiles that have only positive-energy component at t_{in} and negative-energy component at t_{out}.

Both of these tasks reveal how the existence of imaginary m complicates matters. Introducing imaginary m means introducing complex energy values, which means time-translation is no longer unitary and we have to be careful about excluding the possibility of exponential growth. Also, the bipartition between positive and negative energy subspaces is only orthogonal if m is real.

7.1.2.1 Construction of the Representation

As discussed in section 7.1.1, we can define a direct integral representation of $\mathcal{H}_{\text{S.T.}}$ on which $\hat{\Pi}^{\text{in/out}}$ is represented by a multiplication operator,

$$\mathcal{H}_{\text{in/out},\hat{\Pi}} := \int_{\sigma(\hat{\Pi}^{\text{in/out}})}^{\oplus} d\mu_{\text{in/out}}(\Pi)\ \mathcal{H}^{\Pi}_{\text{in/out}}. \tag{7.8}$$

Because γ^0 is a bounded operator that anticommutes with $\hat{\Pi}^{\text{in/out}}$, it can be represented as a transformation between the generalised subspaces, written in the form,

$$(\gamma^0\phi)(\Pi) = \hat{\gamma}^0_{\text{in/out}}(-\Pi)\phi(-\Pi), \tag{7.9}$$

where $\hat{\gamma}^0(\Pi):\ \mathcal{H}^{\Pi}_{\text{in/out}} \to \mathcal{H}^{-\Pi}_{\text{in/out}}$. Since $(\gamma^0)^2 = 1$,

$$\hat{\gamma}^0_{\text{in/out}}(\Pi)\hat{\gamma}^0_{\text{in/out}}(-\Pi) = 1. \tag{7.10}$$

Since this is an invertible unitary transformation, we know from its existence that Π is in the point spectrum if and only if $-\Pi$ is, that Π is in the continuous spectrum if and only if $-\Pi$ is, and that $\dim(\mathcal{H}^{\Pi}_{\text{in/out}}) = \dim(\mathcal{H}^{-\Pi}_{\text{in/out}})$. We can therefore choose the measure to be such that we can define a new representation $\mathcal{H}_{\text{in/out},|\hat{\Pi}|}$,

$$\begin{aligned}\mathcal{H}_{\text{in/out},|\hat{\Pi}|} := &\int^{\oplus}_{\sigma(\hat{\Pi}^{\text{in/out}})>0} d\mu_{\text{in/out}}(\Pi)\ \mathcal{H}^{\Pi}_{\text{in/out}} \oplus \mathcal{H}^{-\Pi}_{\text{in/out}} \\ &+ \mu_{\text{in/out}}(\{0\})\mathcal{H}^0_{\text{in/out}}.\end{aligned} \tag{7.11}$$

We write $\hat{U}^{\text{in/out}}_{|\hat{\Pi}|}$ for the unitary transformation from $\mathcal{H}_{\text{P.T.}}$ to $\mathcal{H}_{\text{in/out},|\hat{\Pi}|}$, and $(a,b)_{\Pi\oplus-\Pi}$ for the product on the generalised subspaces. Note that we can write $\mathcal{H}^0_{\text{in/out}}$ as a true subspace as we only need to include it if 0 is in the point spectrum. If 0 is in the continuous spectrum then we can neglect it from consideration, since two sections that differ on a region of measure 0 are equivalent as elements of the Hilbert space. We write sections in this representation as $\phi^{\text{in/out}}(\Pi)$, with the superscript included to distinguish the representation since in this case the usual practice of distinguishing by the argument would be ambiguous.

Now consider the operators on $\mathcal{H}^{\Pi}_{\text{in/out}} \oplus \mathcal{H}^{-\Pi}_{\text{in/out}}$ for $m \neq 0$, $m \neq \pm i\Pi$,

$$\hat{P}^{\pm}_{\text{in/out},\Pi,m}: \quad \begin{bmatrix} a \\ b \end{bmatrix} \mapsto \frac{1}{2}\begin{bmatrix} a \pm \frac{\sqrt{m^2+\Pi^2}}{m-i\Pi}\hat{\gamma}^0_{\text{in/out}}(-\Pi)b \\ b \pm \frac{\sqrt{m^2+\Pi^2}}{m+i\Pi}\hat{\gamma}^0_{\text{in/out}}(\Pi)a. \end{bmatrix} \tag{7.12}$$

and on $\mathcal{H}^0_{\text{in/out}}$,

$$\hat{P}^{\pm}_{\text{in/out},0,m}: \quad a \mapsto \frac{1}{2}\left(1 \pm \hat{\gamma}^0(0)\right)a. \tag{7.13}$$

We neglect the $\Pi \neq 0$, $m = \pm i\Pi$ case, where the operator $\hat{\mathscr{H}}_m^{\text{in/out}}$ is not diagonalizable. We argue in section 7.4.3 that the assumption that this will not affect our overall argument amounts to a minimal assumption on the spectrum of $\hat{H}_{\text{P.T.}}$ and $\hat{\Pi}^{\text{in/out}}$. These operators obey $(\hat{P}^{\pm}_{\text{in/out},\Pi,m})^2 = \hat{P}^{\pm}_{\text{in/out},\Pi,m}$ and $\sum_{\pm} \hat{P}^{\pm}_{\text{in/out},\Pi,m} = 1$. They are therefore a complete set of projection operators, and we can define their target spaces as $\mathcal{H}^{\Pi,m,\pm}_{\text{in/out}}$, with $\mathcal{H}^{\Pi}_{\text{in/out}} \oplus \mathcal{H}^{-\Pi}_{\text{in/out}} = \mathcal{H}^{\Pi,m,+}_{\text{in/out}} \oplus \mathcal{H}^{\Pi,m,-}_{\text{in/out}}$. Therefore, for every $m \in \mathbb{C}$, there exists a decomposition of every element $\phi \in \mathcal{H}_{\text{S.T.}}$, $\phi^{\text{in/out}}(\Pi) \in \mathcal{H}^{\Pi}_{\text{in/out}} \oplus \mathcal{H}^{-\Pi}_{\text{in/out}}$,

$$\phi(\Pi) = \textstyle\sum_{\pm} {}_{\pm}\phi(\Pi)_m, \quad \left[\hat{\mathscr{H}}^{\text{in}}_m \phi\right](\Pi) = \sum_{\pm} E^{\text{in}}_{\pm}(m,\Pi)\, {}_{\pm}\phi_m(\Pi) \tag{7.14a}$$

$$\phi(\Pi) = \textstyle\sum_{\pm} {}^{\pm}\phi_m(\Pi), \quad \left[\hat{\mathscr{H}}^{\text{out}}_m \phi_m\right](\Pi) = \sum_{\pm} E^{\text{out}}_{\pm}(m,\Pi)\, {}^{\pm}\phi_m(\Pi), \tag{7.14b}$$

where

$${}_{\pm}a_m := \hat{P}^{\pm}_{\text{in},\Pi,m} a, \quad {}^{\pm}a_m := \hat{P}^{\pm}_{\text{out},\Pi,m} a \tag{7.15}$$

$$E^{\text{in/out}}_{\pm}(m,\Pi) := \pm\sqrt{m^2 + \Pi^2} + eA^{\text{in/out}}_0. \tag{7.16}$$

7.1.2.2 The Time-Translation Operator

We can define a time-translation operator for the homogeneous spacetime Dirac equation with mass m on $\mathcal{H}_{\text{in/out},|\hat{\Pi}|}$,

$$[\hat{T}_m(t,t')\phi]^{\text{in}}(\Pi) = \sum_{\pm} {}_{\pm}\phi_m(\Pi) e^{-iE^{\text{in}}_{\pm}(m,\Pi)(t-t')}, \quad t,t' \leq t_{\text{in}} \tag{7.17a}$$

$$[\hat{T}_m(t,t')\phi]^{\text{out}}(\Pi) = \sum_{\pm} {}^{\pm}\phi_m(\Pi) e^{-iE^{\text{out}}_{\pm}(m,\Pi)(t-t')}, \quad t,t' \geq t_{\text{out}}. \tag{7.17b}$$

When acting on the domain of $\hat{\mathscr{H}}^{\text{in}}_m$ in $\mathcal{H}_{\text{S.T.}}$ it returns the unique solution for the spacetime Dirac equation with mass m in $C^1((-\infty, t_{\text{in}}]; \mathcal{H}_{\text{S.T.}})$ or $C^1([t_{\text{out}}, \infty); \mathcal{H}_{\text{S.T.}})$ that equals the input state at t'. The fact that it returns a solution of the Dirac equation with mass m and

leaves it invariant if $t = t'$ is clear from inspection. That the solution it gives is unique and that it is necessarily in the Hilbert space is shown in Appendix G. If m is real then $\hat{T}_m(t, t')$ is unitary.

7.1.2.3 The Bipartition of $\mathcal{H}_{\text{S.T.}}$ and the "Feynman Boundary Condition"

Define ${}_{\pm}\hat{P}^m/{}^{\pm}\hat{P}^m$ as the operators on $\mathcal{H}_{\text{S.T.}}$ induced by the $\hat{P}^{\pm}_{\text{in/out},\Pi,m}$ operators on the generalised subspaces: ${}_{\pm}\hat{P}^m : \ \phi(\Pi) \mapsto \hat{P}^{\pm}_{\text{in},\Pi,m}\phi(\Pi)$ and ${}^{\pm}\hat{P}^m : \ \phi(\Pi) \mapsto \hat{P}^{\pm}_{\text{out},\Pi,m}\phi(\Pi)$. We can then define the target spaces of ${}_{\pm}\hat{P}^{\text{in}}$ as ${}_{\pm}\mathcal{H}^m_{\text{S.T.}}$, and the target spaces of ${}^{\pm}\hat{P}^m$ as ${}^{\pm}\mathcal{H}^m_{\text{S.T.}}$, such that

$$\mathcal{H}_{\text{S.T.}} = {}_{+}\mathcal{H}^m_{\text{S.T.}} \oplus {}_{-}\mathcal{H}^m_{\text{S.T.}} = {}^{+}\mathcal{H}^m_{\text{S.T.}} \oplus {}^{-}\mathcal{H}^m_{\text{S.T.}}. \tag{7.18}$$

Note that this bipartition is orthogonal if m is real, and

$${}_{\pm}\phi_m \in {}_{\pm}\mathcal{H}^m_{\text{S.T.}}, \quad {}^{\pm}\phi_m \in {}^{\pm}\mathcal{H}^m_{\text{S.T.}}. \tag{7.19}$$

Definition (Feynman boundary condition): An element of $C(L; \mathcal{H}_{\text{S.T.}})$, where $t_{\text{in}}, t_{\text{out}} \in L \subseteq \mathbb{R}$ is said to obey the "Feynman boundary condition (with mass m)" if and only if it has 0 component in ${}_{+}\mathcal{H}^m_{\text{S.T.}}$ at t_{in} and 0 component in ${}^{-}\mathcal{H}^m_{\text{S.T.}}$ at t_{out}.

The name is chosen as the boundary condition is a natural generalisation of that discussed by Feynman for the free particle causal propagator [11]. It is a straightforward consequence of the linearity of the boundary condition that it uniquely determines a solution to the inhomogeneous spacetime Dirac equation if and only if there exists no nontrivial solution to the homogeneous spacetime Dirac equation that satisfies the boundary condition. A closely related condition is discussed by FGS (in Ref. [12], chapter 2.4). They demand that the determinant of the transformation matrix between the basis of negative energy in-states and negative energy out-states is non-zero. This would be the case if and only if there are no vectors in the space of negative energy in-states which transform to vectors with no components in the negative energy out-space - i.e. there are no nontrivial solutions to the homogeneous spacetime Dirac

equation which satisfy the Feynman boundary condition. FGS introduce this as a condition for the Fock spaces formed by the action of the creation operators on the in and out vacua to coincide. The physical implications of this condition being violated are unclear, but probably significant: it seems to correspond to a situation where the vacuum states at the in and out times are too radically different to be described in terms of particle perturbations of each other, and hence the whole approach to external-field QED that thinks in terms of perturbative particle processes expanded about the transition from vacuum to vacuum breaks down. Therefore, in physical situations where any of the approaches to external-field QED being considered in this chapter are appropriate, this condition ought to be satisfied.

7.1.3 A Representation of $\mathcal{H}_{\text{P.T.}}$ in which $\hat{H}_{\text{P.T.}}$ is Diagonal

---

We construct the representation of the Hilbert space of spacetime bispinor profiles, $\mathcal{H}_{\text{P.T.}}$, in which $\hat{H}_{\text{P.T.}}$ (the proper-time Hamiltonian) is diagonal. To do this we use the fact that $\hat{H}^2_{\text{P.T.}}$ is Hermitian. This also means we know that the spectrum of $\hat{H}^2_{\text{P.T.}}$ is entirely real, and hence the spectrum of $\hat{H}_{\text{P.T.}}$ is restricted to the real and imaginary axes.

The *spacetime* Dirac equation can be written as $(\hat{H}_{\text{P.T.}} + m)\psi = 0$. This means that eigenstates of $\hat{H}_{\text{P.T.}}$ with eigenvalues λ are solutions of the Dirac equation with mass $m = -\lambda$. The reason we must consider imaginary masses can therefore be stated in the following terms. We want to represent any arbitrary square-integrable spacetime bispinor profile in terms of a sum (or integral) of solutions of the Dirac equation with different masses. This is what it means to use the eigenbasis of $\hat{H}_{\text{P.T.}}$, and it is clearly assumed to be possible by Schwinger. We do not, though, have any good reason to think that any square-integrable spacetime profile can be decomposed as a sum of solutions of the Dirac equation with real masses. In general, it seems that for Dirac equation solutions to provide a complete basis for $\mathcal{H}_{\text{P.T.}}$, we require m to range over both the imaginary and real axes.

As discussed in section 7.1.1, we can define a direct integral representation of $\mathcal{H}_{\text{P.T.}}$ on which $\hat{H}^2_{\text{P.T.}}$ is represented by a multiplication operator,

$$\mathcal{H}_{\hat{H}^2_{\text{P.T.}}} := \int^{\oplus}_{\sigma(\hat{H}^2_{\text{P.T.}})} d\mu_{\hat{H}^2_{\text{P.T.}}}(\lambda^2)\, \mathcal{H}^{\lambda^2}_{\hat{H}^2_{\text{P.T.}}}. \tag{7.20}$$

Consider the representation of $\hat{H}_{\text{P.T.}}$ on this space. Since it commutes with $\hat{H}^2_{\text{P.T.}}$, it must be able to be represented by an operator $\hat{H}_{\text{P.T.}}(\lambda^2)$ on every $\mathcal{H}^{\lambda^2}_{\hat{H}^2_{\text{P.T.}}}$ space, and since $(\hat{H}_{\text{P.T.}}(\lambda^2))^2 = \lambda^2$, we know that if $\lambda \neq 0$ then $\hat{H}_{\text{P.T.}}(\lambda^2)/\lambda$ is defined everywhere on this space [231]. We can therefore define the operators, for $\lambda^2 \neq 0$,

$$\hat{P}_\lambda a := \frac{1}{2}\left(1 + \frac{\hat{H}_{\text{P.T.}}}{\lambda}\right) a. \tag{7.21}$$

These obey $(\hat{P}_\lambda)^2 = \hat{P}_\lambda$ and $1 = \hat{P}_\lambda + \hat{P}_{-\lambda}$. They are therefore a complete set of projection operators, and we can define their target spaces as $\mathcal{H}^{\lambda}_{\hat{H}_{\text{P.T.}}}$ such that

$$\mathcal{H}^{\lambda^2}_{\hat{H}^2_{\text{P.T.}}} = \mathcal{H}^{\lambda}_{\hat{H}_{\text{P.T.}}} \oplus \mathcal{H}^{-\lambda}_{\hat{H}_{\text{P.T.}}}. \tag{7.22}$$

This bipartition is orthogonal if λ is real. Define also $\hat{P}_0 := 1$. We can then define $\mathcal{H}_{\hat{H}_{\text{P.T.}}}$ and $\hat{U}_{\hat{H}_{\text{P.T.}}} : \mathcal{H}_{\text{P.T.}} \to \mathcal{H}_{\hat{H}_{\text{P.T.}}}$ by

$$\mathcal{H}_{\hat{H}_{\text{P.T.}}} := \int^{\oplus}_{\sigma(\hat{H}_{\text{P.T.}})} d\mu_{\hat{H}_{\text{P.T.}}}(\lambda)\, \mathcal{H}^{\lambda}_{\hat{H}_{\text{P.T.}}}, \quad [\hat{U}_{\hat{H}_{\text{P.T.}}}\phi](\lambda) = \hat{P}_\lambda[\hat{U}_{\hat{H}^2_{\text{P.T.}}}\phi](\lambda^2), \tag{7.23}$$

where $\mu_{\hat{H}_{\text{P.T.}}}$ is the push-forward[2] of $\mu_{\hat{H}^2_{\text{P.T.}}}$ by $\lambda = \text{sign}(\lambda)\sqrt{\lambda^2}$. (Considering λ^2 as an independent variable.) Note that since $(\sigma(\hat{H}_{\text{P.T.}}))^2 = \sigma(\hat{H}^2_{\text{P.T.}})$, $\sigma(\hat{H}_{\text{P.T.}})$ is confined to the real and imaginary axes of the complex plane. It directly follows from equations 7.21 and 7.23 that $\hat{H}_{\text{P.T.}}$ is represented in $\mathcal{H}_{\hat{H}_{\text{P.T.}}}$ as a multiplication operator,

$$\hat{H}_{\text{P.T.}} :\ \phi(\lambda) \ \mapsto\ \lambda\phi(\lambda). \tag{7.24}$$

To derive the representation of the Hilbert-space product in $\mathcal{H}_{\hat{H}_{\text{P.T.}}}$, first define

$$\bar{\varphi}(\lambda) := \frac{1}{2}\left(1 + \frac{\hat{H}^\dagger_{\text{P.T.}}}{\lambda^*}\right) \varphi(\lambda^2), \tag{7.25}$$

[2]The "push-forward" of a measure μ on a space V by a transformation $T :\ V \to U$ is the measure ν on U obtained by $\nu(a) = \mu(T^{-1}(a))$.

This gives

$$\begin{aligned}(\varphi,\phi)_{\text{P.T.}} &= \int_{\sigma(\hat{H}^2_{\text{P.T.}})} d\mu_{\hat{H}^2_{\text{P.T.}}}(\lambda^2)\ \sum_{\pm}(\bar{\varphi}(\pm\sqrt{\lambda^2}),\phi(\pm\sqrt{\lambda^2}))_{\pm\sqrt{\lambda^2}} \\ &= \int_{\sigma(\hat{H}_{\text{P.T.}})} d\mu_{\hat{H}_{\text{P.T.}}}(\lambda)\ (\bar{\varphi}(\lambda),\phi(\lambda))_\lambda,\end{aligned} \tag{7.26}$$

where $(a,b)_\lambda$ is the inner product of $\mathcal{H}^\lambda_{\hat{H}_{\text{P.T.}}}$, In the last equality we have moved the sum over $\pm$ outside the integral, which we must assume to be possible, as discussed in section 7.4.3.

7.1.4 Generalised Eigenvectors of $\hat{H}_{\text{P.T.}}$

Properly speaking, unbounded Hermitian operators do not have a complete eigenstate basis, and may not even have any eigenvectors. In regular Schrödinger mechanics, this is clear when considering the momentum and position operators: neither plane waves nor delta functions are square-integrable functions, so they are not vectors in the Hilbert space, never mind eigenvectors. We consider, instead, "generalised eigenvectors", which in general may be defined as *functionals* on some subset of the Hilbert space. As discussed in the last section, these generalised eigenvectors of $\hat{H}_{\text{P.T.}}$ are solutions of the Dirac equation. It is clear that solutions of the Dirac equation with real mass are not in general states in $\mathcal{H}_{\text{P.T.}}$, since they do not reduce in size in the infinite future and past, so do not have finite norm. In this section we discuss the properties of these Dirac equation solutions, some of which we derive, some we must assume. In particular, it is clear that a *true* eigenstate of $\hat{H}_{\text{P.T.}}$ must decrease exponentially in both the future and past, and it seems a reasonable assumption that the generalised eigenstates cannot exponentially *increase* (but can stay at constant magnitude, as a plane wave).

Consider a vector in one of the generalised subspaces that makes up the direct integral $\mathcal{H}_{\hat{H}_{\text{P.T.}}}$, $a \in \mathcal{H}^{\lambda_0}_{\hat{H}_{\text{P.T.}}}$. If λ_0 is in the point spectrum, then a is a true eigenvector of $\hat{H}_{\text{P.T.}}$. If λ_0 is in the continuous spectrum, though, then this "generalised eigenvector" is not a vector in the Hilbert space proper. Whether λ_0 is in the continuous or point spectrum, it can be seen as a representation-independent object by its action as a linear functional,

$$\langle \varphi, a \rangle := (\bar{\varphi}(\lambda_0), a)_{\lambda_0}. \tag{7.27}$$

This functional action is well-defined on any $\varphi \in \mathcal{H}_{\hat{H}_{\text{P.T.}}}$ for which $\bar{\varphi}$ is of finite magnitude at $\lambda = \lambda_0$. This includes the whole Hilbert space if and only if λ_0 is in the point spectrum.

These generalised eigenvectors are functional solutions of the homogeneous spacetime Dirac equation with mass $m = -\lambda_0$. We assume that they are able to be chosen to have some desirable properties. First, we assume that they are classical solutions at $t \leq t_{\text{in}}$ and $t \geq t_{\text{out}}$. Specifically, for every $a \in \mathcal{H}^{\lambda}_{\hat{H}_{\text{P.T.}}}$, there exists $a(t \leq t_{\text{in}}) \in C^1((-\infty, t_{\text{in}}]; \mathcal{H}_{\text{S.T.}})$ and $a(t \geq t_{\text{out}}) \in C^1([t_{\text{out}}, \infty); \mathcal{H}_{\text{S.T.}})$, such that if $\langle \varphi, a \rangle$ exists then,

$$\lim_{n\to\infty} \langle \delta^{(n)}_t \varphi, a \rangle = (\varphi(t), a(t))_{\text{S.T}}, \quad t \leq t_{\text{in}} \quad \text{or} \quad t \geq t_{\text{out}}, \tag{7.28}$$

where $\delta^{(n)}_t$ is a sequence of $\mathbb{C}$-valued functions that act as a nascent delta function centred on t as $n \to \infty$. This means that we can define a mapping from every $\mathcal{H}^{\lambda}_{\hat{H}_{\text{P.T.}}}$ to $\mathcal{H}_{\text{S.T.}}$ for every time $t \leq t_{\text{in}}$ or $t \geq t_{\text{out}}$, $a \mapsto a(t)$, and that for times $t, t' \leq t_{\text{in}}$ or $t, t' \geq t_{\text{out}}$ these are related by $a(t) = \hat{T}_{-\lambda}(t, t')a(t')$ as defined by equation 7.17.

We need two other results. First, it follows straightforwardly from equation 7.17 and $(a, a)_{\text{P.T.}} = \int_{-\infty}^{\infty} dt \ (a(t), a(t))_{\text{S.T.}}$ that for $a \in \mathcal{H}^{\lambda}_{\hat{H}_{\text{P.T.}}}$ to have finite $\mathcal{H}_{\text{P.T.}}$-norm, $E^{\text{in}}_{\pm}(\lambda, \Pi)$ must have positive imaginary component for every non-zero ${}_{\pm}a_{-\lambda}(\Pi; t_{\text{in}})$, and $E^{\text{out}}_{\pm}(\lambda, \Pi)$ must have negative imaginary component for every non-zero ${}^{\pm}a_{-\lambda}(\Pi; t_{\text{in}})$. A true eigenstate of $\hat{H}_{\text{P.T.}}$ cannot have a component of real energy. We want a similar though less strict restriction on the generalised eigenstates, which we assume rather than demonstrate. We assume that the generalised eigenvectors $a \in \mathcal{H}^{\lambda}_{\hat{H}_{\text{P.T.}}}$ do not grow exponentially. This would necessarily be true if the external field is smooth with all derivatives polynomially bounded, as then $\hat{H}_{\text{P.T.}}$ leaves the Schwartz class invariant, and hence we could use the nuclear spectral theorem to determine that our eigenstates are tempered distributions[3] [232].

[3]The "Schwartz class" are smooth functions that, at large distances, decay faster than any polynomial. "Tempered distributions" are functionals with the Schwartz class for their domain. The "nuclear spectral

7.1.5 Projecting a Vector in $\mathcal{H}_{\text{P.T.}}$ onto a Vector in $\mathcal{H}_{\text{S.T.}}$

This section describes mathematical preliminaries needed for the main results in section 7.1.6. Broadly, we want to use Fourier analysis, and to do this, we need to be able to construct Fourier representations of states in $\mathcal{H}_{\text{P.T.}}$ from their representations in the eigenbasis of $\hat{H}_{\text{P.T.}}$. We do so by first projecting $\mathcal{H}_{\text{P.T.}}$ states onto single times, which is a natural generalisation of the projection of generalised eigenvectors discussed in the last section. Then, this projection onto an $\mathcal{H}_{\text{S.T.}}$ state at a single time can be extended to Fourier representations valid on all times $t < t_{\text{in}}$ and $t > t_{\text{out}}$ using the time-translation operators (7.17).

There are details of the procedure we do, though, which will seem arbitrary until their application in section 7.1.6. In particular, our choice of how to label the components of the mass eigenstates gives desirable complex-analytic qualities to the spectral functions (7.39) considered as functions of the complex energy, important to the contour integration techniques used in section 7.1.6. Also, although it would be possible to write actual Fourier representations (by replacing $g^{\text{u/l}}(E) \to g^{\text{u/l}}(p)$ in equation 7.60), we choose not to, but instead write a sum of a Fourier representation and decaying plane waves in equation 7.45. This is, again, to get a simple complex-analytic form of the function which is in the integral: it allows us to preserve the simple analytic structure assumed in equation 7.41 in the integrand in equation 7.45.

Since $\mathcal{H}_{\text{P.T.}} \cong L^2(\mathbb{R}; \mathcal{H}_{\text{S.T.}})$, for any $\phi \in \mathcal{H}_{\text{P.T.}}$ we can assign, for every $t \in \mathbb{R}$, $\phi(t) \in \mathcal{H}_{\text{S.T.}}$. This means of projecting a Hilbert-space state onto a time must be consistent with the projection of the generalised eigenvectors just discussed. Therefore,

theorem" is a version of the spectral theorem appropriate to unbounded self-adjoint operators that leave a "nuclear class" invariant. The definition of a "nuclear class" is technical, but suffice to say that the Schwartz class is an example of a nuclear class. In regular quantum mechanics, the position and momentum operator both leave the Schwartz class invariant, and hence their generalised eigenfunctions, the delta function and plane wave, are tempered distributions.

$$\begin{aligned}\lim_{n\to\infty}(\varphi\delta_t^{(n)},\phi)_{\text{P.T.}} = (\varphi(t),\phi(t))_{\text{S.T.}} &= \int_{\sigma(\hat{H}_{\text{P.T.}})} d\mu_{\hat{H}_{\text{P.T.}}}(\lambda)\ \lim_{n\to\infty}\langle\varphi(\lambda)\delta_t^{(n)},\phi(\lambda)\rangle \\ &= \int_{\sigma(\hat{H}_{\text{P.T.}})} d\mu_{\hat{H}_{\text{P.T.}}}(\lambda)\ (\bar{\varphi}(t),\phi(\lambda;t))_{\text{S.T.}}.\end{aligned} \tag{7.29}$$

Working in the $\mathcal{H}_{\text{in/out},|\hat{\Pi}|}$,

$$\begin{aligned}&\int_{\sigma(\hat{\Pi}^{\text{in/out}})\geq 0} d\mu_{\text{in/out}}(\Pi)\ (\varphi(\Pi),\phi^{\text{in/out}}(\Pi;t))_{\Pi\oplus-\Pi} = \\ &\int_{\sigma(\hat{H}_{\text{P.T.}})} d\mu_{\hat{H}_{\text{P.T.}}}(\lambda)\ \int_{\sigma(\hat{\Pi}^{\text{in/out}})\geq 0} d\mu_{\text{in/out}}(\Pi)\ (\varphi(\Pi),\phi^{\text{in/out}}(\Pi;\lambda;t))_{\Pi\oplus-\Pi}.\end{aligned} \tag{7.30}$$

Assuming that we can change the order the integrals and the implicit sum over the basis sections of $\mathcal{H}_{\text{in/out},|\hat{\Pi}|}$, this gives

$$\phi^{\text{in/out}}(\Pi;t) = \int_{\sigma(\hat{H}_{\text{P.T.}})} d\mu_{\hat{H}_{\text{P.T.}}}(\lambda)\ \phi^{\text{in/out}}(\Pi;\lambda;t). \tag{7.31}$$

The primary aim of this subsection is to convert the RHS of this equation into an inverse Fourier transform for times $t \leq t_{\text{in}}$ and $t \geq t_{\text{out}}$. Define the open vertical half-lines in the complex plane that meet the real axes at $eA_0^{\text{in/out}}$,

$$I^{\pm}_{\text{in/out}} := \{z \in \mathbb{C}\,|\,\exists\, x \in \mathbb{R}^{\pm},\ z = eA_0^{\text{in/out}} + ix\}. \tag{7.32a}$$

and the whole line

$$I_{\text{in/out}} := I^{-}_{\text{in/out}} \cup \{0\} \cup I^{+}_{\text{in/out}}. \tag{7.32b}$$

Call $i\mathbb{R}$ the imaginary axis, and $i\mathbb{R}^{\pm}$ the open positive/negative imaginary axes. Extend the measure $\mu_{\hat{H}_{\text{P.T.}}}$ to the whole imaginary and real axes by stipulating $\mu_{\hat{H}_{\text{P.T.}}}(\rho) = 0$ if $\rho \cap \sigma(\hat{H}_{\text{P.T.}})$ is empty. Then we can use equation 7.17 to write equation 7.31 as

$$\phi^{\text{in}}(\Pi;t) = \sum_{\xi=\pm}\int_{\mathbb{R}\cup i\mathbb{R}} d\mu_{\hat{H}_{\text{P.T.}}}(\lambda)\ {}_{\xi}\phi_{-\lambda}(\Pi;\lambda;t')e^{-iE^{\text{in}}_{\xi}(\lambda,\Pi)(t-t')} \tag{7.33a}$$

$$\phi^{\text{out}}(\Pi;t) = \sum_{\xi=\pm}\int_{\mathbb{R}\cup i\mathbb{R}} d\mu_{\hat{H}_{\text{P.T.}}}(\lambda)\ {}^{\xi}\phi_{-\lambda}(\Pi;\lambda;t')e^{-iE^{\text{out}}_{\xi}(\lambda,\Pi)(t-t')}, \tag{7.33b}$$

where we assume it is possible to bring the sum over $\pm$ outside of the integral. Define

$$\lambda^{\text{in/out}}(E,\Pi) := \sqrt{(E - eA_0^{\text{in/out}})^2 - \Pi^2}, \tag{7.34}$$

and

$$\phi^{\text{in},\pm}_{\xi}(\Pi;E;t) := {}_{\xi}\phi_{\mp\lambda^{\text{in}}(E,\Pi)}(\Pi;\pm\lambda^{\text{in}}(E,\Pi);t) \tag{7.35a}$$

$$\phi^{\text{out},\pm}_{\xi}(\Pi;E;t) := {}^{\xi}\phi_{\mp\lambda^{\text{out}}(E,\Pi)}(\Pi;\pm\lambda^{\text{out}}(E,\Pi);t) \tag{7.35b}$$

such that

$$\phi^{\text{in},\pm}_{\xi}(\Pi;E^{\text{in}}_{\xi'}(\Pi,\lambda);t) = {}_{\xi}\phi_{-\lambda}(\Pi;\lambda;t), \quad \lambda\in\mathbb{R}^{\pm}\cup i\mathbb{R}^{\pm} \tag{7.36a}$$

$$\phi^{\text{out},\pm}_{\xi}(\Pi;E^{\text{out}}_{\xi'}(\Pi,\lambda);t) = {}^{\xi}\phi_{-\lambda}(\Pi;\lambda;t), \quad \lambda\in\mathbb{R}^{\pm}\cup i\mathbb{R}^{\pm}. \tag{7.36b}$$

Then, splitting the integrals in equation 7.33 in half, we use equation 7.36 to write them in a form amenable to a change of variables,

$$\begin{aligned}\int_{\mathbb{R}^{\pm}\cup i\mathbb{R}^{\pm}} d\mu_{\hat{H}_{\text{P.T.}}}(\lambda)\ \phi^{\text{in/out},\pm}_{\xi}(\Pi;E^{\text{in/out}}_{\xi}(\Pi,\lambda);t')e^{-iE^{\text{in/out}}_{\xi}(\Pi,\lambda)(t-t')} = \\ \int_{[\mathbb{R}^{\xi}+\{eA_0^{\text{in/out}}\}]\cup I^{\xi}_{\text{in/out}}} d\mu^{\text{in/out}}_{\hat{E},\Pi}(E)\ \phi^{\text{in/out},\pm}_{\xi}(\Pi;E;t')e^{-iE(t-t')},\end{aligned} \tag{7.37}$$

where $\mu^{\text{in/out}}_{\hat{E},\Pi}$ is the push-forward of the measure $\mu_{\hat{H}_{\text{P.T.}}}$ using the mapping $E^{\text{in/out}}_{\text{sign}(E-eA_0^{\text{in/out}})}(\Pi,\lambda)$, where $\text{sign}(x)$ returns $\pm$ if $x\in\mathbb{R}^{\pm}\cup i\mathbb{R}^{\pm}$. Therefore

$$\begin{aligned}\phi^{\text{in}}(\Pi,t) = \int_{\mathbb{R}\cup I^{+}_{\text{in}}} d\mu^{\text{in}}_{\hat{E},\Pi}(E)\ \Big(&{}_{[\text{sign}(E-eA_0^{\text{in}})]}\phi_{-\lambda^{\text{in}}(E,\Pi)}(\Pi;\lambda^{\text{in}}(E,\Pi);t') \\ &+ {}_{[\text{sign}(E-eA_0^{\text{in}})]}\phi_{\lambda^{\text{in}}(E,\Pi)}(\Pi;-\lambda^{\text{in}}(E,\Pi);t')\Big)e^{-iE(t-t')}\end{aligned} \tag{7.38a}$$

$$\phi^{\text{out}}(\Pi,t) = \int_{\mathbb{R}\cup I^-_{\text{out}}} d\mu^{\text{out}}_{\hat{E},\Pi}(E) \left({}^{[\text{sign}(E-eA_0^{\text{out}})]}\phi_{-\lambda^{\text{out}}(E,\Pi)}(\Pi;\lambda^{\text{in}}(E,\Pi);t') \right. \\ \left. + {}^{[\text{sign}(E-eA_0^{\text{out}})]}\phi_{\lambda^{\text{out}}(E,\Pi)}(\Pi;-\lambda^{\text{out}}(E,\Pi);t') \right) e^{-iE(t-t')}, \tag{7.38b}$$

where we have used our assumption, discussed at the end of section 7.1.4, that generalised eigenvectors cannot exponentially grow to eliminate half the integral over the vertical line. Define

$$\lambda^{\text{u}}(E,\Pi) := \begin{cases} \text{sign}(E-eA_0^{\text{in}})\sqrt{(E-eA_0^{\text{in}})^2-\Pi^2}, & (E-eA_0^{\text{in}})^2 \geq \Pi^2 \\ \sqrt{(E-eA_0^{\text{in}})^2-\Pi^2}, & (E-eA_0^{\text{in}})^2 \leq \Pi^2 \end{cases} \tag{7.39a}$$

$$\lambda^{\text{l}}(E,\Pi) := \begin{cases} \text{sign}(E-eA_0^{\text{out}})\sqrt{(E-eA_0^{\text{out}})^2-\Pi^2}, & (E-eA_0^{\text{out}})^2 \geq \Pi^2 \\ -\sqrt{((E-eA_0^{\text{out}})^2-\Pi^2}, & (E-eA_0^{\text{out}})^2 \leq \Pi^2, \end{cases} \tag{7.39b}$$

where the "u" and "l" superscript refer to the fact that $\lambda^{\text{u/l}}$ can be taken as an analytic function of E on the whole upper/lower half complex plane. Define also

$${}^{\pm}\phi(\Pi;E) := {}_{[\text{sign}(E-eA_0^{\text{in}})]}\phi_{\mp\lambda^{\text{u}}(E,\Pi)}(\Pi;\pm\lambda^{\text{u}}(E,\Pi);t_{\text{in}}) \tag{7.40a}$$

$${}^{\pm}\phi(\Pi;E) := {}^{[\text{sign}(E-eA_0^{\text{out}})]}\phi_{\mp\lambda^{\text{l}}(E,\Pi)}(\Pi;\pm\lambda^{\text{l}}(E,\Pi);t_{\text{out}}), \tag{7.40b}$$

such that

$$\phi^{\text{in}}(\Pi,t) = \sum_{\pm}\int_{\mathbb{R}\cup I^+_{\text{in}}} d\mu^{\text{in}}_{\hat{E},\Pi}(E)\ {}^{\pm}\phi(\Pi;E)e^{-iE(t-t_{\text{in}})}, \quad t \leq t_{\text{in}} \tag{7.40c}$$

$$\phi^{\text{out}}(\Pi,t) = \sum_{\pm}\int_{\mathbb{R}\cup I^-_{\text{out}}} d\mu^{\text{out}}_{\hat{E},\Pi}(E)\ {}^{\pm}\phi(\Pi;E)e^{-iE(t-t_{\text{out}})}, \quad t \geq t_{\text{out}}. \tag{7.40d}$$

We proceed, in the rest of this subsection, to convert the integral over imaginary energies to one over real energies, possible by virtue of the assumption that exponential increase is

forbidden. This completes the conversion of the RHS of equation 7.31 into an inverse Fourier transform. We need quite a general result, for which we assume that we can express ${}_{\pm}\phi(\Pi; E)$ and ${}^{\pm}\phi(\Pi; E)$ in the form

$$ {}_{\pm}\phi(\Pi; E) = g^{\mathrm{u}}(E)\, {}_{\pm}\theta(\Pi; E), \quad {}^{\pm}\phi(\Pi; E) = g^{\mathrm{l}}(E)\, {}^{\pm}\theta(\Pi; E), \tag{7.41} $$

where $g^{\mathrm{u/l}}(E)$ is a complex-valued mereomorphic function on the upper/lower half-planes which is bounded on $I_{\mathrm{in/out}} \cup \mathbb{R}$ and as $|E| \to \infty$. Note that $g^{\mathrm{u/l}}(E)$ could depend on $\pm$ and Π, but since this possible dependence does not affect the following manipulations, we neglect it here. Define

$$ R^{\mathrm{u/l}}(p, t)[g] := \sum_{E_0 \in \mathrm{poles}} \frac{\mathrm{Res}(g(E_0))}{E_0 - p} \exp\left(-iE_0 t\right), \tag{7.42} $$

where the sum runs over poles of $g(E)$ in the upper/lower half plane. Then, by the residue theorem and Jordan's lemma,

$$ \begin{aligned} g^{\mathrm{u}}(p) e^{-ip(t-t_{\mathrm{in}})} = &\int_{\mathbb{R}} dE\, \frac{g^{\mathrm{u}}(E)}{2\pi i(E-p)} e^{-iE(t-t_{\mathrm{in}})} \\ &- R^{\mathrm{u}}(p, t-t_{\mathrm{in}})[g^{\mathrm{u}}], \quad \mathrm{Im}\{p\} > 0 \end{aligned} \tag{7.43a} $$

$$ \begin{aligned} g^{\mathrm{l}}(p) e^{-ip(t-t_{\mathrm{out}})} = -&\int_{\mathbb{R}} dE\, \frac{g^{\mathrm{l}}(E)}{2\pi i(E-p)} e^{-iE(t-t_{\mathrm{out}})} \\ &- R^{\mathrm{l}}(p, t-t_{\mathrm{out}})[g^{\mathrm{l}}], \quad \mathrm{Im}\{p\} < 0, \end{aligned} \tag{7.43b} $$

by closing the E integral in the upper plane for the "in" case and the lower plane for the "out" case. Assuming that we can exchange the order of the integrals along the "vertical" lines, i.e.

$$ \begin{aligned} \int_{I_{\mathrm{in}}^+} d\mu^{\mathrm{in}}_{\hat{E},\Pi}(p) \int_{\mathbb{R}} dE\, \frac{g^{\mathrm{u}}(E)\, {}_{\pm}\theta(\Pi; p)}{2\pi i(E-p)} e^{-iE(t-t_{\mathrm{in}})} = \\ \int_{\mathbb{R}} dE \int_{I_{\mathrm{in}}^+} d\mu^{\mathrm{in}}_{\hat{E},\Pi}(p)\, \frac{g^{\mathrm{u}}(E) {}_{\pm}\theta(\Pi; p)}{2\pi i(E-p)} e^{-iE(t-t_{\mathrm{in}})} \end{aligned} \tag{7.44a} $$

and

$$\begin{aligned}\int_{I^-_{\text{out}}} d\mu^{\text{out}}_{\hat{E},\Pi}(p) \int_{\mathbb{R}} dE\ \frac{g^{\text{l}}(E)\,{}_{\pm}\theta(\Pi;p)}{2\pi i(E-p)} e^{-iE(t-t_{\text{out}})} \\ = \int_{\mathbb{R}} dE \int_{I^-_{\text{out}}} d\mu^{\text{out}}_{\hat{E},\Pi}(p)\ \frac{g^{\text{l}}(E){}^{\pm}\theta(\Pi;p)}{2\pi i(E-p)} e^{-iE(t-t_{\text{out}})}.\end{aligned} \tag{7.44b}$$

This allows us to write

$$\begin{aligned}\phi^{\text{in}}(\Pi,t) = &\sum_{\pm}\int_{\mathbb{R}} dE\ g^{\text{u}}(E)\,{}_{\pm}\check{\theta}(\Pi;E)\exp\left(-iE(t-t_{\text{in}})\right) \\ &- \int_{I^+_{\text{in}}} d\mu^{\text{in}}_{\hat{E},\Pi}(p)\ R^{\text{u}}(p,t-t_{\text{in}})[g^{\text{u}}]\,{}_{\pm}\theta(\Pi;p), \quad t\le t_{\text{in}}\end{aligned} \tag{7.45a}$$

$$\begin{aligned}\phi^{\text{out}}(\Pi,t) = &\sum_{\pm}\int_{\mathbb{R}} dE\ g^{\text{l}}(E)\,{}^{\pm}\check{\theta}(\Pi;E)\exp\left(-iE(t-t_{\text{out}})\right) \\ &- \int_{I^-_{\text{out}}} d\mu^{\text{out}}_{\hat{E},\Pi}(p)\ R^{\text{l}}(p,t-t_{\text{out}})[g^{\text{l}}]\,{}^{\pm}\theta(\Pi;p), \quad t\ge t_{\text{out}},\end{aligned} \tag{7.45b}$$

where,

$${}_{\pm}\check{\theta}(\Pi;E) := \rho^{\text{in}}(\Pi;E)\,{}_{\pm}\theta(\Pi;E) + \int_{I^+_{\text{in}}} d\mu^{\text{in}}_{\hat{E},\Pi}(p)\frac{{}_{\pm}\theta(\Pi;p)}{2\pi i(E-p)} \tag{7.45c}$$

$${}^{\pm}\check{\theta}(\Pi;E) := \rho^{\text{out}}(\Pi;E)\,{}_{\pm}\theta(\Pi;E) - \int_{I^-_{\text{out}}} d\mu^{\text{out}}_{\hat{E},\Pi}(p)\frac{{}_{\pm}\theta(\Pi;p)}{2\pi i(E-p)} \tag{7.45d}$$

and

$$d\mu^{\text{in/out}}_{\hat{E},\Pi}(E) = dE\rho^{\text{in/out}}(\Pi;E) \tag{7.45e}$$

for real E, where $\rho^{\text{in/out}}(\Pi;E)\in[0,\infty)$. This expression for the measure is possible since we know that true eigenvectors of $\hat{H}_{\text{P.T.}}$ cannot have components with real energy, hence $\mu^{\text{in/out}}_{\hat{E},\Pi}$ for real E must be absolutely continuous with respect to the Lebesgue measure.

7.1.6 The Differential Equations

There are two parts to our main mathematical result. The first, given in section 7.1.6.1, is that the *retarded* solution to the inhomogeneous proper-time Dirac equation, when the source profile is a plane wave in proper time with mass m_e, has, at any finite proper-time, a spacetime profile which provides a solution to the spacetime Dirac equation. This follows quite straightforward calculations in the diagonal basis of $\hat{H}_{\text{P.T.}}$, though with some formal subtleties needed to properly define a "retarded" response to an infinite-duration driving source. Then, in section 7.1.6.2, we show that the retarded boundary condition in proper-time corresponds to the *Feynman* boundary condition in spacetime. The work that shows this is a slightly involved piece of complex Fourier analysis and contour integration. Equation 7.62 is a novel solution form of the inhomogeneous spacetime Dirac equation with Feynman boundary condition at times $t < t_{\text{in}}$ and $t > t_{\text{out}}$.

7.1.6.1 The Relationship between Solutions of the Inhomogeneous Spacetime and Proper-Time Dirac Equations

The inhomogeneous proper-time Dirac equation (1.7) can be written in $\mathcal{H}_{\hat{H}_{\text{P.T.}}}$ as

$$(i\partial_\tau - \lambda)\psi(\lambda;\tau) = -J(\lambda;\tau). \tag{7.46}$$

Suppose that the Fourier transform of $J(\tau)$ with respect to proper-time is well-defined and finite on the positive imaginary axis, and denote it

$$\tilde{J}(m) := \frac{1}{2\pi}\int_{\mathbb{R}} d\tau\ J(\tau)e^{im\tau}, \quad m \in \mathbb{C}. \tag{7.47}$$

Consider

$$\psi(\lambda;\tau) = \begin{cases} \int_{-\infty}^{\infty} dm\ \frac{1}{\lambda - m}\tilde{J}(\lambda;m)e^{-im\tau}\ + 2\pi i\tilde{J}(\lambda;\lambda)e^{-i\lambda\tau}, & \mathrm{Im}\{\lambda\} > 0 \\ P\int_{-\infty}^{\infty} dm\ \frac{1}{\lambda - m}\tilde{J}(\lambda;m)e^{-im\tau}\ + \pi i\tilde{J}(\lambda;\lambda)e^{-i\lambda\tau}, & \mathrm{Im}\{\lambda\} = 0 \\ \int_{-\infty}^{\infty} dm\ \frac{1}{\lambda - m}\tilde{J}(\lambda;m)e^{-im\tau}, & \mathrm{Im}\{\lambda\} < 0. \end{cases} \tag{7.48a}$$

Using the Sokhotski-Plemelj theorem this can be rewritten,

$$\psi(\lambda;\tau) = \lim_{\eta\to 0^+}\int_{-\infty}^{\infty} dm\ \frac{-1}{m + i\eta - \lambda}\tilde{J}(\lambda;m)e^{-im\tau} + 2\pi i\Theta(\mathrm{Im}\{\lambda\})\tilde{J}(z;\lambda)e^{-i\lambda\tau}, \tag{7.48b}$$

where we understand the step-function to mean

$$\Theta(x) = \begin{cases} 1, & x > 0 \\ 0, & x \leq 0. \end{cases} \tag{7.48c}$$

$\psi(\lambda;\tau)$ is clearly a solution to the inhomogeneous proper-time Dirac equation if both it and $\lambda\psi(\lambda;\tau)$ exist and are in $C^1(\mathbb{R};\mathcal{H}_{\mathrm{P.T.}})$. We call it the *retarded solution*. To show why, consider the case where $J(\tau)$ is supported only on $\tau > T_1$, $T_1 < 0$. Then we can use equation E.19 to perform the m integrals in equation 7.48b, looking at $\tau < T_1$. This gives

$$\psi(\lambda;\tau < T_1) = 0. \tag{7.49}$$

The term "retarded solution" of course implies that this is the unique solution that satisfies this condition, which seems likely but which we do not have a proof for, due to the awkward properties of $\hat{H}_{\mathrm{P.T.}}$, and hence how little knowledge we have of its spectrum. This does not strictly affect our argument, though, since we do not use this condition as our definition.

We want to consider the response to a plane wave driving source. The solution, though, is not a well-defined section at $\lambda = -m_e$, and it cannot be *directly* defined as being zero before the source acts, since a plane-wave source acts forever. We therefore have to define it as a functional solution of the Dirac equation, reached as a limit of a sequence of $\mathcal{H}_{\mathrm{P.T.}}$ solutions.

Specifically, we say:

Definition (retarded response to a plane wave): Say $J(\tau) = Je^{im_e\tau}$. The retarded response to this source is given by the functional limit of the sequence of solutions given by equation 7.48 to the inhomogeneous proper-time Dirac equation with source profile

$$J_\epsilon(\tau) = A_\epsilon(m_e;\tau)J$$

as $\epsilon \to 0^+$, where

$$A_\epsilon(m_e;\tau) := e^{-\epsilon|\tau|+im_e\tau}.$$

$A_\epsilon(m_e;\tau)$ is a nascent delta function in Fourier space, i.e. $\tilde{A}_\epsilon(m_e;m) \to \delta(m_e+m)$ as $\epsilon \to 0^+$. Define $\psi_\epsilon(\lambda;\tau)$ as the retarded solution to the inhomogeneous proper-time Dirac equation with source $A_\epsilon(m_e;\tau)J$. Using equation 7.48b,

$$\psi_\epsilon(\lambda;\tau) = -\lim_{\eta\to 0^+}\int_{\mathbb{R}} dm\ \frac{\tilde{A}_\epsilon(m_e;m)J(\lambda)}{m+i\eta-\lambda}e^{-im\tau} + \mathcal{O}(\epsilon). \tag{7.50}$$

As $\epsilon \to 0^+$ this does not have a well-defined value for $\lambda = -m_e$, but it does have a well-defined action as a functional. If $J(\lambda)$ and $\bar{\varphi}(\lambda)$ are bounded and continuous at $\lambda = -m_e$,

$$\begin{aligned}\langle\varphi,\psi(\tau)\rangle &= \lim_{\epsilon\to 0^+}(\varphi,\psi_\epsilon(\tau))_{\text{P.T.}} = \lim_{\eta\to 0^+}\int_{\sigma(\hat{H}_{\text{P.T.}})} d\mu_{\hat{H}_{\text{P.T.}}}(\lambda)\ \frac{(\bar{\varphi}(\lambda),J(\lambda))_\lambda}{m_e+\lambda-i\eta}\ e^{im_e\tau} \\ &= \left[P\int_{\sigma(\hat{H}_{\text{P.T.}})} d\mu_{\hat{H}_{\text{P.T.}}}(\lambda)\frac{(\bar{\varphi}(\lambda),J(\lambda))_\lambda}{m_e+\lambda} + i\pi\langle\phi,J(-m_e)\rangle\right]e^{im_e\tau},\end{aligned} \tag{7.51}$$

where it is possible to bring the ϵ limit into the integral, once the η limit has been brought outside. (Strictly, "continuous" should be interpreted as "Hölder-continuous" for the principal value to be well defined [233].) Therefore, the retarded response to a plane wave source $J(\tau) \in \mathcal{H}_{\hat{H}_{\text{P.T.}}}$, of frequency $-m_e$, which is continuous at $\lambda = -m_e$, is a functional,

$\psi(\tau)$, with a defined action on all $\varphi \in \mathcal{H}_{\hat{H}_{\text{P.T.}}}$ for which $\bar{\varphi}$ is also continuous at $\lambda = -m_e$. This solution can also be seen as the limit of the $\mathcal{H}_{\text{P.T.}}$ states

$$\psi_\eta(\lambda) := \frac{J(\lambda)}{m_e + \lambda - i\eta}, \tag{7.52}$$

as $\eta \to 0^+$. Using this,

$$\langle \varphi, -(\hat{H}_{\text{P.T.}} + m_e)\psi(\tau)\rangle = \lim_{\eta\to 0^+} (\varphi, -(\hat{H}_{\text{P.T.}} + m_e)\psi_\eta)_{\text{P.T.}} = -(\varphi, J)_{\text{P.T.}}. \tag{7.53}$$

Therefore $\psi(\tau)$, the retarded response to a plane wave of proper-time frequency $-m_e$, is a functional solution to the inhomogeneous spacetime Dirac equation (1.3b) with mass m_e and source profile J. This is the fundamental result that reflects Schwinger's operator relation (1.6).

7.1.6.2 The Retarded Response to a Plane Wave Obeys the Feynman Boundary Condition

The functional solution to the inhomogeneous proper-time Dirac equation projects onto a functional on some subset of $\mathcal{H}_{\text{S.T.}}$ at a particular time. By equation 7.31 this can be written,

$$\psi^{\text{in/out}}(\Pi; t) = \lim_{\eta\to 0^+} \int_{\sigma(\hat{H}_{\text{P.T.}})} d\mu_{\hat{H}_{\text{P.T.}}}(\lambda)\, \frac{J^{\text{in/out}}(\Pi; \lambda; t)}{m_e + \lambda - i\eta}, \tag{7.54}$$

with $t \le t_{\text{in}}$ or $t \ge t_{\text{out}}$. Use equation 7.40c,d to write

$$\psi^{\text{in}}_\eta(\Pi; t) = \sum_{\pm} \int_{\mathbb{R}\cup iI^+_{\text{in}}} d\mu^{\text{in}}_{\hat{E},\Pi}(E)\, \frac{{}^{\pm}J(\Pi; E)e^{-iEt}}{m_e \pm \lambda^{\text{u}}(E,\Pi) - i\eta}, \quad t < t_{\text{in}} \tag{7.55a}$$

$$\psi^{\text{out}}_\eta(\Pi, t) = \sum_{\pm} \int_{\mathbb{R}\cup iI^-_{\text{out}}} d\mu^{\text{out}}_{\hat{E},\Pi}(E)\, \frac{{}^{\pm}J(\Pi; E)e^{-iEt}}{m_e \pm \lambda^{\text{l}}(E,\Pi) - i\eta}, \quad t > t_{\text{out}}, \tag{7.55b}$$

Define

$$g^{\mathrm{u/l}}_{\eta,\pm}(E,\Pi) := 1/(m_e \pm \lambda^{\mathrm{u/l}}(E,\Pi) - i\eta), \tag{7.56}$$

which is a meromorphic function in the upper/lower plane and uniformly bounded as $|E| \to \infty$. We can therefore use equation 7.45c,d with $g^{\mathrm{u/l}}(E) = 1$ to write

$$J^{\mathrm{in}}(\Pi;t) = \sum_{\pm} \int_{\mathbb{R}} dE \; {}_{\pm}\check{J}(\Pi;E) e^{-iE(t-t_{\mathrm{in}})} \tag{7.57a}$$

$$J^{\mathrm{out}}(\Pi,t) = \sum_{\pm} \int_{\mathbb{R}} dE \; {}^{\pm}\check{J}(\Pi;E) e^{-iE(t-t_{\mathrm{out}})} \tag{7.57b}$$

and with $g^{\mathrm{u/l}}(E)$ as defined in equation 7.56,

$$\begin{aligned}\psi^{\mathrm{in}}_{\eta}(\Pi;t) = &\sum_{\pm} \int_{\mathbb{R}} dE \; g^{\mathrm{u}}_{\eta,\pm}(E,\Pi) \, {}_{\pm}\check{J}(\Pi;E) e^{-iE(t-t_{\mathrm{in}})} \\ &- \int_{I^{+}_{\mathrm{in}}} d\mu^{\mathrm{in}}_{\hat{E},\Pi}(p) \; R^{\mathrm{u}}(p, t-t_{\mathrm{in}}) [g^{\mathrm{u}}_{\eta,\pm}] \, {}_{\pm}J(\Pi;p)\end{aligned} \tag{7.58a}$$

$$\begin{aligned}\psi^{\mathrm{out}}_{\eta}(\Pi;t) = &\sum_{\pm} \int_{\mathbb{R}} dE \; g^{\mathrm{l}}_{\eta,\pm}(E,\Pi) \, {}^{\pm}\check{J}(\Pi;E) e^{-iE(t-t_{\mathrm{out}})} \\ &- \int_{I^{-}_{\mathrm{out}}} d\mu^{\mathrm{out}}_{\hat{E},\Pi}(p) \; R^{\mathrm{l}}(p, t-t_{\mathrm{out}}) [g^{\mathrm{l}}_{\eta,\pm}] \, {}^{\pm}J(\Pi;p).\end{aligned} \tag{7.58b}$$

We know that $J^{\mathrm{in}}(\Pi,t)$ is supported only on $t > t_{\mathrm{in}}$ and $J^{\mathrm{out}}(\Pi,t)$ is supported only on $t < t_{\mathrm{out}}$. It is shown in Appendix F that both $\pm$ components in the sum on the RHS of equation 7.57a,b also independently satisfy this condition. Therefore, we can use equation E.19 to carry out the integrals,

$$\begin{aligned}&\sum_{\pm} \int_{\mathbb{R}} dE \; g^{\mathrm{u}}_{\eta,\pm}(E,\Pi) \, {}_{\pm}\check{J}(\Pi;E) \exp\left(-iE(t-t_{\mathrm{in}})\right) = \\ &\qquad 2\pi i \sum_{\pm, E_0 \in \mathrm{poles}} \mathrm{Res}(g^{\mathrm{u}}_{\eta,\pm}(E_0,\Pi)) \, {}_{\pm}\check{J}(\Pi;E_0) e^{-iE_0(t-t_{\mathrm{in}})}\end{aligned} \tag{7.59a}$$

$$\begin{aligned}&\sum_{\pm} \int_{\mathbb{R}} dE \; g^{\mathrm{l}}_{\eta,\pm}(E,\Pi) \, {}^{\pm}\check{J}(\Pi;E) \exp\left(-iE(t-t_{\mathrm{out}})\right) = \\ &\qquad -2\pi i \sum_{\pm, E_0 \in \mathrm{poles}} \mathrm{Res}(g^{\mathrm{l}}_{\eta,\pm}(E_0,\Pi)) \, {}^{\pm}\check{J}(\Pi;E_0) e^{-iE_0(t-t_{\mathrm{out}})},\end{aligned} \tag{7.59b}$$

where the sum runs over poles in the upper/lower half plane in equation 7.59a/*b*. This gives

$$\psi_\eta^{\text{in}}(\Pi;t) = 2\pi i \sum_{\pm, E_0 \in \text{poles}} \text{Res}(g^{\text{u}}_{\eta,\pm}(E_0,\Pi))\rho(\Pi;E_0)\,{}_{\pm}J(\Pi;E_0)e^{-iE_0(t-t_{\text{in}})} \tag{7.60a}$$

$$\psi_\eta^{\text{out}}(\Pi;t) = -2\pi i \sum_{\pm, E_0 \in \text{poles}} \text{Res}(g^{\text{l}}_{\eta,\pm}(E_0,\Pi))\rho(\Pi;E_0)\,{}^{\pm}J(\Pi;E_0)e^{-iE_0(t-t_{\text{out}})}. \tag{7.60b}$$

Note that the integral over p in equation 7.58a/b has cancelled with that in the definition of $\check{J}$ in equation 7.45c/*d*. $g^{\text{u/l}}_{\eta,\pm}(E,\Pi)$ has poles at

$$E_0 = \mp\sqrt{m_e^2+\Pi^2} + A_0^{\text{in/out}} \pm \frac{i\eta}{\sqrt{1+(\Pi^2/m_e^2)}} + \mathcal{O}(\eta^2), \tag{7.61}$$

with residues $\pm m_e/\sqrt{m_e^2+\Pi^2} + \mathcal{O}(\eta)$. Therefore in the "in" case we capture the negative energy pole, and in the "out" case we capture the positive energy pole. Taking $\eta \to 0^+$

$$\begin{aligned}\psi^{\text{in}}(\Pi;t) =& \frac{2\pi i m_e \rho(\Pi; E_-^{\text{in}}(m_e,\Pi))}{\sqrt{m_e^2+\Pi^2}}\,{}_{-}J^{\text{in}}_{m_e}(\Pi;-m_e;t_{\text{in}}) \\ &\cdot \exp\left(-i\left[-\sqrt{m_e^2+\Pi^2}+eA_0^{\text{in}}\right](t-t_{\text{in}})\right)\end{aligned} \tag{7.62a}$$

$$\begin{aligned}\psi^{\text{out}}(\Pi;t) =& \frac{2\pi i m_e \rho(\Pi; E_+^{\text{out}}(m_e,\Pi))}{\sqrt{m_e^2+\Pi^2}}\,{}^{+}J^{\text{out}}_{m_e}(\Pi;-m_e;t_{\text{out}}) \\ &\cdot \exp\left(-i\left[\sqrt{m_e^2+\Pi^2}+eA_0^{\text{out}}\right](t-t_{\text{out}})\right),\end{aligned} \tag{7.62b}$$

where we have used equation 7.40 to write the RHS. It is clear that this is in $\mathcal{H}_{\text{S.T.}}$ as a direct consequence of our assumption that the generalised eigenvectors projected onto times $t \le t_{\text{in}}$ and $t \ge t_{\text{out}}$ take values in $\mathcal{H}_{\text{S.T.}}$ (7.28). It is also clear from equation 7.19 that it obeys the Feynman boundary condition.

7.2 The "Causal Propagator" of Fradkin, Gitman & Schvartsman

In this section it is shown that if we interpret FGS's "causal propagator" (2.19) as a solver of the inhomogeneous Dirac equation (as in equation 1.3), then it returns solutions of the inhomogeneous Dirac equation which satisfy the Feynman boundary condition. The relationship between this result, and that given in section 6, is that between the use of the same Green's function to solve the homogeneous and inhomogeneous equation.

Define the "causal" solution to the inhomogeneous spacetime Dirac equation,

$$\psi^c(x) := \int d^4x' \; S^c(x,x')J(x'). \tag{7.63}$$

Take the $\mathcal{H}_{\text{S.T.}}$-product of some $f \in \mathcal{H}_{\text{S.T.}}$ with the causal solution at t_{in},

$$\begin{aligned}(f,\psi^c(t_{\text{in}}))_{\text{S.T.}} &= -i\sum_l \int d^4y \; J_l(y) \left\langle 0,\text{out}\right| \hat{\bar{\psi}}_{H|l}(y) \left[(f,\hat{\psi}_H(t_{\text{in}}))_{\text{S.T.}}\right] \left|0,\text{in}\right\rangle \\ &= -i\sum_l \int d^4y \; J_l(y) \left\langle 0,\text{out}\right| \hat{\bar{\psi}}_{H|l}(y)\hat{U}(0,t_{\text{in}}) \left[(f,\hat{\psi}_S)_{\text{S.T.}}\right] \left|0,t_{\text{in}}\right\rangle \\ &= 0 \quad \text{if} \quad f \in {}_+\mathcal{H}^{m_e}_{\text{S.T.}},\end{aligned} \tag{7.64}$$

where in the second line we have injected two pairs of $1 = \hat{U}^\dagger(0,t_{\text{in}})\hat{U}(0,t_{\text{in}})$ and in the last line we have used equation 6.6a. At t_{out},

$$\begin{aligned}(f,\psi^c(t_{\text{out}})) &= i\sum_l \int d^4y \; J_l(y) \left\langle 0,\text{out}\right| \left[(f,\hat{\psi}_H(t_{\text{out}}))_{\text{S.T.}}\right] \hat{\bar{\psi}}_{H|l}(y) \left|0,\text{in}\right\rangle \\ &= i\sum_l \int d^4y \; J_l(y) \left\langle 0,t_{\text{out}}\right| \left[(f,\hat{\psi}_S)_{\text{S.T.}}\right] \hat{U}(t_{\text{out}},0)\hat{\bar{\psi}}_{H|l}(y) \left|0,\text{in}\right\rangle, \\ &= 0 \quad \text{if} \quad f \in {}^-\mathcal{H}^{m_e}_{\text{S.T.}}.\end{aligned} \tag{7.65}$$

where in the third line we have used equation 6.6d. Due to the orthogonality of the subspaces for real m_e, these are equivalent to the Feynman boundary condition.

7.3 Three Other Equivalent Solution Forms

This section lists three other propagators and show that they return solutions of the inhomogeneous spacetime Dirac equation which obey the Feynman boundary condition

7.3.1 Schwinger's Proper-time Propagator

Use equation 7.52 and the mathematical relation

$$\frac{1}{x - i\eta} = i \int_0^\infty ds\, e^{-i(x-i\eta)s}, \quad x \in \mathbb{R},\ \eta > 0 \tag{7.66}$$

to get

$$\psi_\eta(\lambda) = i \int_0^\infty ds\, e^{-i(m_e - i\eta)s} e^{-i\lambda s} J(\lambda) = \left[\left(i \int_0^\infty ds\, e^{-i(m_e - i\eta)s} e^{-i\hat{H}_{\text{P.T.}} s} \right) J \right](\lambda). \tag{7.67}$$

The term in round brackets is Schwinger's expression for his Green's function (1.6) in the diagonal basis, with an infinitesimal negative imaginary number inserted. Schwinger inserted the infinitesimal negative imaginary number during calculations that would otherwise explicitly return a divergence. Later authors [69] formalised this procedure, and say that the expression is defined for negative imaginary mass, with the prescription that solutions for the real mass are to be derived by then taking the limit of the imaginary component to zero, perhaps after appropriate integrations. In this work this procedure is understood as returning a functional solution to the Dirac equation with a domain smaller than $\mathcal{H}_{\text{P.T.}}$, with action

$$\langle \phi, \psi \rangle = \lim_{\eta \to 0^+} (\phi, \psi_\eta)_{\text{P.T.}}. \tag{7.68}$$

7.3.2 The $m_e^2 - i\epsilon$ Prescription and Continuation from Euclidean Time

Consider a solution to the inhomogeneous spacetime Dirac equation with mass m_e that takes values in $\mathcal{H}_{\text{S.T.}}$ for $t \leq t_{\text{in}}$ and $t \geq t_{\text{out}}$, before and after the source acts. At these times they are just solutions to the homogeneous spacetime Dirac equation, so we can write, in the $\mathcal{H}_{\text{in/out},|\hat{\Pi}|}$ representations according to equation 7.17,

$$\psi^{\text{in}}(\Pi;t) = \sum_{\pm} {}_{\pm}\psi_{m_e}(\Pi;t') \exp\left(-i\left[\pm\sqrt{m_e^2+\Pi^2} + eA_0^{\text{in}}\right](t-t')\right) \tag{7.69a}$$

$$\psi^{\text{out}}(\Pi;t) = \sum_{\pm} {}^{\pm}\psi_{m_e}(\Pi;t') \exp\left(-i\left[\pm\sqrt{m_e^2+\Pi^2} + eA_0^{\text{out}}\right](t-t')\right). \tag{7.69b}$$

Now consider that we demand that these solutions are each analytic functions of m_e in some open region, confined to the lower half complex plane, which has m_e as a limit point. Further, we demand that in this region, no component grows exponentially. The m_e dependence in the ${}_{\pm}\psi_{m_e}(\Pi;t')$ and ${}^{\pm}\psi_{m_e}(\Pi;t')$ terms are here insignificant, so we can focus on the mass-dependence in the exponential, which is in fact a dependence on m_e^2. Specifically, we can enforce this demand by asking that there exists an $\epsilon > 0$ such that for all masses $m^2(\delta) := m_e^2 - i\delta$, for all $\delta \in (0,\epsilon]$, the expression 7.69 does not grow exponentially as $t \to \pm\infty$. This is true iff

$${}_{+}\psi_{m_e}(\Pi; t \leq t_{\text{in}}) \equiv {}^{-}\psi_{m_e}(\Pi; t \geq t_{\text{out}}) \equiv 0. \tag{7.70}$$

Next, consider making the same demand, that the solution does not grow exponentially, if we enact the replacement

$$t \to e^{-i\phi}t, \quad \phi \in (0, \pi/2]. \tag{7.71}$$

So long as $|eA_0^{\text{in/out}}| < m_e$, this enforces exactly the same requirement. This is a version of the idea that the causal solutions are to be derived by analytic continuation of solutions for "Euclidean time" [234]. Both these requirements are therefore equivalent to imposing the

Feynman boundary condition.

We have chosen to treat the Green's function as a mapping from source profiles to solutions of the inhomogeneous equation. That this is a reasonable approach is discussed in section 7.4.3.1. To show that our specific demands on the solutions with complex mass - that there is no exponential growth - are equivalent to other author's demands on the analytical properties of Green's functions would have to be done case-by-case. It is worth mentioning two of the most common approaches here, though. First, less mathematically rigorous works that use the "$m_e^2 - i\epsilon$ prescription" often implicitly assume that the Green's function can be represented in Fourier space. This certainly implies that the homogeneous equation solutions it gives have Fourier representations, which necessarily requires them to not have exponential growth. Second, as specifically discussed in section 7.4.3.1, in more mathematically rigorous works based on Euclidean time, Green's functions are defined such that they must return tempered distributional solutions to the inhomogeneous Dirac equation. Again, a lack of exponential growth is a necessary condition for being a tempered distribution.

There is cause for caution here. To get the same boundary condition, we have needed to demand that the *actual solutions* for imaginary mass or imaginary time obey certain constraints on growth at infinity, *not* the terms of a perturbative series. If we were to demand that each of the solutions that form the asymptotic series approximation to the correct solution do not exponentially grow at infinity, then this would be neither necessary nor sufficient for their sum to not exponentially grow at infinity. This explains Gitman's observation [52] that FGS's causal propagator does not equal that derived by applying the $m_e^2 - i\epsilon$ prescription to the perturbative series expression of the propagator. In Feynman-diagrammatic terms, the important thing for the $m_e^2 - i\epsilon$ or Euclidian-time prescriptions to give the Feynman boundary condition is that the "leg" connecting the input and output particles to infinity is treated as propagation under the external field, not as a free propagator.

7.4 Discussion

7.4.1 The Result

The principal result of this chapter is the demonstration that, for a broad class of external fields (those satisfying the form (7.1)) and under reasonable mathematical assumptions, Schwinger's proper-time propagator, FGS's causal propagator, and propagators derived by analytic continuation of the complexified mass or time all obey what we call the "Feynman boundary condition". This can loosely be stated as the requirement that they propagate positive-energy solutions into the future and negative-energy solutions into the past. Under a further assumption discussed in section 7.1.2.3, that there exists no solution to the homogeneous equation which is wholly negative-energy at the initial time and wholly positive-energy at the final time, this is a demonstration of the equivalence of all these propagators. To derive this result, we have interpreted Schwinger's operator relationship (1.6) as a statement relating the solutions of two partial differential equations: the retarded solution to the inhomogeneous proper-time Dirac equation (1.7) for a plane-wave driving source of proper-time frequency $-m_e$ is a solution of the inhomogeneous spacetime Dirac equation (1.3b) with mass m_e. When applied to fields of form (7.1), this also gives a novel expression for this solution before the in-time and after the out-time in terms of the decomposition of the source profile in the generalised eigenbasis of $\hat{H}_{\text{P.T.}}$ (7.62). This result might be of independent interest. We now discuss the two caveats just mentioned, the class of external field and the mathematical assumptions made, in turn.

7.4.2 Conditions on the External Field

While Schwinger's propagator and the proper-time method described in Section 7.1 have been demonstrated to be wholly equivalent for any external field, the other three propagators considered have only been demonstrated as equivalent by their obedience of the Feynman boundary condition. Their obedience of the Feynman boundary condition is contingent on the field satisfying the conditions (7.1), so equivalence has only been demonstrated for fields satisfying these conditions. There are also some subtle distinctions in the conditions applied to some of the

propagators, which we now discuss.

First, the continuation from Euclidean time and FGS's causal propagator require $|eA_0^{\text{in/out}}| < m_e$, such that the "negative energy" states genuinely all have negative energy and the "positive energy" states all have positive energy. The proper-time method and the $m_e^2 - i\epsilon$ prescription do not. This is a technicality entangled with issues to do with the normalisation with respect to the vacuum, and besides can be fixed by a partial gauge constraint.

More substantially, FGS's causal propagator is only defined for times $t_{\text{out}} \geq t \geq t_{\text{in}}$. Say the field used for FGS's causal propagator is $A_\mu(x)$, and define

$$A'_\mu(t, \mathbf{x}; t_{\text{in}}, t_{\text{out}}) := \begin{cases} A_\mu(t_{\text{out}}, \mathbf{x}), & t \geq t_{\text{out}} \\ A_\mu(t, \mathbf{x}), & t_{\text{out}} \geq t \geq t_{\text{in}} \\ A_\mu(t_{\text{in}}, \mathbf{x}), & t \leq t_{\text{in}}. \end{cases} \tag{7.72}$$

A'_μ satisfies the conditions (7.1) if and only if $A_0(x)$ has no spatial variation at t_{in} or t_{out}. Therefore, the solution derived using the proper-time method, the $m_e^2 - i\epsilon$ prescription and continuation from Euclidean time matches on this temporal region if we use the field $A'_\mu(x; t_{\text{in}}, t_{\text{out}})$ and $A_0(x)$ has no spatial variation at t_{in} or t_{out}. We can therefore, using equation 7.72, derive a solution using any of the former three methods that matches that derived using FGS's causal propagator on the region $t_{\text{out}} \geq t \geq t_{\text{in}}$ with a field constrained only by a partial gauge condition.

FGS derive a solution for all time by taking the limits $t_{\text{in}} \to -\infty$, $t_{\text{out}} \to \infty$. We therefore have

$$\lim_{t_{\text{in}} \to -\infty,\, t_{\text{out}} \to \infty} \psi[A'_\mu(t_{\text{in}}, t_{\text{out}})](x) = \lim_{t_{\text{in}} \to -\infty,\, t_{\text{out}} \to \infty} \psi_{\text{FGS}}^{t_{\text{in}}, t_{\text{out}}}[A_\mu](x), \tag{7.73}$$

where $\psi_{\text{FGS}}^{t_{\text{in}}, t_{\text{out}}}[A_\mu]$ returns the solutions to the inhomogeneous equation with the external field $A_\mu(x)$ derived using FGS's causal propagator with the given in and out times, and $\psi[A_\mu]$ returns the solution derived by any other the other three methods. If $A_\mu(x)$ satisfies conditions (7.1) for any finite t_{in} and t_{out}, then $A'_\mu(x; t_{\text{in}}; t_{\text{out}}) = A_\mu(x)$ for sufficiently large-magnitude t_{in} and t_{out}, and hence we get equality of all four methods on all time,

$$\psi[A_\mu](x) = \lim_{t_{\text{in}}\to-\infty,\, t_{\text{out}}\to\infty} \psi_{\text{FGS}}^{t_{\text{in}},t_{\text{out}}}[A_\mu](x). \tag{7.74}$$

We have therefore demonstrated the equality of all four propagators for all fields that obey the constraints (7.1) for all time. In this sense, equality has been proven for all "physical" situations, in which we can confine the action of the external field to some finite time. The limitation is important to state, though, since fields that do not obey condition (7.1) include such important theoretical cases as the everywhere uniform electric field considered by Schwinger [6]. FGS prove equivalence in this specific case by direct calculation [12], though, so there is some reason to suspect that the proper time and FGS propagators are equivalent in all cases. This chapter's result could be extended to cover this general case if we knew that the mapping from external field profiles to inhomogeneous spacetime Dirac equation solutions, with fixed source profile, was continuous, and hence

$$\lim_{t_{\text{in}}\to-\infty,\, t_{\text{out}}\to\infty} \psi[A'_\mu(t_{\text{in}}, t_{\text{out}})](x) = \psi[A_\mu(x)]. \tag{7.75}$$

7.4.3 Mathematical Assumptions

7.4.3.1 The Green's Function is Well-Defined as a Mapping from Compactly Supported Source Profiles

We assume that the ascription of a (functional) solution to the inhomogeneous equation for every source profile that is compactly supported in time defines the Green's function well. There is no single mathematical result that justifies this, since we are demonstrating the equivalence of Green's functions as used in literature which does not share a strict definition of what mathematical object the Green's function is. Schwinger's definition of $\hat{G}$ as an operator on the Hilbert space is insufficient, as even when looking at our restricted class of source profiles, the solutions returned are not necessarily in the Hilbert space. To give the idea plausibility, consider that in axiomatic treatments of QFT [234] the Green's functions are often treated as tempered distributions on $\mathbb{R}^{3\oplus1} \otimes \mathbb{R}^{3\oplus1}$. In this case, we can use the Schwartz kernel theorem to prove an isomorphism between this class and continuous linear mappings from source profiles

in the Schwartz class to tempered-distributional solutions of the inhomogeneous equation [235]. The continuity of this mapping ensures that defining it on the compactly supported functions defines it well on the Schwartz class, since the compactly supported functions are dense in the Schwartz class.

7.4.3.2 Neglecting the $m = \pm i\Pi$ Case in Section 7.1.2

All uses we make of our $\mathcal{H}_{\text{S.T.}}$ representations in which $\hat{\mathscr{H}}_m^{\text{in/out}}$ for imaginary m is diagonal proceeds from equation 7.31. Suppose in this equation, we set $\phi^{\text{in/out}}(\Pi; \lambda; t) = 0$ for $\lambda = \pm i\Pi$. This would only alter the LHS of the equation if $i\Pi$ or $-i\Pi$ were in the point spectrum of $\hat{H}_{\text{P.T.}}$. Assuming this to be the case, for this alteration of the LHS to affect the Hilbert space state that $\phi^{\text{in/out}}(\Pi; t)$ represents, we require $\phi^{\text{in/out}}(\Pi; t)$ to be altered on a region of finite $\mu_{\text{in/out}}$-measure. Since the point spectrum of $\hat{H}_{\text{P.T.}}$ covers a region of Lebesgue-measure 0, the only way for this to be the case would be if Π were in the point spectrum of $\hat{\Pi}^{\text{in/out}}$. Therefore, the neglect of the case where $m = \pm i\Pi$ can only matter if there exists a real number α which is in the point spectrum of $\hat{\Pi}^{\text{in/out}}$, and $\pm i\alpha$ is in the point spectrum of $\hat{H}_{\text{P.T.}}$. We therefore must assume this not to be the case.

7.4.3.3 Other Assumptions

There are three further classes of substantial mathematical assumptions made in this chapter. The first class is that two operators which are known to by symmetric, $\hat{\Pi}$ and $\hat{H}^2_{\text{P.T.}}$, are self-adjoint, as mentioned in section 7.1.1. Proving that Hamiltonians with various potentials are self-adjoint is a known, difficult problem in the case of non-relativistic quantum mechanics [236]. The extension of this work to the proper-time case would be substantial. The second class is that the relevant solutions to the homogeneous and inhomogeneous spacetime Dirac equation are equal to $\mathcal{H}_{\text{S.T.}}$ states at times $t \leq t_{\text{in}}$ and $t \geq t_{\text{out}}$ (7.28), and that they do not grow exponentially in the future or past. The third class is that we can exchange the order of various infinite sums and integrals, as done to derive equations 7.26, 7.31, 7.33 and 7.45c,*d*.

These are all the sorts of assumptions that are frequently made implicitly in calculations performed in the bra-ket formalism, where, respectively, unbounded operators are treated as

operating on the whole Hilbert space, their eigenvectors are treated as if in the Hilbert space, and integrals and infinite summations over ket-vector bases are manipulated symbolically as finite summations. A significant reason it has been necessary to make them is that we have used very little knowledge of $\hat{H}_{\text{P.T.}}$: in particular its spectrum and the properties of its generalised eigenstates are largely unknown. A substantial work of functional analysis of $\hat{H}_{\text{P.T.}}$ as an operator on $\mathcal{H}_{\text{P.T.}}$ would be needed to validate our assumptions, which would probably necessitate some regularity constraints on the external field $A_\mu(x)$. This would act as an extension of some of the results derived from functional analysis for putting regular quantum mechanics on a mathematically rigorous footing [31,237] to Schwinger's proper-time quantum mechanics.[4] We have not supplied the proofs needed for this extension. We believe it is clear, though, that the assumptions made are no more egregious than are commonplace in physics literature that uses the bra-ket formalism, and in making its assumptions explicit acts as a derivation of some plausible sufficient conditions for the validity of the proper-time method. The validation of these assumptions, or the derivation of fewer or less restrictive assumptions, is a substantial area for future work.

[4]This extension is non-trivial because, as a differential operator, $\hat{H}_{\text{P.T.}}$ has very different properties to the Hamiltonians considered in regular quantum mechanics: in particular, it is hyperbolic rather than elliptic. Very roughly speaking, it is in general harder to prove regularity properties for functions related to hyperbolic operators than elliptic operators.

Chapter 8

Conclusion

In chapter 3 we used simple, empirical cross-sections to derive "correction factors" for collision, ionisation, de-excitation and recombination from free-electron/ion collisions that account for the effects of special relativity on the free electron motion. The correction factors are closed-form algebraic combinations of special functions, dependent on both temperature and the "reaction threshold", the parameter on which the empirical cross-sections are dependent. This expands on existing correction factors, dependent on the temperature only and independent of cross-section, which are derived only from the ratio of partition functions.

In chapters 4 and 5, we examined particle creation in a black-body field using Breit-Wheeler and external field methods in the $k_B T \gg mc^2$ regime. For Breit-Wheeler we found a simple expression for the largest-scaling two terms, which scaled with $\log(k_B T/(m_e c^2))T^4$ and T^4. The log term is the only term that retains a dependence on the electron rest mass. Using external field methods is more novel. We derived the relevant formal expressions, and outlined how to exploit them with a procedure of representative sampling of external field profiles. We then gave explicit results from a numerical procedure that simplifies these sampled external fields as an ensemble of spatial Sauter pulses, and found that the pair-production rate scales with T^4, though significantly surpasses the Breit-Wheeler rate for all temperatures above $k_B/(m_e c^2)$ in relevant regimes.

Treating the black-body field as one-dimensional spatial Sauter pulses, though, is not an assumption that can be rigorously justified, and as such we cannot draw strong conclusions about the actual particle-production rate in a black-body from our model. An approximation

as extreme as ours was needed for an analytical result for particle production. To get a figure that could be seen as a legitimate estimate of the true value, it would be necessary to use a numerical method to calculate particle production of the sampled external field profiles. Though the full four-dimensional external field calculation is intractable, we could simplify external fields that are much more complicated than the 1D Sauter pulse, and would capture much more relevant physics. The fields could vary in two spatial dimensions and time, extend over a larger spatial region, and could include a magnetic field component. (Though there would be a trade-off between the number of fields we could sample and the complexity of the applied fields modelled, given finite computational resources.) The obvious choice for a numerical method would be a numerical integration of the Dirac equation (which has been applied to both two-dimensional spatial variation [139] and rotating fields [150, 151]), though the numerical worldline technique [82] provides an alternative. We are restricted, of course, by the inapplicability of semiclassical methods in our regime.

There would remain problems even if the particle-production rate for each external field could be calculated with complete accuracy, though. Even our formal method assumes that the black-body field is a free field. In terms of the real and imaginary time evolution mentioned in section 2.5, imaginary time evolution has been carried out without interactions. We made the same approximation for Breit-Wheeler and the external field method, but it makes somewhat less sense in the latter case. To see why, consider that Breit-Wheeler is the lowest-order perturbative approximation. To include particle interactions in the definition of the black-body would, essentially, mean including fermion-mediated interactions in determining the Boltzmann factors of photon states. To include these particle reactions in addition to the reactions that lead to pair-creation means working to a higher-order in perturbation theory. Neglecting them is part of the truncation to lowest order in perturbation theory. External field calculations, though, can include processes from all orders of perturbation theory: it is restricted only by being a single loop. However, in this case, it seems likely that virtual fermion exchanges, which alter the photon equilibrium state, and particle-creating real-fermion production, could well both occur together at the one-loop level, and therefore neglecting virtual-fermion interactions is a much more arbitrary truncation.

Incorporating interactions in the definition of equilibrium within the external-field picture would be a substantial, exciting, novel development of theory. Broadly, as fermion interactions in the time-evolution of the external field to one loop are incorporated by solving the Dirac equation in real time, it seems likely that including interactions in the definition of equilibrium would involve solving the Dirac equation in imaginary time.

This could be accompanied by a more thorough investigation of the process by the more standard techniques developed for the study of thermal particle production. As described in Ref [47, 181], different approximation schemes are appropriate for different momentum scales. The total pair creation rate will span momentum scales, so a calculation of total particle creation rate would need to be sensitive to this: standard perturbation theory is good when all external momenta are hard, "HTL resummation" when all are soft. Applying these methods to the black-body field is, in principle, a straightforward application of well-studied methods. The details would be very involved, though, and much would need to be done from scratch, since the case of the photon and electron fields out of equilibrium has not been much studied in the thermal QFT formalism. Since these techniques include "resummation" of infinite orders of perturbation theory, it is not remotely clear *a priori* whether or not they would capture the same physics as the methods based on treating the black-body as an ensemble of external fields. If all this could be achieved, then the theoretical grounding of the external-field method of treating the black-body field would be strong, and perhaps at a stage where it would be worth seeking extensions to areas beyond QED, where particle production (and other effects) in plasmas with temperatures beyond the rest mass of the relevant particles are of more widespread concern, such as photon production in the quark-gluon plasma [182, 183] or dark matter production in the early universe [184–187].

In chapter 6, we used the "Bogoliubov transformation" formalism (section 2.2) to show how $\mathbb{C}$-valued solutions of the "Feynman-Cauchy" problem for the homogeneous Dirac equation fit into QED with a background field. This means solutions which have a given positive-energy component in the past, and a given negative-energy component in the future. This includes a concise "interpretation" of the bispinor profiles, by which is meant a mapping from the bispinor profiles that satisfy the Dirac equation to quantum-mechanical states, as well as a

proof that taking correct inner products with the Dirac equation solutions can provide the correct probability amplitudes for electron scattering, positron scattering, pair annihilation or pair creation.

Chapter 7 achieved two main aims. First, it demonstrated the equivalence of four causal propagators in a very broad class of vacuum-destabilising external fields, for which equivalence had previously only been demonstrated in special cases. Second, it provided a new formulation of Schwinger's proper-time quantum mechanics, which is both more mathematically rigorous, and conceptually novel: it replaces formal operator relations with relations between solutions of differential equations. This work could be expanded in two directions. First, part of what it set out to achieve is manifestly incomplete. The work uses the language of rigorous mathematics, and makes statements which are well-defined, but it has not rigorously *proven* its results. This is because the extension of mathematically rigorous formulations of quantum mechanics, which acknowledge the difficulties of working with unbounded operators on a Hilbert space, do not straightforwardly generalise to proper-time quantum mechanics. The problem is difficult because the proper-time Hamiltonian, considered as a differential operator, has very different mathematical properties to the regular Schrödinger Hamiltonian. The nature of its generalised eigenbasis and spectrum are therefore unknown. Completing this task, of extending rigorous mathematical formulations of non-relativistic quantum mechanics to proper-time quantum mechanics, is a well-defined incomplete mathematical exercise.

Excepting the possibility that this exercise would prove the negative, and invalidate Schwinger's result, it is really a task of more mathematical than physical interest. There is, perhaps, a way in which developing the work of chapter 7 could lead somewhere with potential novel physical application, though. Where something like Schwinger's proper-time has had success in application is in the worldline formulation of effective actions [73–75], generalisable to applications beyond external fields by its relation to the quantum effective action (the "background field method" [38–41] discussed briefly in section 2.1). This has all been formulated in terms of Euclidian path integrals, though, which is a starkly contrasting formulation to our relations between real-time differential equations. Therefore, it seems likely that the way to apply our rigorous formulation of the proper-time method in terms of differential equations to

an actual physics problem would be to relate it to the effective action, which could provide alternative evaluation methods to the Euclidean path integrals currently in wide use. Schwinger's expression for the effective action can be written

$$W^{(1)} = i \int^{-m_e c} d\lambda \, \mathrm{Tr}[\hat{G}_\lambda]. \tag{8.1}$$

In terms of inhomogeneous differential equations, $\mathrm{Tr}[\hat{G}_\lambda]$ is calculated by taking the sum of the inner product of some complete basis of source profiles $\{J_i(x)\}_i$, with the corresponding solutions of the inhomogenous proper-time Dirac equation, $\psi[J](\tau; x)$, $(i\partial_\tau - \hat{H})\psi_\lambda[J](\tau; x) = -J(x)e^{-i\lambda\tau}$ obeying the correct (Feynman) boundary condition,

$$W^{(1)} = i \int^{-m_e c} d\lambda \, \sum_{J_i} (J_i, \psi_\lambda[J_i](\tau = 0))_{\mathrm{P.T.}}. \tag{8.2}$$

Could this expression be useful for calculations? We can only say "possibly". If we knew that some small number of source profiles dominated the sum, for instance, then it is likely that some sort of numerical method or analytical approximation would work. It is also possible that some natural expression in terms of differential equation solutions could be discovered without the formal integration with respect to the mass. In general, this gives an entirely different mathematical formulation of the effective action than the usual path integrals, with its own possibilities of useful simplifications and estimates. It is, though, impossible ahead to time to know what these possibilities might really be, or if they are practically realisable.

Appendices

Appendix A

The Quantum Effective Action in a Background Field

This appendix derives equation 2.8. The argument used is a straightforward generalisation of that given in Ref [40, 41], with adjustments to include explicit field profiles at the boundaries at finite times. Consider the partition functionals between particular field profile $\phi_i(t_{\rm in})$ at $t_{\rm in}$ and $\phi_i(t_{\rm out})$ at $t_{\rm out}$. They can be written in the path-integral formalism, for the theories with and without an external field, as, respectively,

$$Z[J;\phi'_{\rm out},\phi'_{\rm in}] := \int_{\phi(t_{\rm in})=\phi'_{\rm in}}^{\phi'(t_{\rm out})=\phi_{\rm out}} \mathcal{D}\phi\; e^{i(S[\phi]+J\cdot\phi)} \tag{A.1a}$$

$$\tilde{Z}[B,J;\phi_{\rm out},\phi_{\rm in}] := \int_{\phi(t_{\rm in})=\phi_{\rm in}}^{\phi(t_{\rm out})=\phi_{\rm out}} \mathcal{D}\phi\; e^{i(S[\phi+B]+J\cdot\phi)}. \tag{A.1b}$$

where it is understood that $J\cdot\phi := \int d^4x\ \sum_i J_i(x)\phi_i(x)$. From these, we define the generator of connected graphs, with and without the background,

$$W[J;\phi'_{\rm out},\phi'_{\rm in}] := -\,i\ln Z[J;\phi'_{\rm out},\phi'_{\rm in}] \tag{A.2a}$$

$$\tilde{W}[J;\phi_{\rm out},\phi_{\rm in}] := -\,i\ln \tilde{Z}[B,J;\phi_{\rm out},\phi_{\rm in}], \tag{A.2b}$$

and the quantum effective action, the generator of 1PI graphs,

$$\Gamma[\bar{\phi};\phi'_{\text{out}},\phi'_{\text{in}}] := W[J;\phi'_{\text{out}},\phi'_{\text{in}}] - J\cdot\bar{\phi} \tag{A.3a}$$

$$\tilde{\Gamma}[\tilde{\phi};\phi_{\text{out}},\phi_{\text{in}}] := \tilde{W}[B,\tilde{J};\phi_{\text{out}},\phi_{\text{in}}] - \tilde{J}\cdot\tilde{\phi}, \tag{A.3b}$$

where

$$\bar{\phi} = \frac{\delta W}{\delta J} \quad \text{and} \quad \tilde{\phi} = \frac{\delta \tilde{W}}{\delta \tilde{J}}. \tag{A.4a}$$

We can, in equation A.3, imagine either that $\bar{\phi}/\ \tilde{\phi}$ are both functionals of $J/\tilde{J}$, or that $J/\tilde{J}$ are functionals of $\bar{\phi}/\tilde{\phi}$. It is the standard assumption of the Legendre transform that these functionals are invertible. We now set $\phi'_{\text{out/in}} = \phi_{\text{out/in}} + B$ and shift the variable of integration in equation A.2b from $\phi \to \phi - B$, such that

$$\tilde{Z}[B,J;\phi_{\text{out}},\phi_{\text{in}}] = Z[J;\phi_{\text{out}}+B,\phi_{\text{in}}+B]e^{-iJ\cdot B}. \tag{A.5}$$

Taking a logarithm of this equation gives

$$\tilde{W}[B,J;\phi_{\text{out}},\phi_{\text{in}}] = W[J;\phi_{\text{out}}+B,\phi_{\text{in}}+B] - J\cdot B. \tag{A.6}$$

Differentiating this with respect to J gives

$$\tilde{\phi}[B,J;\phi_{\text{out}},\phi_{\text{in}}] = \bar{\phi}[J;\phi_{\text{out}}+B,\phi_{\text{in}}+B] - B. \tag{A.7}$$

Because, for fixed B and in and out fields, the functionals $\tilde{\phi}[J]$ and $\bar{\phi}[J]$ are invertible, we can write this relation instead as

$$\tilde{J}[B,\tilde{\phi};\phi_{\text{out}},\phi_{\text{in}}] = J[\tilde{\phi}+B;\phi_{\text{out}}+B,\phi_{\text{in}}+B]. \tag{A.8}$$

Therefore

$$\tilde{\Gamma}[B, \phi; \phi_{\text{out}}, \phi_{\text{in}}] = \Gamma[\phi + B; \phi_{\text{out}} + B, \phi_{\text{in}} + B]. \tag{A.9}$$

Summing over in and out states formed as linear superpositions of field eigenstates gives the desired result (2.8).

Appendix B

A Toy Model for the Correction Factor

This appendix explains, using a toy model, why the inverse ratio of two partition functions of two systems can form an estimate for the ratio of the expectation values of a thermodynamic quantity measured in the two systems. Consider measuring the expectation value of a quantity v in two thermodynamic systems, A and B. Both of these systems can be in any of a set of microstates, labelled $i = 1, ..., N$, with value $v = v_i$, with Boltzmann factors $p_{A/B,i}$. Call their partition functions

$$Z_{A/B} = \sum_{i=1}^{N} p_{A/B,i}. \tag{B.1}$$

Suppose that $p_{A,i} = p_{B,i}$ if $v_i \neq 0$. Then, the ratio of expectation values for v measured in system A over system B is

$$\begin{aligned} R &= \frac{Z_A^{-1} \sum_{i=1}^{N} p_{A,i} v_i}{Z_B^{-1} \sum_{i=1}^{N} p_{B,i} v_i} = \frac{Z_B \sum_{i=1}^{N} p_{A,i} v_i}{Z_A \sum_{i=1}^{N} p_{A,i} v_i} \\ &= \frac{Z_B}{Z_A}. \end{aligned} \tag{B.2}$$

The ratio of the thermodynamic quantity in the two systems will therefore precisely equal the inverse ratio of partition functions if the non-normalised Boltzmann factors for microstates in the two systems are equal for all microstates with non-zero values of the quantity. It will form an approximate estimate of the true ratio if this is approximately true. In the case where system A describes the relativistic physics of a system, while B describes the classical physics, the inverse ratio of partition functions will form a good estimate of the correction

factor if the states that contribute most to the thermodynamic quantity all have energy in the non-relativistic regime.

Appendix C

Pair-Production in a Temporal Sauter Pulse

Adorno *et al.* [102] find, for an electric field with profile

$$E(t) = E_0 \operatorname{sech}^2(\omega_c t), \tag{C.1}$$

that the pair-creation rate for a given mode of momentum p_x in the direction of the applied field is

$$N_n^{\mathrm{cr}} = \frac{\sinh\{\pi c\hbar^{-1}\omega_c^{-1}[eE_0\omega_c^{-1} + \frac{1}{2}(\omega_+ - \omega_-)]\}\sinh\{\pi c\hbar^{-1}\omega_c^{-1}[eE_0\omega_c^{-1} - \frac{1}{2}(\omega_+ - \omega_-)]\}}{\sinh(\pi c\hbar^{-1}\omega_c^{-1}\omega_+)\sinh(\pi c\hbar^{-1}\omega_c^{-1}\omega_-)} \tag{C.2}$$

where

$$\omega_\pm := \sqrt{(p_x \mp \omega_c^{-1}eE_0)^2 + p_\perp^2 + m^2c^2}. \tag{C.3}$$

We now define

$$\begin{aligned} \kappa &= \frac{p_x\omega_c}{eE_0}, \quad & \Omega_\pm &= \sqrt{(\kappa_x \mp 1)^2 + \kappa_\perp^2 + \gamma^2} \\ \gamma &= \frac{mc\omega_c}{eE_0}, & \lambda &= \frac{c\pi eE_0}{\hbar\omega_c^2}. \end{aligned} \tag{C.4}$$

Note that $N_n^{\mathrm{cr}} = N_n^{\mathrm{cr}}(\kappa, \gamma)$, such that we can write the total pair production per unit

spatial volume,

$$n = \frac{m^3}{4\pi^2}\gamma^{-3}\int_0^\infty d(\kappa_\perp^2)\int_{-\infty}^\infty d\kappa_x\; N_n^{\rm cr}(\kappa;\lambda,\gamma). \tag{C.5}$$

This can be rewritten, for ease of computation,

$$n = \frac{m^3}{4\pi^2}\gamma^{-3}\int_{\gamma^2}^\infty d\Omega_+\int_{\sqrt{4-4\sqrt{\Omega_+^2-\gamma^2}+\Omega_+^2}}^{\sqrt{4+4\sqrt{\Omega_+^2-\gamma^2}+\Omega_+^2}} d\Omega_-\;\Omega_+\Omega_- N_n^{\rm cr}(\lambda,\Omega_+,\Omega_-). \tag{C.6}$$

The inner integral can be computed analytically and the outer numerically. The locally-constant field approximation to the total particle production rate can be written

$$\begin{aligned} n^{\rm LCFA} &= \frac{(eE_0)^2}{4\pi^3 c\hbar^2}\int_{-\infty}^\infty dt\;\mathrm{sech}^4(\omega_c t)\exp\left(-\frac{\pi E_S}{E_0}\cosh^2(\omega_c t)\right) \\ &= \frac{(eE_0)^2}{4\pi^3 c\hbar^2\omega_c}\left(\frac{\pi E_S}{E_0}\right)^2\int_{\pi E_S/E_0}^\infty du\;\frac{1}{\sqrt{u-\pi E_S/E_0}\;u^{5/2}}e^{-u} \\ &= \frac{m^3c^3}{3\pi^2\hbar^3}\lambda^{-1}\gamma^{-3}\left[1+\mathcal{O}\left(\frac{\pi E_S}{E_0}\right)\right], \end{aligned} \tag{C.7}$$

where the last line can be demonstrated using the first term of a Taylor expansion of e^{-u}, noting that its remainder ~ -1 for large u. Putting in parameters appropriate to the black-body, using equations 5.1 and 5.2, we find that $\gamma \to 0$ as as $k_B T$ grows much larger than $m_e c^2$, and

$$\lambda = \frac{\pi c e E_{\rm bb}}{\hbar\omega_{c,\rm bb}^2} = \frac{\pi}{\tilde{\beta}_{\rm c}^2}\sqrt{\frac{8\pi^3\alpha}{15}}. \tag{C.8}$$

This is constant with temperature and of order of magnitude ~ 1. The ratio of equation C.6 over equation C.7 for $\gamma = 0$ is plotted in figure C.1. We can see, first, that large λ corresponds to the locally-constant limit, and second, that the exact result only ever exceeds the locally-constant approximation, $n \geq n^{\rm LCFA}$ for all λ when $\gamma = 0$.

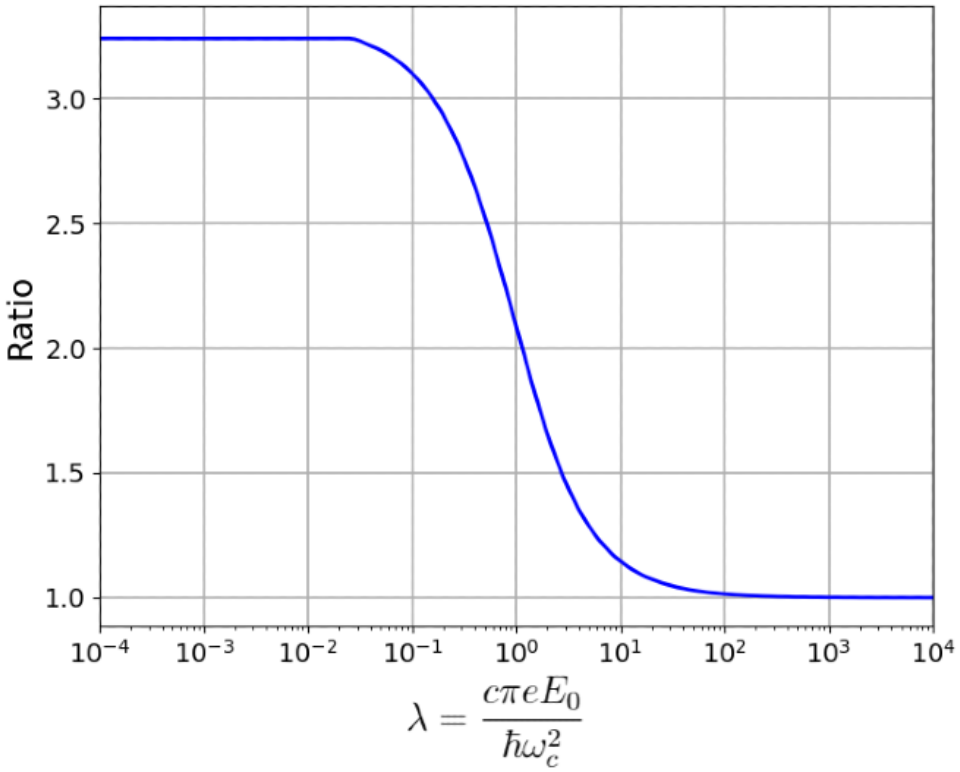

Figure C.1: Ratio of particle production rate in a temporal Sauter pulse external field over the locally-constant field estimate for $\gamma = 0$. Note that the the x-axis is logarithmic while the y-axis is not. The ratio approaching one as λ grows corresponds to the locally-constant field approximation being accurate in this limit.

Appendix D

The Feynman-Cauchy Problem from FGS

In this appendix we show that equation 6.15 agrees with FGS's results [12]. We restrict attention to electron scattering and pair annihilation for brevity; the method for positron scattering and pair creation is very similar. We first note that FGS's $G({}^{\xi}|_{\chi})$ matrices (2.24) act as solvers of the advanced and retarded Dirac equation in the following sense. First, consider a general bispinor profile $f_l(x)$, and denote its components in FGS's in and out bases as

$$f_l(x) = \sum_{\alpha,\pm} {}_{\pm}f_{\alpha}(t)\, {}_{\pm}\varphi_{\alpha}(\mathbf{x}) \tag{D.1a}$$

$$= \sum_{\alpha,\pm} {}^{\pm}f_{\alpha}(t)\, {}^{\pm}\varphi_{\alpha}(\mathbf{x}). \tag{D.1b}$$

If we write ${}_{\pm}f_{\alpha}$ and ${}^{\pm}f_{\alpha}$ as column vectors, and assembled the matrix

$$G = \begin{pmatrix} G({}^{+}|_{+}) & G({}^{+}|_{-}) \\ G({}^{-}|_{+}) & G({}^{-}|_{-}) \end{pmatrix}, \tag{D.2}$$

then we have the relations

$$\begin{pmatrix} {}^{+}f \\ {}^{-}f \end{pmatrix} = G \begin{pmatrix} {}_{+}f \\ {}_{-}f \end{pmatrix}, \quad \begin{pmatrix} {}_{+}f \\ {}_{-}f \end{pmatrix} = G^{\dagger} \begin{pmatrix} {}^{+}f \\ {}^{-}f \end{pmatrix}, \tag{D.3}$$

i.e. G can be used to solve the advanced and retarded Dirac equation, with components in two different bases at the in and out times. Now take $f_l(\mathbf{x})$ to be f_{in} defined in equation 6.13, with components $\{ {}_{\pm}f_{\text{in},\alpha}(t)\}_{\pm,\alpha}$ or $\{ {}^{\pm}f_{\text{in},\alpha}(t)\}_{\pm,\alpha}$. Equations D.3 and 2.25 give

$${}_{+}f(t_{\text{in}}) = G({}_{+}|^{+}) \, {}^{+}f(t_{\text{out}}) + G({}_{+}|^{-}) \, {}^{-}f(t_{\text{out}}) \tag{D.4a}$$

$${}_{-}f(t_{\text{in}}) = G({}_{-}|^{+}) \, {}^{+}f(t_{\text{out}}) + G({}_{-}|^{-}) \, {}^{-}f(t_{\text{out}}) \tag{D.4b}$$

but since ${}^{-}f_{\text{in}} \equiv 0$,

$${}^{+}f_{\text{in}}(t_{\text{out}}) = G^{-1}({}_{+}|^{+}) \, {}_{+}f_{\text{in}}(t_{\text{in}})(t_{\text{in}}) \tag{D.5a}$$

$${}_{-}f_{\text{in}}(t_{\text{in}}) = G({}_{-}|^{+}) \, {}^{+}f_{\text{in}}(t_{\text{out}}) = G({}_{-}|^{+}) G^{-1}({}_{+}|^{+}) \, {}_{+}f_{\text{in}}(t_{\text{in}})(t_{\text{in}}). \tag{D.5b}$$

Write an output electron profile as ${}^{+}g_l(\mathbf{x})$. Then we have

$$\begin{aligned} ({}^{+}g, \, f_{\text{in}}(t_{\text{out}})) &= ({}^{+}g, \, {}^{+}\hat{P}^m f_{\text{in}}(t_{\text{out}})) \\ &= \sum_{\alpha\beta} {}^{+}g^{*}_{\beta} G^{-1}({}_{+}|^{+})_{\beta\alpha} \, {}_{+}f_{\text{in},\alpha}(t_{\text{in}}). \end{aligned} \tag{D.6}$$

Write an input positron profile as ${}_{-}g_l(\mathbf{x})$. Then we have

$$\begin{aligned} ({}_{-}g, f_{\text{in}}(t_{\text{in}})) &= ({}_{-}g, \, {}_{-}\hat{P}^m f_{\text{in}}(t_{\text{in}})) \\ &= \sum_{\alpha\beta} {}_{-}g^{*}_{\beta} \left[G({}_{-}|^{+}) G^{-1}({}_{+}|^{+}) \right]_{\beta\alpha} \, {}_{+}f_{\text{in},\alpha}(t_{\text{in}}). \end{aligned} \tag{D.7}$$

Relating these to FGS's expressions 2.26a,c, we see that 6.15a,b is equivalent to FGS's expression, though in a basis-independent form.

Appendix E

Complex Fourier Analysis

The methods in this subsection are guided closely by Ref. [238], chapter 19. Following its notation, we label the real-variable we are transforming in this section t, the real Fourier variable x, and the complex variable $z = x + iy$. We can write the complex Fourier transform as

$$f(z) = \int_{\mathbb{R}} dt\ e^{izt} F(t). \tag{E.1}$$

We write a real Fourier transform and its inverse as

$$\mathcal{F}_{x,t}[G(t)] = \int_{-\infty}^{\infty} dt\ e^{ixt} G(t) \tag{E.2}$$

$$\mathcal{F}^{-1}_{t,x}[g(x)] = \frac{1}{2\pi} \int_{-\infty}^{\infty} dx\ e^{-ixt} g(x). \tag{E.3}$$

Suppose $F^{\mathrm{l}}(t)$ is supported only on $(-\infty, A)$, and $F^{\mathrm{u}}(t)$ only on (B, ∞), with $A > 0$, $B < 0$. $f^{\mathrm{u/l}}(z)$ is the complex Fourier transform of these functions. Both functions are square-integrable, and by the Placherel theorem,

$$\int_{-\infty}^{\infty} dt\ |F^{\mathrm{u/l}}(t)|^2 = \int_{\mathbb{R}} dx\ |f^{\mathrm{u/l}}(x)|^2 = C > 0. \tag{E.4}$$

By the Paley-Weiner theorems, we know that $f^{\mathrm{u/l}}(z)$ is analytic on the upper/lower half complex plane. Now, define the inverse Fourier transform along some horizontal line defined

by y constant as

$$\tilde{f}_y(t) = \frac{1}{2\pi}\int_{-\infty}^{\infty} dx\; e^{-ixt} f(x+iy) = \mathcal{F}^{-1}_{t,x}[f(x+iy)] \tag{E.5}$$

and write

$$f(x+iy) = \int_{-\infty}^{\infty} dt\; e^{i(x+iy)t} F(t) = \mathcal{F}_{x,t}[e^{-yt}F(t)] \tag{E.6}$$

to give

$$\tilde{f}_y(t) = \mathcal{F}^{-1}_{t,x}[\mathcal{F}_{x,t}[e^{-yt}F(t)]] = e^{-yt}F(t). \tag{E.7}$$

Now consider

$$\begin{aligned}\int_{-\infty}^{\infty} dx |f^{\mathrm{u/l}}(x+iy)|^2 &= \int_{-\infty}^{\infty} dt\; |\mathcal{F}^{-1}_{t,x}[f^{\mathrm{u/l}}(x+iy)]|^2 \\ &= \int_{-\infty}^{\infty} dt\; |\tilde{f}^{\mathrm{u/l}}_y(t)|^2 = \int_{-\infty}^{\infty} dt\; e^{-2ty}|F^{\mathrm{u/l}}(t)|^2 \\ &\leq \begin{cases} e^{-2Ay}C, & l \text{ case, } y<0 \\ e^{-2By}C, & u \text{ case, } y>0, \end{cases}\end{aligned} \tag{E.8}$$

where in the first line we have used the Plancherel theorem, in the second we have used equation E.7 and in the third we have used the known support of $F^{\mathrm{u/l}}(t)$ to extract a maximum value of e^{-2ty} and used equation E.4. Now write

$$\begin{aligned}\int_{-\infty}^{\infty} dx\; |f^{\mathrm{u/l}}(x+iy)e^{-it(x+iy)}|^2 &= e^{2yt}\int_{-\infty}^{\infty} dx\; |f^{\mathrm{u/l}}(x+iy)|^2 \\ &\leq \begin{cases} e^{2(t-A)y}C, & l \text{ case, } y<0 \\ e^{2(t-B)y}C, & u \text{ case, } y>0. \end{cases}\end{aligned} \tag{E.9}$$

Next, write the interval $I^{\mathrm{u}}_y = [y, 0]$, with $y < 0$ assumed, and $I^{\mathrm{l}}_y = [0, y]$, with $y > 0$ assumed. Then define the positive integral

$$\Lambda^{\mathrm{u/l}}(\alpha; y) := \int_{I^{\mathrm{u/l}}_y} du\; |f^{\mathrm{u/l}}(\alpha+iu)e^{-it(\alpha+iu)}|^2. \tag{E.10}$$

Now consider

$$\int_{-\infty}^{\infty} d\alpha\ \Lambda^{\mathrm{u/l}}(\alpha;y) = \int_{I_y^{\mathrm{u/l}}} du \left(\int_{-\infty}^{\infty} d\alpha\ |f^{\mathrm{u/l}}(\alpha+iu)e^{-it(\alpha+iu)}|^2 \right), \tag{E.11}$$

where Fubini's theorem allows us to change the order of the integral. We can now use equation E.9 to get

$$\int_{-\infty}^{\infty} d\alpha\ \Lambda^{\mathrm{l}}(\alpha;y) \leq C \int_{I_y^{\mathrm{l}}} du\ e^{2(t-A)u} = \frac{C}{2(t-A)} \left(1 - 2e^{2(t-A)y}\right) \tag{E.12}$$

$$\int_{-\infty}^{\infty} d\alpha\ \Lambda^{\mathrm{u}}(\alpha;y) \leq C \int_{I_y^{\mathrm{u}}} du\ e^{2(t-B)u} = \frac{C}{2(t-B)} \left(1 - e^{2(t-B)y}\right). \tag{E.13}$$

Therefore for every fixed y, $\Lambda^{\mathrm{u/l}}(\alpha, y)$ is an integrable function of α on the real line. This means that there exists a sequence, $\{\gamma_j \in \mathbb{R}\}_j$, such that as $j \to \infty$ [**?**],

$$\gamma_j \to +\infty, \qquad \Lambda^{\mathrm{u/l}}(\gamma_j, y) = 0. \tag{E.14}$$

Define $\Gamma^{\mathrm{u}}_{\alpha,\beta}$ as the anticlockwise rectangular contour with corners at $(\pm\alpha, 0)$, $(\pm\alpha, \beta)$, $\alpha, \beta \in \mathbb{R}^+$, which does not include the real line. Define, similarly, $\Gamma^{\mathrm{l}}_{\alpha,\beta}$ as the clockwise contour with corners at $(\pm\alpha, 0)$, $(\pm\alpha, -\beta)$ which does not include the real line. Also suppose the function $h^{\mathrm{u/l}}(z)$ has bounded absolute value $|h^{\mathrm{u/l}}(z)|$ as $|z| \to \infty$ on the upper/lower complex plane, and is meromorphic on the upper/lower complex plane. Then we can write

$$\begin{aligned} \int_{\Gamma^{\mathrm{l}}_{\gamma_j,\beta}} |dz|\ |h^{\mathrm{l}}(z)f^{\mathrm{l}}(z)e^{-izt}|^2 \leq\ & \mathrm{Sup}_{\Gamma^{\mathrm{l}}_{\gamma_j,\beta}} \left(|h^{\mathrm{l}}(z)|^2\right) \cdot \\ & \left(\int_{-\gamma_j}^{\gamma_j} dx\ |f^{\mathrm{l}}(x-i\beta)e^{-it(x-i\beta)}|^2 + \Lambda^{\mathrm{l}}(\gamma_j, -\beta) + \Lambda^{\mathrm{l}}(-\gamma_j, -\beta) \right) \end{aligned} \tag{E.15}$$

$$\begin{aligned} \int_{\Gamma^{\mathrm{u}}_{\gamma_j,\beta}} |dz|\ |h^{\mathrm{u}}(z)f^{\mathrm{u}}(z)e^{-izt}|^2 \leq\ & \mathrm{Sup}_{\Gamma^{\mathrm{u}}_{\gamma_j,\beta}} \left(|h^{\mathrm{u}}(z)|^2\right) \cdot \\ & \left(\int_{-\gamma_j}^{\gamma_j} dx\ |f^{\mathrm{u}}(x+i\beta)e^{-it(x+i\beta)}|^2 + \Lambda^{\mathrm{u}}(\gamma_j, \beta) + \Lambda^{\mathrm{u}}(-\gamma_j, \beta) \right). \end{aligned} \tag{E.16}$$

If we take $j \to \infty$, then the second two terms in the brackets vanishes by equation E.14.

If we then take $\beta \to \infty$ then the first term vanishes by equation E.9, so long as $t < B$ in the "u" case and $t > A$ in the "l" case.. $\mathrm{Sup}_{\substack{\Gamma^{\mathrm{u/l}} \\ \gamma_j,\beta}} \left(|h^{\mathrm{u/l}}(z)|^2\right)$ stays finite by assumption, and hence

$$\lim_{\beta\to\infty} \lim_{j\to\infty} \int_{\substack{\Gamma^{\mathrm{u/l}} \\ \gamma_j,\beta}} |dz|\ |h^{\mathrm{u/l}}(z) f^{\mathrm{u/l}}(z) e^{-izt}|^2 = 0. \tag{E.17}$$

Therefore, there exists a way of taking $\Gamma^{\mathrm{u/l}}$ to be an infinite rectangular contour in the upper/lower half plane excluding the real line, such that

$$\int_{\Gamma^{\mathrm{u/l}}} dz\ h^{\mathrm{u/l}}(z) f^{\mathrm{u/l}}(z) e^{-izt} = 0, \tag{E.18}$$

and hence, by the residue theorem,

$$\int_{\mathbb{R}} dz\ h^{\mathrm{u/l}}(z) f^{\mathrm{u/l}}(z) e^{-izt} = \pm 2\pi i \sum_{z_0 \in \mathrm{poles}} f(z_0) \mathrm{Res}(h^{\mathrm{u/l}}(z_0)), \tag{E.19}$$

if $t < B$ in the "u" case and if $t > A$ in the case "l" case. $\pm = +/-$ in the "u/l" case, and the z_0 sum runs over poles in the upper/lower half plane.

Appendix F

The ± Components of a Source Supported on Finite Time

Consider equation 7.57a. Define

$$ {}_{\pm}J^{\text{in}}(\Pi;t) := \int_{\mathbb{R}} dE\ {}_{\pm}\check{J}(\Pi;E)e^{-iE(t-t_{\text{in}})}, \tag{F.1} $$

and define ${}_{\pm}J(t)$ as the t-dependent vectors in $\mathcal{H}_{\text{S.T.}}$ for which ${}_{\pm}J^{\text{in}}(\Pi;t)$ are representations. In this appendix we argue that if the support of $J(t)$ is in the interval (t_{in},∞), then the same is true of both ${}_{\pm}J(t)$ individually. Consider

$$ \begin{aligned} \hat{H}_{\text{P.T.}}: \quad {}_{\pm}J^{\text{in}}(\Pi,t) \ \mapsto\ {}_{\pm}J'^{\text{in}}(\Pi,t) &= \pm\int_{\mathbb{R}\cup I^{+}_{\text{in}}} d\mu^{\text{in}}_{\hat{E},\Pi}(E)\ \lambda^{\text{u}}(\Pi,E)\,{}_{\pm}J(\Pi;E)e^{-iE(t-t_{\text{in}})} \\ &= \pm\int_{\mathbb{R}} dE\ \lambda^{\text{u}}(\Pi,E)\,{}_{\pm}\check{J}(\Pi;E)e^{-iE(t-t_{\text{in}})}, \end{aligned} \tag{F.2} $$

where in the first line we have used the notation of equation 7.40, and in the second line that of equation 7.45, with $g^{\text{u}}(E)=\lambda^{\text{u}}(\Pi,E)$. A Paley-Wiener theorem says that a function's Fourier transform is of exponential type t_{in} in the upper half-plane if and only if its support is within (t_{in},∞) [238]. $\lambda^{\text{u}}(\Pi,E)$ is of exponential type 0, so $\lambda^{\text{u}}(\Pi,E)\sum_{\pm}\pm\,{}_{\pm}\check{J}(\Pi;E)$ is of the same exponential type as $\sum_{\pm}\pm\,{}_{\pm}\check{J}(\Pi;E)$, and hence $[\hat{H}_{\text{P.T}}J](t)$ is supported in (t_{in},∞) if and only if $\sum_{\pm}\pm\,{}_{\pm}J(t)$ is.

If $J(t) = 0$ at some t, then ${}_+J(t) = -{}_-J(t)$, and therefore $\sum_\pm \pm {}_\pm J(t) = 2\,{}_+J(t) = -2\,{}_-J(t)$. Therefore if $J(t) = 0$ and either ${}_+J(t) \neq 0$ or ${}_-J(t) \neq 0$ at a particular t, then $\sum_\pm \pm {}_\pm J(t) \neq 0$. Therefore, if $J(t)$ is supported in (t_{in}, ∞), and ${}_+J(t)$ or ${}_-J(t)$ is not, then $[\hat{H}_{\text{P.T.}} J](t)$ is also not supported in (t_{in}, ∞). But if $\hat{H}_{\text{P.T.}}$ acts on a profile that equals zero in some open interval that includes t, it must return zero, since it is a local differential operator of finite order. Therefore, if $J(t) = 0$ in any open region, both its ± components must also, ${}_\pm J(t) = 0$. Applied to the open interval $(-\infty, t_{\text{in}})$, this gives the desired result. The result for the "out" representation proceeds analogously.

Appendix G

The Time-Translation Operator of the Dirac Equation

We here prove that the classical initial value problem for the Dirac equation with an complex mass is well-posed: any initial value gives one and only one classical solution. To do this, we write the Dirac equation in the form

$$\partial_t \psi = (\hat{A} + \hat{B})\psi \tag{G.1a}$$

$$\hat{A} := -\gamma^0 \hat{\Pi}^{\text{in/out}} - iA_0^{\text{in/out}}, \quad \hat{B} := -im\gamma^0, \tag{G.1b}$$

and use known results from semigroup operator methods for solving evolution equations, specifically as presented in Ref. [239], chapter 12.1-2. The classical initial-value problem gives a unique classical solution if $\hat{C} := \hat{A} + \hat{B}$ is an infinitesimal generator for a strongly continuous semigroup, $\hat{T}_m(t)$. We write of such an operator,

$$\hat{C} \in \mathcal{G}(M, \omega) \quad \text{iff} \quad ||\hat{T}_m(t)|| \leq Me^{\omega t}, \quad M, \omega \in \mathbb{R}. \tag{G.2}$$

Any operator that is skew-adjoint is in $\mathcal{G}(1, 0)$. This is true of $\hat{A}$ always, and $\hat{A} + \hat{B}$ iff m is real. If m is not real, we can use the result that if $\hat{A} \in \mathcal{G}(1, \omega)$ and $\hat{B}$ is bounded, with $||\hat{B}|| = |m|$, then $\hat{A} + \hat{B} \in \mathcal{G}(1, \omega + |m|)$, or in this case, $\hat{A} + \hat{B} \in \mathcal{G}(1, |m|)$.

Bibliography

[1] J. J. Beesley and S. J. Rose. Free electron relativistic correction factors to collisional excitation and ionisation rates in a plasma. *High Energy Density Phys.*, 33:100716, 2019.

[2] J. J. Beesley. On the equivalence of causal propagators of the dirac equation in vacuum-destabilising external fields. *Found. Phys.*, 52(1):27, Feb. 2022.

[3] J. J. Beesley and S. J. Rose. High-temperature limit of breit–wheeler pair production in a black-body field. *Results Phys.*, 41:105917, 2022.

[4] G. Breit and J. A. Wheeler. Collision of two light quanta. *Phys. Rev.*, 46:1087–1091, Dec. 1934.

[5] T. A. Weaver. Reaction rates in a relativistic plasma. *Phys. Rev. A*, 13:1563–1569, 1976.

[6] J. Schwinger. On gauge invariance and vacuum polarization. *Phys. Rev.*, 82:664–679, June 1951.

[7] E. C. G. Sudarshan. Equivalence of semiclassical and quantum mechanical descriptions of statistical light beams. *Phys. Rev. Lett.*, 10:277–279, Apr. 1963.

[8] C. L. Mehta and E. C. Sudarshan. Relation between Quantum and Semiclassical Description of Optical Coherence. *Phys. Rev.*, 138(1B):274–280, Apr. 1965.

[9] R. J. Glauber. Coherent and incoherent states of the radiation field. *Phys. Rev.*, 131:2766–2788, Sep. 1963.

[10] A. I. Nikishov. Barrier scattering in field theory removal of klein paradox. *Nucl. Phys. B*, 21(2):346–358, 1970.

[11] R. P. Feynman. The theory of positrons. *Phys. Rev.*, 76:749–759, Sep. 1949.

[12] E. S. Fradkin, D. M. Gitman, and Sh. M. Shvartsman. *Quantum electrodynamics with unstable vacuum.* Jan. 1991.

[13] F. Gieres. Mathematical surprises and dirac's formalism in quantum mechanics. *Rep. Prog. Phys.*, 63(12):1893–1931, Nov. 2000.

[14] N. Bohr. Can quantum-mechanical description of physical reality be considered complete? *Phys. Rev.*, 48:696–702, Oct. 1935.

[15] N. Bohr. Causality and complementarity. *Philos. Sci.*, 4(3):289–298, 1937.

[16] P. A. M. Dirac. The quantum theory of the electron. *Proc. Roy. Soc. Lond. A*, 117:610–624, 1928.

[17] P. A. M. Dirac. A Theory of Electrons and Protons. *Proc. Roy. Soc. Lond. A*, 126(801):360–365, 1930.

[18] M. Planck. Ueber das Gesetz der Energieverteilung im Normalspectrum. *Ann. Phys.*, 309(3):553–563, Jan. 1901.

[19] A. Einstein. über einen die erzeugung und verwandlung des lichtes betreffenden heuristischen gesichtspunkt. *Ann. Phys.*, 322(6):132–148, 1905.

[20] F. J. Dyson. The s matrix in quantum electrodynamics. *Phys. Rev.*, 75:1736–1755, June 1949.

[21] S. Tomonaga. On a Relativistically Invariant Formulation of the Quantum Theory of Wave Fields. *Prog. Theor. Phys.*, 1(2):27–42, Aug. 1946.

[22] R. P. Feynman. Space-time approach to quantum electrodynamics. *Phys. Rev.*, 76:769–789, Sep. 1949.

[23] R. P. Feynman. Mathematical formulation of the quantum theory of electromagnetic interaction. *Phys. Rev.*, 80:440–457, Nov. 1950.

[24] J. Schwinger. Quantum electrodynamics. i. a covariant formulation. *Phys. Rev.*, 74:1439–1461, Nov. 1948.

[25] J. Schwinger. Quantum electrodynamics. ii. vacuum polarization and self-energy. *Phys. Rev.*, 75:651–679, Feb. 1949.

[26] J. Schwinger. Quantum electrodynamics. iii. the electromagnetic properties of the electron—radiative corrections to scattering. *Phys. Rev.*, 76:790–817, Sep. 1949.

[27] W. Heisenberg and H. Euler. Folgerungen aus der Diracschen Theorie des Positrons. *Z. Phys.*, 98(11-12):714–732, Nov. 1936.

[28] W. H. Furry. On bound states and scattering in positron theory. *Phys. Rev.*, 81:115–124, Jan. 1951.

[29] P. A. M. Dirac. *The Principles of Quantum Mechanics*. Clarendon Press, 1981.

[30] J. von Neumann and R. T. Beyer. *Mathematical Foundations of Quantum Mechanics*. Goldstine Printed Materials. Princeton University Press, 1955.

[31] B. C. Hall. *Quantum theory for mathematicians*. Springer, New York, 2013.

[32] R. de la Madrid. The role of the rigged hilbert space in quantum mechanics. *Eur. J. Phys.*, 26(2):287–312, Feb. 2005.

[33] P. A. M. Dirac and R. H. Fowler. The fundamental equations of quantum mechanics. *Proc. R. Soc. Lond. A*, 109(752):642–653, 1925.

[34] P.A.M. Dirac. *Lectures on Quantum Mechanics*. Belfer Graduate School of Science. Monographs series. Belfer Graduate School of Science, Yeshiva University, 1964.

[35] N. M. J. Woodhouse. *Geometric Quantization*. Oxford mathematical monographs. Clarendon Press, 1997.

[36] S. Weinberg. *The Quantum Theory of Fields*, volume 1. Cambridge University Press, 1995.

[37] H. Lehmann, K. Symanzik, and W. Zimmermann. Zur Formulierung quantisierter Feldtheorien. *Il Nuovo Cimento*, 1(1):205–225, Jan. 1955.

[38] D. G. Boulware. Gauge dependence of the effective action. *Phys. Rev. D*, 23:389–396, Jan. 1981.

[39] Bryce S. DeWitt. A Gauge Invariant Effective Action. In *Oxford Conference on Quantum Gravity*, July 1980.

[40] L. F. Abbott. The Background Field Method Beyond One Loop. *Nucl. Phys. B*, 185:189–203, 1981.

[41] L. F. Abbott. Introduction to the Background Field Method. *Acta Phys. Polon. B*, 13:33, 1982.

[42] S. Weinberg. A model of leptons. *Phys. Rev. Lett.*, 19:1264–1266, Nov. 1967.

[43] A. Salam. Weak and Electromagnetic Interactions. *Conf. Proc. C*, 680519:367–377, 1968.

[44] J. Schwinger. Brownian motion of a quantum oscillator. *J. Math. Phys.*, 2(3):407–432, 1961.

[45] L. V. Keldysh. Diagram technique for nonequilibrium processes. *Zh. Eksp. Teor. Fiz.*, 47:1515–1527, 1964.

[46] N. P. Landsman and Ch. G. van Weert. Real- and imaginary-time field theory at finite temperature and density. *Phys. Rep.*, 145(3):141–249, 1987.

[47] M. Le Bellac. *Thermal Field Theory*. Cambridge Monographs on Mathematical Physics. Cambridge University Press, Mar. 2011.

[48] J. Schwinger. *Particles, Sources, and Fields*. Number v. 1 in Addison-Wesley series in physics. Addison-Wesley Publishing Company, 1970.

[49] A. I. Nikishov. Pair Production by a Constant External Field. *Sov. J. Exp. Theor. Phys.*, 30:660, Jan. 1969.

[50] N. B. Narozhnyi and A. I. Nikishov. The simplest processes in the pair-creating electric field. *Yadern. Fiz.*, 1(11):1072–7, May 1970.

[51] A. I. Nikishov. S matrix in quantum electrodynamics with external field. *Theor. Math. Phys.*, 20(1):653–659, July 1974.

[52] D. M. Gitman. Processes of Arbitrary Order in Quantum Electrodynamics with a Pair Creating External Field. *J. Phys. A*, 10:2007–2020, 1977.

[53] D. M. Gitman. *Problems in QED with an External Field*. PhD thesis, Institute of Nuclear Physics (Novosibirsk), 1979.

[54] D. M. Gitman. Quantum processes in an intense electromagnetic field. i. *Sov. Phys. J.*, 19(10):1309–1313, Oct. 1976.

[55]

[56] E. S. Fradkin and D. M. Gitman. Problems of Quantum Electrodynamics with Intensive Field: Appendix. Technical report, 1979.

[57] E. S. Fradkin and D. M. Gitman. Furry picture for quantum electrodynamics with pair-creating external field. *Fortschritte der Phys.*, 29(9):381–411, 1981.

[58] S. P. Gavrilov, D. M. Gitman, and Sh. M. Shvartsman. Unitarity relation in quantum electrodynamics with a pair-generating external field. *Sov. Phys. J.*, 23(3):257–260, Mar. 1980.

[59] E. S. Fradkin, D. M. Gitman, and Sh. M. Shvartsman. Optical theorem in quantum electrodynamics with unstable vacuum. *Fortschritte der Phys.*, 36(8):643–669, 1988.

[60] V. P. Barashev, A. E. Shabad, and Sh. M. Shvartsman. Polarization Operator in Quantum Electrodynamics With Pair Creating External Field. *Sov. J. Nucl. Phys.*, 43:617, 1986.

[61] V. P. Barashev, A. E. Shabad, and S. M. Shvartsman. Polarization operator in quantum electrodynamics with a pair-creating external field. *Sov. J. Nucl. Phys.*, 4(43), 1986.

[62] D. M. Gitman, E. S. Fradkin, and Sh. M. Shvartsman. Quantum electrodynamics with an external field disturbing vacuum stability. *Moscow Izdatel Nauka*, 193:3–207, Jan. 1989.

[63] S. P. Gavrilov and D. M. Gitman. Vacuum radiational processes in pair-generating fields. *Sov. Phys. J.*, 25(9):775–777, Sep. 1982.

[64] V. Fock. Proper time in classical and quantum mechanics. *Phys. Z. Sowjetunion*, 12:404–425, 1937.

[65] E. C. G. Stueckelberg. La Mecanique du point materiel en theorie de relativite et en theorie des quanta. *Helv. Phys. Acta*, 15:23–37, 1942.

[66] R. P. Feynman. Relativistic cut-off for quantum electrodynamics. *Phys. Rev.*, 74:1430–1438, Nov. 1948.

[67] R. P. Feynman. Space-time approach to non-relativistic quantum mechanics. *Rev. Mod. Phys.*, 20:367–387, Apr. 1948.

[68] J. R. Fanchi. Review of invariant time formulations of relativistic quantum theories. *Found. Phys.*, 23:487–548, 1993.

[69] B. S. DeWitt. Dynamical theory of groups and fields. 1965.

[70] A. O. Barvinsky and G. A. Vilkovisky. The Generalized Schwinger-Dewitt Technique in Gauge Theories and Quantum Gravity. *Phys. Rept.*, 119:1–74, 1985.

[71] R. Camporesi. Harmonic analysis and propagators on homogeneous spaces. *Phys. Rep.*, 196(1):1 – 134, 1990.

[72] W. Dittrich and H. Gies. *Probing the quantum vacuum. Perturbative effective action approach in quantum electrodynamics and its application*, volume 166. 2000.

[73] Z. Bern and D. A. Kosower. The computation of loop amplitudes in gauge theories. *Nucl. Phys. B*, 379(3):451–561, 1992.

[74] M. J. Strassler. Field theory without Feynman diagrams: One loop effective actions. *Nucl. Phys. B*, 385:145–184, 1992.

[75] C. Schubert. An introduction to the worldline technique for quantum field theory calculations. 1996.

[76] K. Costello. *Renormalization and Effective Field Theory*. American Mathematical Society, Providence, R.I, 2011.

[77] S. Coleman. *Classical Lumps and Their Quantum Descendants*, pages 297–421. Springer US, Boston, MA, 1977.

[78] G. V. Dunne and C. Schubert. Worldline instantons and pair production in inhomogenous fields. *Phys. Rev. D*, 72:105004, Nov. 2005.

[79] G. V. Dunne, Q. Wang, H. Gies, and C. Schubert. Worldline instantons and the fluctuation prefactor. *Phys. Rev. D*, 73:065028, Mar. 2006.

[80] T. D. Cohen and D. A. McGady. Schwinger mechanism revisited. *Phys. Rev. D*, 78:036008, Aug. 2008.

[81] C. Itzykson and J. B. Zuber. *Quantum Field Theory*. International series in pure and applied physics. McGraw-Hill International Book Company, 1980.

[82] H. Gies and K. Klingmüller. Pair production in inhomogeneous fields. *Phys. Rev. D*, 72:065001, Sep. 2005.

[83] I. A. Aleksandrov, G. Plunien, and V. M. Shabaev. Locally-constant field approximation in studies of electron-positron pair production in strong external fields. *Phys. Rev. D*, 99:016020, Jan. 2019.

[84] F. V. Bunkin and I. I. Tugov. Possibility of creating electron-positron pairs in a vacuum by the focusing of laser radiation. In *Soviet Physics Doklady*, volume 14, page 678, 1970.

[85] J. K. Daugherty and I. Lerche. Theory of pair production in strong electric and magnetic fields and its applicability to pulsars. *Phys. Rev. D*, 14:340–355, July 1976.

[86] V. G. Bagrov, D. M. Gitman, and Sh. M. Shvartsman. Concerning the production of electron-positron pairs from vacuum. *Zh. Eksp. Teor. Fiz*, 68:392–399, 1975.

[87] D. M. Gitman, V. M. Shakhmatov, and Sh. M. Shvartsman. Pair production in an electric field applied for a short time. *Sov. Phys. J.*, 18(4):455–460, Apr. 1975.

[88] N. B. Narozhnyi and A. I. Nikishov. Pair production by a periodic electric field. *Zh. Eksp. Teor. Fiz.*, 65(3):862–874, 1973.

[89] V. M. Mostepanenko and V. M. Frolov. Particle creation from vacuum by homogeneous electric field with a periodical time dependence. *Yad. Fiz.*, 19:885–896, 1974.

[90] V. G. Bagrov, D. M. Gitman, and Sh. M. Shvartsman. Pair creation from vacuum by an electromagnetic field in the zero-plane formalism. *Sov. Journ. Nucl. Phys.*, 23:394–400.

[91] S. P. Gavrilov and D. M. Gitman. Processes of pair-creation and scattering in constant field and plane-wave field. *Sov. Phys. Journ.*, 5:108–111.

[92] N. B. Narozhnyi and A. I. Nikishov. Solutions of the klein-gordon and dirac equations for a particle in a constant electric field and a plane electromagnetic wave propagating along the field. *Theor. Math. Phys.*, 26(1):9–20, Jan. 1976.

[93] Yu. Yu. Vol'fengaut and Sh. M. Shvartsman. Vacuum creation of $e\hat{+}e\hat{-}$ pairs in coherent states. *Sov. Phys. J.*, 21(11):1499–1500, Nov. 1978.

[94] S. P. Gavrilov and D. M. Gitman. Scattering and pair creation by a constant electric field between two capacitor plates. *Phys. Rev. D*, 93:045033, Feb. 2016.

[95] T. C. Adorno, S. P. Gavrilov, and D. M. Gitman. Vacuum instability in a constant inhomogeneous electric field: a new example of exact nonperturbative calculations. *Eur. Phys. J. C*, 80(2):88, Feb. 2020.

[96] T. C. Adorno, S. P. Gavrilov, and D. M. Gitman. Particle creation from the vacuum by an exponentially decreasing electric field. *Phys. Scr.*, 90(7):074005, June 2015.

[97] T. C. Adorno, S. P. Gavrilov, and D. M. Gitman. Particle creation by peak electric field. *Eur. Phys. J. C*, 76(8):447, Aug. 2016.

[98] T. Adorno, S. Gavrilov, D. Gitman, and R. Ferreira. Peculiarities of pair creation by a peak electric field. *Russian Physics Journal*, 60, July 2017.

[99] T. Adorno, R. Ferreira, S. Gavrilov, and D. Gitman. Role of switching-on and -off effects in the vacuum instability. *Int. J. Mod. Phys. A*, 33, Feb. 2018.

[100] T. C. Adorno, S. P. Gavrilov, and D. M. Gitman. Violation of vacuum stability by inverse square electric fields. *Eur. Phys. J. C*, 78(12):1021, Dec. 2018.

[101] A. I. Breev, S. P. Gavrilov, D. M. Gitman, and A. A. Shishmarev. Vacuum instability in time-dependent electric fields: New example of an exactly solvable case. *Phys. Rev. D*, 104:076008, Oct. 2021.

[102] T. Adorno, S. P. Gavrilov, and D. M. Gitman. Exactly solvable cases in qed with t-electric potential steps. *Int. J. Mod. Phys. A*, 32:1750105, 2017.

[103] S. P. Gavrilov and D. M. Gitman. Quantization of charged fields in the presence of critical potential steps. *Phys. Rev. D*, 93:045002, Feb. 2016.

[104] V. S. Popov. Production of e^+e^–pairs in an alternating external fields. *JETP Lett.*, 13:185, 1971.

[105] MS Marinov and Vladimir Stepanovich Popov. On the production of e^+e^–pairs from the vacuum under the influence of an electric field. *Teoreticheskaya i Matematicheskaya Fizika*, 17(1):34–46, 1973.

[106] V. S. Popov. Method of "imaginary time" for periodical fields. *Sov. J. Nucl. Phys.*, 19:584, 1974.

[107] E. Brezin and C. Itzykson. Pair production in vacuum by an alternating field. *Phys. Rev. D*, 2:1191–1199, Oct. 1970.

[108] L. DiMauro, M. Frolov, K. L. Ishikawa, and M. Ivanov. 50 years of optical tunneling. *J. Phys. B*, 47(20):200301, Oct. 2014.

[109] W. Greiner, B. Müller, and J. Rafelski. *Quantum Electrodynamics of Strong Fields*. Springer-Verlag, Berlin, 1985.

[110] J. Rafelski, L. P. Fulcher, and A. Klein. Fermions and bosons interacting with arbitrarily strong external fields. *Phys. Rep.*, 38(5):227–361, 1978.

[111] K. Parker and J. Tiomno. Pair-Producing Electric Fields and Pulsars. *Astrophys. J*, 178:809–818, Dec. 1972.

[112] N. D. Birrell and P. C. W. Davies. *Quantum Fields in Curved Space*. Cambridge Monographs on Mathematical Physics. Cambridge Univ. Press, Cambridge, UK, Feb. 1984.

[113] S. G. Grib, A. A. Mamaev and V. M. Mostepanenko. Quantum effects in intense external fields (methods and results not connected with the perturbation theory), Jan. 1980.

[114] D. Strickland and G. Mourou. Compression of amplified chirped optical pulses. *Optics Communications*, 55(6):447–449, 1985.

[115] A. Di Piazza, C. Müller, K. Z. Hatsagortsyan, and C. H. Keitel. Extremely high-intensity laser interactions with fundamental quantum systems. *Rev. Mod. Phys.*, 84:1177–1228, Aug. 2012.

[116] G. A. Mourou, T. Tajima, and S. V. Bulanov. Optics in the relativistic regime. *Rev. Mod. Phys.*, 78:309–371, Apr. 2006.

[117] B. Acharya et al. Search for magnetic monopoles produced via the schwinger mechanism. *Nature*, 602(7895):63–67, Feb 2022.

[118] S. Schmidt, D. Blaschke, G. Röpke, S. A. Smolyansky, A. V. Prozorkevich, and V. D. Toneev. A quantum kinetic equation for particle production in the schwinger mechanism. *Int. J. Mod. Phys. E*, 07(06):709–722, Dec. 1998.

[119] S. A. Smolyansky, G. Roepke, S. Schmidt, D. Blaschke, V. D. Toneev, and A. V. Prozorkevich. Dynamical derivation of a quantum kinetic equation for particle production in the schwinger mechanism, 1997.

[120] Y. Kluger, E. Mottola, and J. M. Eisenberg. Quantum vlasov equation and its markov limit. *Phys. Rev. D*, 58:125015, Nov. 1998.

[121] R. Alkofer, M. B. Hecht, C. D. Roberts, S. M. Schmidt, and D. V. Vinnik. Pair creation and an x-ray free electron laser. *Phys. Rev. Lett.*, 87:193902, Oct. 2001.

[122] C. D. Roberts, S. M. Schmidt, and D. V. Vinnik. Quantum effects with an x-ray free-electron laser. *Phys. Rev. Lett.*, 89:153901, Sep. 2002.

[123] D. B. Blaschke, A. V. Prozorkevich, C. D. Roberts, S. M. Schmidt, and S. A. Smolyansky. Pair production and optical lasers. *Phys. Rev. Lett.*, 96:140402, Apr. 2006.

[124] F. Hebenstreit, R. Alkofer, G. V. Dunne, and H. Gies. Momentum signatures for schwinger pair production in short laser pulses with a subcycle structure. *Phys. Rev. Lett.*, 102:150404, Apr. 2009.

[125] C. K. Dumlu and G. V. Dunne. Stokes phenomenon and schwinger vacuum pair production in time-dependent laser pulses. *Phys. Rev. Lett.*, 104:250402, June 2010.

[126] N. Abdukerim, Z. L. Li, and B. Xie. Effects of laser pulse shape and carrier envelope phase on pair production. *Phys. Lett. B*, 726(4):820–826, 2013.

[127] C. Banerjee and M. P. Singh. Imprint of the temporal envelope of ultra-short laser pulses on the longitudinal momentum spectrum of e^+e^- pairs. *Phys. Rev. D*, 105:076021, Apr. 2022.

[128] A. Otto, H. Oppitz, and B. Kämpfer. Assisted vacuum decay by time-dependent electric fields. *Eur. Phys. J. A*, 54(2):23, Feb. 2018.

[129] N. Abdukerim, Z. L. Li, and B. Xie. Enhanced electron–positron pair production by frequency chirping in one- and two-color laser pulse fields. *Chin. Phys. B*, 26(2):020301, Feb. 2017.

[130] M. Ruf, G. R. Mocken, C. Müller, K. Z. Hatsagortsyan, and C. H. Keitel. Pair production in laser fields oscillating in space and time. *Phys. Rev. Lett.*, 102:080402, Feb. 2009.

[131] I. A. Aleksandrov, G. Plunien, and V. M. Shabaev. Pulse shape effects on the electron-positron pair production in strong laser fields. *Phys. Rev. D*, 95:056013, Mar. 2017.

[132] I. A. Aleksandrov, G. Plunien, and V. M. Shabaev. Momentum distribution of particles created in space-time-dependent colliding laser pulses. *Phys. Rev. D*, 96:076006, Oct. 2017.

[133] Q. Z. Lv, S. Dong, Y. T. Li, Z. M. Sheng, Q. Su, and R. Grobe. Role of the spatial inhomogeneity on the laser-induced vacuum decay. *Phys. Rev. A*, 97:022515, Feb. 2018.

[134] M. Jiang, W. Su, X. Lu, Z. M. Sheng, Y. T. Li, Y. J. Li, J. Zhang, R. Grobe, and Q. Su. Electron-positron pair creation induced by quantum-mechanical tunneling. *Phys. Rev. A*, 83:053402, May 2011.

[135] L. F. Granz, O. Mathiak, S. Villalba-Chávez, and C. Müller. Electron-positron pair production in oscillating electric fields with double-pulse structure. *Phys. Lett. B*, 793:85–89, 2019.

[136] M. Jiang, W. Su, Z. Q. Lv, X. Lu, Y. J. Li, R. Grobe, and Q. Su. Pair creation enhancement due to combined external fields. *Phys. Rev. A*, 85:033408, Mar. 2012.

[137] L. Wang, B. Wu, and B. S. Xie. Electron-positron pair production in an oscillating sauter potential. *Phys. Rev. A*, 100:022127, Aug. 2019.

[138] X. X. Zhou, C. K. Li, N. S. Lin, and Y. J. Li. Electron-positron pair creation induced by two sequential short pulses. *Phys. Rev. A*, 103:012229, Jan. 2021.

[139] I. A. Aleksandrov, G. Plunien, and V. M. Shabaev. Electron-positron pair production in external electric fields varying both in space and time. *Phys. Rev. D*, 94:065024, Sep. 2016.

[140] I. Bialynicki-Birula, P. Górnicki, and J. Rafelski. Phase-space structure of the dirac vacuum. *Phys. Rev. D*, 44:1825–1835, Sep. 1991.

[141] F. Hebenstreit, A. Ilderton, M. Marklund, and J. Zamanian. Strong field effects in laser pulses: The wigner formalism. *Phys. Rev. D*, 83:065007, Mar. 2011.

[142] F. Hebenstreit, R. Alkofer, and H. Gies. Schwinger pair production in space- and time-dependent electric fields: Relating the wigner formalism to quantum kinetic theory. *Phys. Rev. D*, 82:105026, Nov. 2010.

[143] F. Hebenstreit, R. Alkofer, and H. Gies. Particle self-bunching in the schwinger effect in spacetime-dependent electric fields. *Phys. Rev. Lett.*, 107:180403, Oct. 2011.

[144] A. Blinne and H. Gies. Pair production in rotating electric fields. *Phys. Rev. D*, 89:085001, Mar. 2014.

[145] Z. L. Li, D. Lu, and B. S. Xie. Effects of electric field polarizations on pair production. *Phys. Rev. D*, 92:085001, Oct. 2015.

[146] Z. L. Li, Y. J. Li, and B. S. Xie. Momentum vortices on pairs production by two counter-rotating fields. *Phys. Rev. D*, 96:076010, Oct. 2017.

[147] O. Olugh, Z. L. Li, B. S. Xie, and R. Alkofer. Pair production in differently polarized electric fields with frequency chirps. *Phys. Rev. D*, 99:036003, Feb. 2019.

[148] O. Olugh, Z. L. Li, and B. S. Xie. Dynamically assisted pair production for various polarizations. *Phys. Lett. B*, 802:135259, 2020.

[149] F. Fillion-Gourdeau, F. Hebenstreit, D. Gagnon, and S. MacLean. Pulse shape optimization for electron-positron production in rotating fields. *Phys. Rev. D*, 96:016012, July 2017.

[150] A. Wöllert, H. Bauke, and C. H. Keitel. Spin polarized electron-positron pair production via elliptical polarized laser fields. *Phys. Rev. D*, 91:125026, June 2015.

[151] A. Wöllert, H. Bauke, and C. H. Keitel. Multi-pair states in electron–positron pair creation. *Phys. Lett. B*, 760:552–557, 2016.

[152] A. Blinne and E. Strobel. Comparison of semiclassical and wigner function methods in pair production in rotating fields. *Phys. Rev. D*, 93:025014, Jan. 2016.

[153] E. Strobel and S. S. Xue. Semiclassical pair production rate for rotating electric fields. *Phys. Rev. D*, 91:045016, Feb. 2015.

[154] S. P. Kim and D. N. Page. Schwinger pair production in electric and magnetic fields. *Phys. Rev. D*, 73:065020, Mar. 2006.

[155] S. P. Kim and D. N. Page. Improved approximations for fermion pair production in inhomogeneous electric fields. *Phys. Rev. D*, 75:045013, Feb. 2007.

[156] H. Kleinert, R. Ruffini, and S. S. Xue. Electron-positron pair production in space- or time-dependent electric fields. *Phys. Rev. D*, 78:025011, July 2008.

[157] J. Oertel and R. Schützhold. Wkb approach to pair creation in spacetime-dependent fields: The case of a spacetime-dependent mass. *Phys. Rev. D*, 99:125014, June 2019.

[158] R. Schützhold, H. Gies, and G. Dunne. Dynamically assisted schwinger mechanism. *Phys. Rev. Lett.*, 101:130404, Sep. 2008.

[159] M. Orthaber, F. Hebenstreit, and R. Alkofer. Momentum spectra for dynamically assisted schwinger pair production. *Phys. Lett. B*, 698(1):80–85, 2011.

[160] M. F. Linder, C. Schneider, J. Sicking, N. Szpak, and R. Schützhold. Pulse shape dependence in the dynamically assisted sauter-schwinger effect. *Phys. Rev. D*, 92:085009, Oct. 2015.

[161] I. A. Aleksandrov, G. Plunien, and V. M. Shabaev. Dynamically assisted schwinger effect beyond the spatially-uniform-field approximation. *Phys. Rev. D*, 97:116001, June 2018.

[162] A. Di Piazza, E. Lötstedt, A. I. Milstein, and C. H. Keitel. Barrier control in tunneling e^+-e^- photoproduction. *Phys. Rev. Lett.*, 103:170403, Oct. 2009.

[163] G. V. Dunne, H. Gies, and Ralf Schützhold. Catalysis of schwinger vacuum pair production. *Phys. Rev. D*, 80:111301, Dec. 2009.

[164] A. Monin and M. B. Voloshin. Semiclassical calculation of photon-stimulated schwinger pair creation. *Phys. Rev. D*, 81:085014, Apr. 2010.

[165] C. Fey and R. Schützhold. Momentum dependence in the dynamically assisted sauter-schwinger effect. *Phys. Rev. D*, 85:025004, Jan. 2012.

[166] M. J. A. Jansen and C. Müller. Strongly enhanced pair production in combined high- and low-frequency laser fields. *Phys. Rev. A*, 88:052125, Nov. 2013.

[167] S. Augustin and C. Müller. Nonperturbative bethe–heitler pair creation in combined high- and low-frequency laser fields. *Phys. Lett. B*, 737:114–119, 2014.

[168] Otto A., D. Seipt, D. Blaschke, B. Kämpfer, and S. A. Smolyansky. Lifting shell structures in the dynamically assisted schwinger effect in periodic fields. *Phys. Lett. B*, 740:335–340, 2015.

[169] G. V. Dunne and Q. Wang. Multidimensional worldline instantons. *Phys. Rev. D*, 74:065015, Sep. 2006.

[170] C. Schneider and R. Schützhold. Dynamically assisted sauter-schwinger effect in inhomogeneous electric fields. *J. High Energy Phys.*, 2016(2):164, Feb. 2016.

[171] G. Torgrimsson, C. Schneider, and R. Schützhold. Sauter-schwinger pair creation dynamically assisted by a plane wave. *Phys. Rev. D*, 97:096004, May 2018.

[172] J. von Neumann. Wahrscheinlichkeitstheoretischer aufbau der quantenmechanik. *Nachrichten von der Gesellschaft der Wissenschaften zu Göttingen, Mathematisch-Physikalische Klasse*, pages 245–272, 1927.

[173] J. von Neumann. Thermodynamik quantenmechanischer gesamtheiten. *Nachrichten von der Gesellschaft der Wissenschaften zu Göttingen, Mathematisch-Physikalische Klasse*, pages 273–291, 1927.

[174] U. Fano. Description of states in quantum mechanics by density matrix and operator techniques. *Rev. Mod. Phys.*, 29:74–93, Jan. 1957.

[175] K. C. Chou, Z. B. Su, B. L. Hao, and Yu L. Equilibrium and nonequilibrium formalisms made unified. *Phys. Rep.*, 118(1):1–131, 1985.

[176] J. P. Blaizot, E. Iancu, and A. Rebhan. Approximately self-consistent resummations for the thermodynamics of the quark-gluon plasma: Entropy and density. *Phys. Rev. D*, 63:065003, Feb. 2001.

[177] E. Braaten. Solution to the perturbative infrared catastrophe of hot gauge theories. *Phys. Rev. Lett.*, 74:2164–2167, Mar. 1995.

[178] D. Bödeker. Effective dynamics of soft non-abelian gauge fields at finite temperature. *Phys. Lett. B*, 426(3):351–360, 1998.

[179] D. Bödeker. From hard thermal loops to langevin dynamics. *Nucl. Phys. B*, 559:502–538, 1999.

[180] F. Flechsig and A. K. Rebhan. Improved hard-thermal-loop effective action for hot qed and qcd. *Nucl. Phys. B*, 464(1):279–297, 1996.

[181] D. Besak. *Thermal particle production in the early universe.* PhD thesis, Universität Bielefeld, 2010.

[182] P. Arnold, G. D. Moore, and L. G. Yaffe. Photon emission from ultrarelativistic plasmas. *J. High Energy Phys.*, 2001(11):057–057, Nov. 2001.

[183] P. Arnold, G. D. Moore, and L. G. Yaffe. Photon emission from quark gluon plasma: Complete leading order results. *JHEP*, 12:009, 2001.

[184] M. Bolz, A. Brandenburg, and W. Buchmüller. Thermal production of gravitinos. *Nucl. Phys. B*, 606(1):518–544, 2001.

[185] J. Pradler. Electroweak Contributions to Thermal Gravitino Production. Master's thesis, Vienna U., 2006.

[186] V. S. Rychkov and A. Strumia. Thermal production of gravitinos. *Phys. Rev. D*, 75:075011, Apr. 2007.

[187] A. Brandenburg and F. D. Steffen. Axino dark matter from thermal production. *J. Cosmol. Astropart. Phys.*, 2004(08):008–008, Aug. 2004.

[188] T. A. Weaver and G. F. Chapline. Dissipation in supernova shock waves. *Astrophys. J., Lett.*, 192:L57–L60, Sep. 1974.

[189] R. Ramaty and R. E. Lingenfelter. Positron-electron annihilation radiation from the galactic center. *Highlights Astron.*, 6:525–529, 1983.

[190] S. J. Rose. Electron–positron pair creation in burning thermonuclear plasmas. *High Energy Density Phys.*, 9:480–483, 2013.

[191] E. Haug. Pair production by photons in a hot maxwellian plasma. *Astron. Astrophys.*, 416:437–440, 2004.

[192] I. Kuznetsova, D. Habs, and J. Rafelski. Thermal reaction processes in a relativistic qed plasma drop. *Phys. Rev. D*, 81:053007, 2010.

[193] J. Larsen. *Foundations of High-Energy-Density Physics*. Cambridge University Press, May 2017.

[194] H. A. Scott. Collisional-radiative modeling for radiation hydrodynamics codes. In Y. Ralchenko, editor, *Modern Methods in Collisional-Radiative Modeling of Plasmas*, chapter 4, pages 81–104. Springer International Publishing, Berlin, 2016.

[195] G. J. Tallents. Free electron degeneracy effects on collisional excitation, ionization, de-excitation and three-body recombination. *High Energy Density Phys.*, 20:9–16, Sep. 2016.

[196] M. Tabak. What is the role of tritium-poor fuels in ICF? *Nucl. Fusion*, 36(2):147–157, Feb. 1996.

[197] H. Chen et al. On krypton-doped capsule implosion experiments at the national ignition facility. *Phys. Plasmas*, 24:072715, July 2017.

[198] W. Biel et al. Diagnostics for plasma control – from iter to demo. *Fusion Eng. Des.*, Jan. 2019.

[199] B. W. Smith et al. Oso-8 x-ray spectra of clusters of galaxies. 1. observations of twenty clusters: Physical correlations - nasa-tm-78097. Technical report, 1978.

[200] J. L. Synge. *The Relativistic Gas*. Series in Physics. North-Holland, 1957.

[201] H. Sampson, D. L. Zhang, and C. J. Fontes. A fully relativistic approach for calculating atomic data for highly charged ions. *Phys. Rep.*, 477:111–214, July 2009.

[202] R. W. B. Best. Clean fusion concepts and efforts - a survey. *Nucl. Instrum. Methods*, 144:1–7, 1977.

[203] O. J. Pike. *Particle Interactions in High Temperature Plasmas*. PhD thesis, Imperial College London, July 2015.

[204] H. Van Regemorter. Rate of collisional excitation in stellar atmospheres. *Astrophys. J.*, 136:906–915, 1962.

[205] W. Z. Lotz. Electron-impact ionization cross-sections and ionization rate coefficients for atoms and ions from hydrogen to calcium. *Z. Phys.*, 216(3):241–247, June 1968.

[206] M. Abramowitz and I. A. Stegun. *Handbook of Mathematical Functions: With Formulas, Graphs, and Mathematical Tables*. Number 55 in Applied Mathematics Series. Dover Publications, New York, 1965.

[207] M. N. Saha. Liii. ionization in the solar chromosphere. *Philos. Mag.*, 40(238):472–488, 1920.

[208] M. N. Saha. On a physical theory of stellar spectra. *Proc. R. Soc. Lond. A*, 99(697):135–153, 1921.

[209] A. Kramida, Yu. Ralchenko, J. Reader, and and NIST ASD Team. NIST Atomic Spectra Database (ver. 5.10), [Online]. Available: `https://physics.nist.gov/asd` [2023, May 12]. National Institute of Standards and Technology, Gaithersburg, MD., 2022.

[210] J. M. Jauch and F. Rohrlich. *The theory of photons and electrons.* Texts and Monographs in Physics. Springer, Berlin, 2nd edition, 1976.

[211] E. W. Kolb and M. S. Turner. *The Early Universe*. Frontiers in physics. Addison-Wesley, Boston, 1990.

[212] J. Bernstein. *Kinetic theory in an expanding universe*. Cambridge Monographs on Mathematical Physics. Cambridge University Press, Cambridge, U.K., 1988.

[213] R. Svensson. The pair annihilation process in relativistic plasmas. *Astrophys. J*, 258:321–334, 1982.

[214] R. Svensson. Electron-Positron Pair Equilibria in Relativistic Plasmas. *Astrophys. J.*, 258:335, July 1982.

[215] G. S. Bisnovatyi-Kogan, Y. B. Zel'dovich, and R. A. Syunyaev. Physical Processes in a Low-Density Relativistic Plasma. *Soviet Astron.*, 15:17–22, 1971.

[216] R. J. Gould and G. Schréder. Opacity of the universe to high-energy photons. *Phys. Rev. Lett.*, 16:252–254, 1966.

[217] A. P. Lightman. Relativistic thermal plasmas - Pair processes and equilibria. *Astrophys. J.*, 253:842–858, 1982.

[218] S. S. Masood. Renormalization of qed near decoupling temperature. *Phys. Res. Int.*, 2014:489163, Jun 2014.

[219] D. Seipt, M. Bluhm, and B. Kämpfer. Quark mass dependence of thermal excitations in QCD in one-loop approximation. *J. Phys. G*, 36(4):045003, Mar. 2009.

[220] M. Bluhm, B. Kämpfer, R. Schulze, and D. Seipt. Qcd equation of state: Physical quark masses and asymptotic temperatures. *Prog. Part. Nucl. Phys.*, 62(2):512–517, 2009. Heavy-Ion Collisions from the Coulomb Barrier to the Quark-Gluon Plasma.

[221] R. C. Bourret. Coherence properties of blackbody radiation. *Nuovo Cimento*, 18(2):347, 1960.

[222] C. L. Mehta and E. Wolf. Coherence properties of blackbody radiation. i. correlation tensors of the classical field. *Phys. Rev.*, 134:A1143–A1149, June 1964.

[223] L. Mandel and E. Wolf. *Optical Coherence and Quantum Optics*. Cambridge University Press, 1995.

[224] H. Gies and G. Torgrimsson. Critical Schwinger pair production. *Phys. Rev. Lett.*, 116(9):090406, 2016.

[225] H. Gies and G. Torgrimsson. Critical schwinger pair production. ii. universality in the deeply critical regime. *Phys. Rev. D*, 95:016001, Jan. 2017.

[226] V.N. Baier and V.M. Katkov. Concept of formation length in radiation theory. *Phys. Rep.*, 409(5):261–359, 2005.

[227] M. D'Onofrio and K. Rummukainen. Standard model cross-over on the lattice. *Phys. Rev. D*, 93:025003, Jan. 2016.

[228] O. Klein. Die reflexion von elektronen an einem potentialsprung nach der relativistischen dynamik von dirac. *Z. Phys.*, 53(3):157–165, Mar. 1929.

[229] A. Hansen and F. Ravndal. Klein's Paradox and Its Resolution. *Phys. Scripta*, 23:1036, 1981.

[230] J. von Neumann. On rings of operators. reduction theory. *Ann. Math.*, 50(2):401–485, 1949.

[231] M. H. Mortad. Unbounded operators: (square) roots, nilpotence, closability and some related invertibility results, 2020.

[232] P. Blanchard and E. Brüning. *Mathematical Methods in Physics*. Birkhäuser, Basel, 2015.

[233] M. Guiggiani. The evaluation of cauchy principal value integrals in the boundary element method—a review. *Math. Comput. Model.*, 15(3):175–184, 1991.

[234] K. Osterwalder and R. Schrader. Axioms for Euclidean Green's functions. *Commun. Math. Phys.*, 31(2):83–112, June 1973.

[235] M. S. Friedlander, F. G. Joshi. *Introduction to the Theory of Distributions*. Cambridge University Press, 1998.

[236] B. Simon. Essential self-adjointness of schrödinger operators with positive potentials. *Math. Ann.*, 201:211–220, 1973.

[237] M. Reed and B. Simon. *I: Functional Analysis*. Methods of Modern Mathematical Physics. Elsevier Science, 1981.

[238] W. Rudin. *Real and Complex Analysis, 3rd Ed.* McGraw-Hill, Inc., USA, 1987.

[239] M. Renardy and R.C. Rogers. *An Introduction to Partial Differential Equations*. Texts in Applied Mathematics. Springer New York, 2004.